UNIVERSITY OF CALIFORNIA,
IRVINE

Nonperturbative Dynamics of Monopoles in Quantum Field Theory

DISSERTATION

submitted in partial satisfaction of the requirements
for the degree of

DOCTOR OF PHILOSOPHY

in Physics and Astronomy

by

Michael Waterbury

DISSERTATION COMMITTEE:
Professor Yuri Shirman, Chair
Professor Mu-Chun Chen
Professor Michael Ratz

2021

TABLE OF CONTENTS

LIST OF FIGURES

LIST OF TABLES

ACKNOWLEDGMENTS

The completion of this dissertation would not have been possible without the wide network of support I received from my family, friends, teachers, colleagues, and collaborators. I am paricularly grateful to have had such a wise and understanding advisor, Yuri Shirman, who supported and guided me on the path which lead to my interest and research in the subject of this thesis.

I thank the present and past members of the UCI particle theory group for a plethora of insightful conversations. Particularly, the wonderful courses lead by Arvind Rajaraman, Michael Ratz, Yuri Shirman, and Tim Tait were instrumental in developing and reinforcing my understanding of quantum field theory and particle physics. I would like to acknowledge my many collaborators: Dillon Berger, Csaba Csàki, Sungwoo Hong, Seyda Ipek, Michael Ratz, Yuri Shirman, Shreya Shukla, Tim Tait, Ofri Telem, and John Terning without which many of the ideas and developments present in this work would not have happened.

I would also like to show my appreciation to my network of friends which began developing as early as elementary school and continues to grow today for their support and encouragement. There are so many of you who deserve recognition, but I feel particularly indebted to Louis Farley, Daniel Gartrell, Parker Thompson, Caleb Berberich, Carlo Suits, Catherine Chambers, John Bollenbacher, Nick Beier, Amanatullah Khan, and Drew Welser for their encouragment and help in overcoming many of the obstacles which have stood in my way.

I am particularly beholden to my brother, Christopher Waterbury, my mother, Margaret Waterbury, and father, Scott Waterbury, for their love and support throughout my entire life. Without the nurturing environment they provided, many of the early seeds which later developed into the pursuit of this degree would not have sprouted.

Aspects of this work received funding by NSF grants PHY-2014071, PHY-1915005, PHY-1620638, PHY-131622, DGE-1839285 and DOE grants DE SC-0009999, DE-AC02-05CH11231.

VITA

Michael Waterbury

EDUCATION

Doctor of Philosophy in Physics and Astronomy **2021**
University of California, Irvine *Irvine, CA*

Bachelor of Science in Physics and Astronomy **2016**
Georgia Institute of Technology *Atlanta, GA*

RESEARCH EXPERIENCE

Graduate Research Assistant **2017–2021**
University of California, Irvine *Irvine, California*

TEACHING EXPERIENCE

Teaching Assistant **2016–2021**
University of California, Irvine *Irvine, California*

ABSTRACT OF THE DISSERTATION

Nonperturbative Dynamics of Monopoles in Quantum Field Theory

By

Michael Waterbury

Doctor of Philosophy in Physics and Astronomy

University of California, Irvine, 2021

Professor Yuri Shirman, Chair

It is common for quantum field theories to lack a consistent, perturbative treatment. In most cases, this is because the couplings flow to a strongly-coupled regime, and the perturbative series diverges at all orders in these regimes. In some cases, such as those we will investigate for magnetic monopoles, the dynamics are inherently nonperturbative. In three dimensions, monopoles play the role of instantons and induce important corrections to the theory which are absent in a naive perturbative expansion around the trivial vacuum. In four dimensions, they appear as charged states, and the scattering processes involving electric and magnetic states fail to converge at any order in perturbation theory.

We begin by studying the conditions for fundamental zero modes of the Kaluza-Klein monopole which arises in compactified four dimensional theories. The existence of fundamental zero modes provide a path to decouple the Kaluza-Klein monopole in the zero radius limit such that the theory is purely three dimensional. We study the correspondence between the three and four dimensional theories under these effects.

Next, we study the moduli space for three dimensional supersymmetric SU(N) gauge theories with $F < N$ chiral superfields in the fundamental and anti-fundamental representations. We calculate quantum constraints induced by monopoles and find a novel interpretation of the constraints as transition functions between the moduli of different subwedges of the

moduli space. Although the subwedges are classically disjoint, these quantum modifications smooth out their boundaries and allow for a consistent description of the system's physics independent of the choice of classical vacua. We emphasize how these quantum modifications to the moduli space allow one to flow from the F flavor theory to the $F-1$ flavor theory which was not previously understood.

We now shift focus to an on-shell description of electric-magnetic scattering. Magnetically charged particles are theoretically well-motivated, but it is difficult to calculate the signatures of scattering events involving both magnetic and electrically charged particles. This cause for this difficulty is two-fold: there remains no local, Lorentz invariant Lagrangian description of such theories, and due to Dirac quantization, the coupling strength of the interactions are never weakly-coupled. We develop on-shell methods to study these processes, derive new selection rules, and calculate fermion-monopole scattering.

We end by changing gears and presenting a phenomenological study of dark matter freeze-out where the universe experiences an early QCD phase transition. Where dark matter freeze out is typically driven by annihilation into quarks, here the active degrees of freedom are mesons which alter the correspondence between the dark matter couplings to the Standard Model and the relic abundance of dark matter. We show that this model can explain the observed dark matter relic density while evading experimental constraints from direct detection.

Chapter 1

Introduction

Magnetic monopoles can play a variety of roles in quantum field theory (QFT) depending on the geometry of the theory. On $\mathbb{R}^4$ (4D), they appear as massive extended objects in grand unified theories [101] and are responsible for nonperturbative effects in strongly coupled gauge theories. In fact, it has been conjectured that confinement is a symptom of a monopole condensate [78]. As a dynamical explanation for confinement in quantum chromodynamics (QCD) is a long-standing goal for theoretical particle physics, this is particularly intriguing idea. Much of the recent progress in this direction has been in supersymmetric (SUSY) theories. For instance, in Seiberg-Witten $\mathcal{N} = 2$ theories [94], one can explicitly show how electric confinement is connected to a monopole condensate. In contrast, if magnetic monopoles are extended objects in an ultraviolet (UV) completion of the Standard Model (SM), then, at long distances, they behave as magnetically charged states coupled by electromagnetism. Such states were initially theorized by Dirac [41], and their interactions with matter are frequently incalculable. Despite the long history of these ideas, there is still much to understand about the dynamics of magnetic monopole of both theoretical and phenomenological interest.

To further understand the role of magnetic monopoles, we can compactify the dimension along their world-line, such that they behave as instantons in theories on $\mathbb{R}^3$ (3D) or theories on a cylinder ($\mathbb{R}^3 \times \mathbb{S}^1$). The theory on a cylinder can interpolate between the 3D and 4D theories [3, 4, 32, 38, 88, 95]. Many nonperturbative effects in 4D SUSY theories are best understood by considering the theory on a cylinder and taking the limit of an infinitely large compact dimension. Similarly, the limit of infinitesimally small compact dimension allows us to find new results for 3D theories from 4D theories.

The rest of this chapter attempts to make the above notions more precise and provides the background for the chapters that follow. We begin by discussing 4D instantons with the goal of epxlaining their topological origins, their zero modes, and how to calculate their dynamics. We then discuss monopole-instantons and their zero modes in detail before discussing the Kaluza-Klein (KK) monopole which appears in the theory on a cylinder. The KK monopole is paramount to the connection between 3D and 4D theories. Next we review exact results in $\mathcal{N} = 1$ 4D SUSY QCD and $\mathcal{N} = 2$ 3D SUSY QCD. We explicitly show that $\mathcal{N} = 2$ 3D SUSY QCD deformed by the KK monopole flows to $\mathcal{N} = 1$ 4D SUSY QCD in the limit of a large compact dimension. These sections provide the necessary background for Chapters 2 and 3. In Chapter 2, we study the conditions for KK monopole fundamental zero modes by constructing the solutions. As a result, we find an elegant, dynamical explanation for the KK monopole to decouple under the real mass deformations discussed in [4] and illustrate how the appearance of these zero modes explain the 3D origins of the ADS superpotential of a 4D SUSY $SU(2) \times SU(2)$ gauge theory with bifundamental matter. In Chapter 3, we calculate chiral, squark correlation functions in monopole backgrounds. Their non-zero value implies the existence of quantum deformations of the moduli space which can be implemented by a constraint with a Lagrange multiplier in the superpotential. The quantum constraint ensures that the superpotentails generated in different sub-wedges of the moduli space agree despite being classically disjoint regions. Moreover, the quantum constraint is necessary for the theory to properly flow to theories with less flavors under large mass deformations.

After introducing monopoles and their role as instantons in SUSY gauge theories, we discuss electromagnetism with magnetic monopoles by beginning with the Dirac monopole. We emphasize that although the dynamics of the theory is difficult to calculate, the theory remains consistent with the laws of quantum mechanics and relativity. The problem of calculating is revisted in Chapter 4 using the language of scattering amplitudes. We find that theories with mutually non-local electric and magnetic charges require new representations of the Lorentz group which were not previously considered. With these new representations, we construct spinor-helicity variables and derive selection rules for the scattering processes from their little group properties. Additionally, we perform a relativistic calculation of fermion-monopole scattering and find results which agree with previous non-relativistc calculations.

We end this chapter by discussing thermal freeze out. This section on thermal freeze out focuses on its prospects as a mechanism to produce the observed dark matter relic abundance. Although the model works for a variety of masses and coupling strengths, the weak-scale couplings are of particular interest. Dark matter with these couplings is often referred as a weakly interacting massive particle (WIMP) and the coincidence between dark matter and the weak scale is often called the "WIMP miracle." Despite being compelling, WIMP-like dark matter produced by thermal freeze out is in tension with direct detection experiments and its prospects seem dim. In Chapter 5, we explore a dark matter model where thermal freeze out occurs during a period of early QCD confinement. We find that, in the context of a non-standard cosmology, the WIMPs can evade current direction detection bounds while explaining the entire dark matter abundance, maintaining the "WIMP miracle."

We conclude this dissertation in Chapter 6 with final remarks on the work presented in Chapters 2 to 5.

1.1 Instantons and Monopole-Instantons

QFTs are defined on a given manifold $\mathcal{M}$, and instantons, as we shall see, are deeply connected with the topology of the given manifold. We will need to deal with them for each manifold on which we wish to study QFT. In this section, we will develop the theory of instantons on $\mathbb{R}^4$ (4D), $\mathbb{R}^3$ (3D), and $\mathbb{R}^3 \times \mathbb{S}^1$ (cylinder) each with a Euclidean metric. While the 4D scenario most closely resembles models for fundmental physics, the motivation for studying 3D theories and theories on a cylinder is less direct. 3D QFTs can model electrons in metals which may be effectively constrained to two spatial dimensions, while QFT on a cylinder corresponds to thermal systems where the size of the compact direction $\mathbb{S}^1$ corresponds with the inverse temperature of the system. From a purely theoretical point of view, 3D QFTs are more tractable than 4D QFTs, and the cylinder serves as an interpolating theory where large compact dimensions behave 4D-like and small compact dimensions behave 3D-like. Although there is no proof of such a correspondence between these theories, all known examples follow this schematic, and presenting examples is a key point of this work.

In this section, we will begin by discussing 4D instantons, developing the philosophy behind their existence and how to calculate their effects. Next, we investigate 3D instantons which require symmetry breaking. These instantons correspond with 't Hooft-Polyakov magnetic monopoles in 4D, and thus we often refer to them as monopole-instantons or simply monopoles. Finally, we establish the role of the compact dimension on the instantons of $\mathbb{R}^3 \times \mathbb{S}^1$. The $\mathbb{R}^3$ factor reproduces the monopole-instantons in the pure 3D theory, while the $\mathbb{S}^1$ allows novel configurations called the KK monopoles. Importantly, the KK monopole along with the fundamental monopole-instantons form a caloron which can be identified with the 4D instanton when the compact dimension is large.

1.1.1 Instantons on $\mathcal{M} = \mathbb{R}^4$ (4D Instantons)

Instantons were first discovered in [10]. In an illuminating paper [102], 't Hooft calculated their quantum effects. Since then, many more calculations and reviews been published adding detail and insight into instanton calculus. We find [25, 28, 42, 96, 109] to be particularly insightful.

We begin by considering the path integral for the parition function of 4D Yang Mills (YM) with gauge group G coupled to Weyl fermions ψ and scalars ϕ

$$\mathcal{Z} = \int DA_\mu D\phi D\bar{\psi} D\psi e^{-S[A_\mu, \phi, \bar{\psi}, \psi]} \,. \tag{1.1}$$

This expression can be interpreted as the "sum over all field configurations with finite action weighted by their probability amplitude" where "their probability amplitude" is given by $\exp(-S[A_\mu, \phi, \bar{\psi}, \psi])$. The action for pure YM is

$$S_{\text{YM}}[A_\mu] = \int d^4x \left[-\frac{1}{2g^2} \operatorname{Tr}(F^{\mu\nu} F_{\mu\nu}) + \frac{\mathrm{i}\theta}{16\pi^2} \operatorname{Tr}(F^{\mu\nu} \tilde{F}_{\mu\nu}) \right] \tag{1.2}$$

where $F^{\mu\nu} = [\mathcal{D}_\mu, \mathcal{D}_\nu]$ is the field strength tensor, and $\tilde{F}_{\mu\nu} = \frac{1}{2}\varepsilon_{\mu\nu\rho\sigma} F^{\rho\sigma}$ is the dual field strength tensor. The requirement that the action be finite is equivalent to the condition that the field strength must vanish sufficiently quickly at infinity

$$\lim_{x\to\infty} F_{\mu\nu}(x) = 0 \,. \tag{1.3}$$

This implies that the gauge field becomes pure gauge at infinity

$$\lim_{x\to\infty} A_\mu(x) = \mathrm{i} U^{-1}(x) \partial_\mu U(x) \,, \tag{1.4}$$

where $U(x) \in G$ is a gauge transformation. Fundamentally $U(x)$ is a map from spacetime to

the gauge group. Restricting ourselves to the condition at infinity, the domain of the map becomes S^3 such that

$$U : S^3 \to G\,, \qquad U : x \mapsto U(x)\,. \tag{1.5}$$

If we consider the set of all possible maps, they fall into classes based on their homotopy group $\pi_3(G)$. Thus, there are $|\pi_3(G)|$ distinct classes of field configurations which satisfy our finite action condition. By nature of homotopy, one cannot continuous deform between maps which are characterized by different elements of $\pi_3(G)$. It follows that the path integral written in Equation (1.1) decomposes into a sum over these different classes

$$\mathcal{Z} = \sum_{k\in\pi_3(G)} \mathcal{Z}^k, \qquad \mathcal{Z}^k = \int DA_\mu^{[k]} D\phi D\bar{\psi} D\psi e^{-S[A_\mu^{[k]},\phi,\bar{\psi},\psi]}\,. \tag{1.6}$$

Due to a correspondence with the θ-vacuum, we interpret this sum as the effect of tunneling between the different vacua of the theory. It is often said that the instanton is the effect of tunneling between topological distinct vacua. The above decomposition of the path integral is the justification for this statement.

Now we turn to the question of calculating the partition function in the different k-instanton sectors of the theory with gauge group $G = \mathrm{SU}(N)$ where $\pi_3(\mathrm{SU}(N)) = \mathbb{Z}$. The path integral is computed by considering the classical, minimum action field configuration and then summing over the perturbative modes of the classical solution. Thus we need to find both the minimum action in the k-instanton sector and the field configuration to which this corresponds. To determine the minimum action, we turn to the so-called Bogomolny bound

[15] which is easily derived by rewriting the action as

$$S[A_\mu^{[k]}] = \int d^4x \left[-\frac{1}{4g^2} \operatorname{Tr}\left((F_{\mu\nu} \mp \tilde{F}_{\mu\nu})^2 \right) + \left(\frac{\mathrm{i}\theta}{16\pi^2} \mp \frac{1}{2g^2} \right) \operatorname{Tr}(F_{\mu\nu}\tilde{F}^{\mu\nu}) \right] \tag{1.7}$$

$$\geq \int d^4x \left(\frac{\mathrm{i}\theta}{8\pi} \mp \frac{1}{2g^2} \right) \operatorname{Tr}(F_{\mu\nu}\tilde{F}^{\mu\nu}) = \left(\mp \frac{8\pi^2}{g^2} + \mathrm{i}\theta \right) k \tag{1.8}$$

where the bound is saturated if the field strength is self-dual or anti-self-dual ($F_{\mu\nu} = \pm\tilde{F}_{\mu\nu}$), and we used that the integral over the Pontyragin square is given by

$$\int d^4x \operatorname{Tr}(F_{\mu\nu}\tilde{F}^{\mu\nu}) = 16\pi^2 k \,. \tag{1.9}$$

One can easily verify that the minimum action is then given by $k > 0$ for self-dual configurations and $k < 0$ for anti-self-dual configurations. Therefore the k-instanton partition function is given by

$$\mathcal{Z}^k = \int DA_\mu^{\mathrm{qu.}} e^{-\frac{8\pi^2}{g^2}|k| + \mathrm{i}\theta k} e^{-S[A_\mu^{\mathrm{qu.}}]} \tag{1.10}$$

where we expanded the gauge field around its classical value by $A_\mu = A_\mu^{\mathrm{cl.}} + A_\mu^{\mathrm{qu.}}$. $A_\mu^{\mathrm{cl.}}$ is the k-instanton solution which we will discuss in a moment. We are interested in the leading order corrections to the path integral due to instantons. Due to the $\exp(-\frac{8\pi^2}{g^2})$ factor from the classical action, its effects are dominated by single instanton configurations at weak coupling. Thus we will only discuss the $k = \pm 1$ effects from here on. The general k instanton solution can be constructed via the ADHM construction [8].

We now cite the instanton solution for $k = 1$ and $G = \mathrm{SU}(2)$

$$A_\mu^{\mathrm{cl.}[k=1]} = \partial_\nu \log[(x - z)^2 + \rho^2]\sigma_{\nu\mu} \tag{1.11}$$

up to local gauge transformations.[1] For $k = -1$, simply replace $\sigma_{\nu\mu}$ with $\bar{\sigma}_{\nu\mu}$. z is a 4-vector

[1] By local gauge transformations, we mean those which are in the trivial class of $\pi_3(\mathrm{SU}(2))$.

which is interpreted as the location of the center of the instanton, and ρ is a real number which is interpreted as the size of the instanton. Note that the value of z and ρ do not change the classical action of the configuration. For general $G = \mathrm{SU}(N)$, one simply embeds the above solution into an SU(2) subgroup of SU(N). The choice of SU(2) subgroup is irrelevant since any choice is gauge equivalent to any other choice.

We are now ready to study the measure $DA_\mu^{\mathrm{qu.}}$. It describes all possible modes for the quantum fluctuations around the classical, instanton vacuum. Some of these modes incur no additional action called zero modes. For the SU(2) instanton, there are a total of 8 bosonic zero modes originating from the location of the instanton, the size of the instanton, and three spatial rotations.[2] For general SU(N), there are a total of $4N$ total bosonic zero modes. The additional zero modes originate from the components of the SU(N) gauge field which transform as doublets under the SU(2) subgroup of the instanton. Simple counting gives $4(N-2)$ doublet components which when added to the 8 SU(2) zero modes gives $4N$.

The fermions charged under the gauge group also have zero modes in the instanton background. The precise number of zero eigenvalues depends on the representations underwhich the fermions transform and can be determined by various index theorems. Fermions which transform under the fundamental (or anti-fundamental) representation have a single zero mode in the instanton background, while fermions which transform under the adjoint representation have $2N$ zero modes in the instanton background. To see the importance of these zero modes, we will decompose the fermion fields in the eigenmodes of $-\mathrm{i}\not{D}$

$$-\mathrm{i}\not{D}\psi(x) = \sum_i \lambda_i \psi_i(x) c_i \tag{1.12}$$

where λ_i is the eigenvalue of the mode, $\psi_i(x)$ is the eigenmode, and c_i is a Grassman number.

[2]Due to the $\sigma_{\mu\nu}$, the instanton only transforms under $\mathrm{SU}(2)_{\mathrm{L}}$ subgroup of SO(4), thus there are only three independent rotations.

In the path integral, this becomes

$$\int \prod_i dc_i d\bar{c}_i e^{\sum_j \lambda_j \bar{c}_j c_j} = \int \prod_i dc_i d\bar{c}_i \prod_j \lambda_j \bar{\psi}_j \psi_j \bar{c}_j c_j \tag{1.13}$$

If $\lambda_j \neq 0$ for all j, then the Grassman numbers are simply absorbed by the Grassman measure and the integral simplifies to $\prod_j \lambda_j = \det(\mathrm{i}\mathcal{D})$. However, whenever $\lambda_j = 0$, those Grassman measures and not absorbed, and the integral goes to zero. Thus, whenever the instanton carries fermionic zero modes, the instanton partition function vanishes. However, this does not mean that the instanton cannot impart dynamics on the field theory. Recall that, in the path integral formulation of QFT, the expectation value of an operator $\mathcal{O}$ is calculated as

$$\langle \mathcal{O} \rangle = \frac{1}{\mathcal{Z}} \int [D\phi] \mathcal{O} e^{-S[\phi]} \tag{1.14}$$

thus those fermionic zero modes which kill the instanton contributions to vacuum expectation values can be absorbed from the operator $\mathcal{O}$. Therefore, in theories with fermions, instantons can only contribute to correlation functions with a fermion operator for each fermionic zero mode. This can be interpreted as generating an effective operator, known as the 't Hooft operator, in an effective field theory where the instantons have been 'integrated out.' The coefficient of this effective operator can be determined by completing the calculation we have been outlining.

Additionally, the fermion zero modes are exclusive to left-handed (right-handed) Weyl fermions for instantons (anti-instantons), so the instanton only generates operators containing left-handed fermions. These correlation functions are always guaranteed to violate a U(1) symmetry of the classical vacuum and therefore vanish if we only considered the $k = 0$ instanton sector. The charge of the operators which violate this U(1) always corresponds to the anomaly coefficient of said U(1). From this perspective, it is clear what the instanton calculation does for us as field theorists. It computes the effects of anomalies in the field

theory.

Let us finish this section by completing the calculation we have been outlining. The non-zero anomalous correlation function is

$$\langle \prod_i \psi(x_i) \rangle = \frac{1}{\mathcal{Z}^{[k=0]}} \int \left(\prod_i D\psi_i^{\emptyset} \right) \left(\prod_{i=1}^{4N} DA_{\mu,i}^{\emptyset} \right) \prod_i \psi(x_i) e^{-\frac{8\pi^2}{g^2} + \mathrm{i}\theta} \times (\det M_A)^{-1/2} (\det M_\psi)(\det M_{\text{gh.}})(\det M_\phi)^{-1} , \quad (1.15)$$

where $\det M_A, \det M_{\text{gh.}}, \det M_\psi, \det M_\phi$ are the factors which arise from the integral over the Gaussian modes.[3] Recall that some of the operators have zero modes, in these cases, it is implied that the det is taken without said zero modes. This can be made concrete by defining the determinant as

$$\det(\Delta) = \lim_{\mu \to 0} \frac{\det(\Delta + \mu)}{\mu^{\mathcal{I}(\Delta)}} \quad (1.16)$$

where $\mathcal{I}(\Delta)$ is the number of zero eigenvalues. At zeroth order in the gauge coupling, $\mathcal{Z}^{[k=0]}$ is simply the same expression without the zero modes, instanton weight, and the determinants evaluated with $A_\mu^{\text{cl.}} = 0$

$$\mathcal{Z}^{[k=0]} = (\det M_A^{(0)})^{-1/2} (\det M_\psi^{(0)})(\det M_{\text{gh.}}^{(0)})(\det M_\phi^{(0)})^{-1} \quad (1.17)$$

where the $^{(0)}$ indicates $A_\mu^{\text{cl.}} = 0$. The correlation function simplies to

$$\langle \prod_i \psi(x_i) \rangle = \int \left(\prod_{i=1}^{4N} DA_{\mu,i}^{\emptyset} \right) \prod_i \psi^{\emptyset}(x_i) e^{-\frac{8\pi^2}{g^2} + \mathrm{i}\theta} \times \left(\frac{\det M_A}{\det M_A^{(0)}} \right)^{-1/2} \left(\frac{\det M_\psi}{\det M_\psi^{(0)}} \right) \left(\frac{\det M_\phi}{\det M_\phi^{(0)}} \right)^{-1} \left(\frac{\det M_{\text{gh.}}}{\det M_{\text{gh.}}^{(0)}} \right) \quad (1.18)$$

[3]The non-Gaussian terms are proportional to the gauge coupling and result in higher order corrections.

The bosonic zero integral can be converted to a collective coordinate integral

$$\int \left(\prod_{i=1}^{4N} DA^{\emptyset}_{\mu,i} \right) = \int d^4z d\rho \rho^{4N-5} \frac{2^{4N+5}\pi^{4N-2}}{(N-1)!(N-2)!} \tag{1.19}$$

such that the correlation function becomes

$$\begin{aligned} \langle \prod_i \psi(x_i) \rangle = \frac{2^{4N+5}\pi^{4N-2}}{(N-1)!(N-2)!} \int d^4z d\rho \rho^{4N-5} \prod_i \psi^{\emptyset}(x_i) e^{-\frac{8\pi^2}{g^2} + \mathrm{i}\theta} \\ \times \left(\frac{\det M_A}{\det M_A^{(0)}} \right)^{-1/2} \left(\frac{\det M_\psi}{\det M_\psi^{(0)}} \right) \left(\frac{\det M_\phi}{\det M_\phi^{(0)}} \right)^{-1} \left(\frac{\det M_{\text{gh.}}}{\det M_{\text{gh.}}^{(0)}} \right) \end{aligned} \tag{1.20}$$

where the determinants and zero mode function secretly depend on ρ.

The intent of this subsection was to motivate and introduce instanton calculations by example using $\mathbb{R}^4$ instantons. In the following subsection, we will investigate and discuss instantons on $\mathbb{R}^3$ and $\mathbb{R}^3 \times \mathbb{S}^1$, using this subsection as a backbone.

1.1.2 Instantons on $\mathcal{M} = \mathbb{R}^3$ (3D Monopole-Instantons)

In this section, we will introduce the fundamental or BPS monopole-instantons of QFTs on $\mathbb{R}^3$ using the previous section as a backbone.

If we follow the beginning arguments for the sum over instanton sectors of YM on $\mathbb{R}^4$ and repeat them for YM on $\mathbb{R}^3$, we will arrive at the homotopy groups $\pi_2(G)$. It turns out that $\pi_2(G)$ is trivial for all semi-simple Lie groups, thus pure YM theories in $\mathbb{R}^3$ do not have instantons. However, if we consider YM theories which undergo spontaneous symmetry breaking via a scalar vacuum expectation value (VEV)

$$G \xrightarrow{\langle\phi\rangle \neq 0} H \tag{1.21}$$

then the finite action field configurations are defined by the asymptotic behavior

$$\lim_{x\to\infty} \phi(x) = U\langle\phi\rangle \tag{1.22}$$

$$\lim_{x\to\infty} A_\mu(x) = \mathrm{i}U^{-1}\partial_\mu U\,. \tag{1.23}$$

Here U is a gauge transformation which changes the asymptotic behavior of ϕ if $U \in G/H$. Therefore the asymptotic behavior of ϕ is given by the map

$$U : S^2 \to G/H\,, \quad U : x \mapsto U(x) \tag{1.24}$$

which falls into classes $\pi_2(G/H) \simeq \pi_1(H)$ which is nontrivial for generic H.

Let us consider the situation where $G = \mathrm{SU}(2)$ and ϕ transforms in the adjoint representation of SU(2) such that $\langle\phi\rangle \neq 0$ triggers the breaking pattern

$$\mathrm{SU}(2) \xrightarrow{\langle\phi\rangle\neq 0} \mathrm{U}(1)\,. \tag{1.25}$$

In this scenario, $\pi_2(\mathrm{SU}(2)/\mathrm{U}(1)) \simeq \pi_1(\mathrm{U}(1)) \simeq \mathbb{Z}$ and the partition function will be a sum over k sectors similar to the story for 4D instantons. The minimum action can be found again from the Bogomolny bound [15]

$$S = \int d^3x \left[-\frac{1}{2g^2}\,\mathrm{Tr}(F_{\mu\nu}F^{\mu\nu}) + \frac{1}{g^2}\,\mathrm{Tr}(\mathcal{D}_\mu\phi\mathcal{D}^\mu\phi)\right] \tag{1.26}$$

$$= \int d^3x \left[-\frac{1}{g^2}\,\mathrm{Tr}(B_\mu B^\mu) + \frac{1}{g^2}\,\mathrm{Tr}(\mathcal{D}_\mu\phi\mathcal{D}^\mu\phi)\right] \tag{1.27}$$

$$= \int d^3x \left[\mathrm{Tr}\left(B_\mu \mp \mathcal{D}_\mu\phi\right)^2 \pm \frac{1}{g^2}\,\mathrm{Tr}(B_\mu\mathcal{D}^\mu\phi)\right] \tag{1.28}$$

$$\geq \pm\int_{S^2} d^2y_\mu \frac{2}{g^2}\,\mathrm{Tr}(B^\mu\phi) \tag{1.29}$$

where we defined $B_\mu = \frac{1}{2}\varepsilon_{\mu\nu\rho}F^{\nu\rho}$ and the bound is saturated for $B_\mu = \pm\mathcal{D}_\mu\phi$. For $k = 1$, we

can choose the asymptotic behavior of ϕ to be

$$\lim_{x\to\infty} \phi(x) = vn^a \frac{\sigma^a}{2} \tag{1.30}$$

where the idea is that the group vector σ^a points in the direction of the unit vector. This particular expression is for the hedgehog gauge and cannot be continuously deformed to the trivial vacuum due to the hairy ball theorem. It follows that the action is bounded by

$$S \geq \pm \int_{S^2} d^2 y_\mu \frac{v}{g^2} B^{\mu,a}(x) n^a \tag{1.31}$$

where we expanded $B^\mu = B^{\mu,a}\sigma^a$. The bounding 2-sphere S^2 originates from Gauss's law and bounds $\mathbb{R}^3$. It follows that this integral is performed at $r \to \infty$, thus it only survives if

$$\lim_{x\to\infty} B^{\mu,a}(x) = \frac{n^\mu n^a}{r^2} \,. \tag{1.32}$$

Therefore the minimum action is

$$S_{\text{cl.}} = \frac{4\pi v}{g^2} \,. \tag{1.33}$$

Note that this action corresponds to a field configuration of a magnetic charge. For this reason, the instanton in this model is called a monopole-instanton and we shall refer to it as a monopole. The monopole field configuration can be solved from the asymptotic behavior of Equations (1.30) and (1.32) alongside $B_\mu = \pm \mathcal{D}_\mu \phi$ from the Bogomolny bound. The field configuration in hedgehog gauge is

$$\phi(x) = vH(vr) n^a \frac{\sigma^a}{2} \,, \qquad A_\mu(x) = \varepsilon_{\mu ab} \frac{F(vr)}{r} n^a \frac{\sigma^b}{2} \,, \tag{1.34}$$

$$H(vr) = \frac{\cosh(vr)}{\sinh(vr)} - \frac{1}{vr} \,, \qquad F(vr) = 1 - \frac{vr}{\sinh vr} \,. \tag{1.35}$$

where $r = |x - z|$ is the distance from the center of the monopole z. Similarly to the $\mathbb{R}^4$

instanton, the action is independent of, z and z makes up 3 bosonic zero modes. There is one additional zero mode associated to U(1) rotations around the Dirac string.[4] Altogether there are 4 bosonic zero modes.

Monopole-instantons can also carry fermionic zero modes. An SU(2) monopole carries a single zero mode for each fundamental or anti fundamental fermion so long as their real mass satisfies $|m_{\mathbb{R}}| < v/2$ and 2 zero modes for each adjoint fermion.

The generalization to SU(N) is fairly straightforward. A non-degenerate $\langle\phi\rangle$ induces breaking

$$\mathrm{SU}(N) \xrightarrow{\langle\phi\rangle\neq 0} \mathrm{U}(1)^{N-1}\,. \tag{1.36}$$

It follows from the homotopy group $\pi_2(\mathrm{SU}(N)/\mathrm{U}(1)^{N-1}) = \mathbb{Z}^{N-1}$ that there are $N-1$ kinds of monopole-instantons. This is because there are $N-1$ different U(1) subgroups of SU(N) in which we can embed the SU(2) monopole solution discussed above. Unlike in the case of the $\mathbb{R}^4$ instanton, these embeddings are distinct because the vacuum is only invariant under $\mathrm{U}(1)^{N-1}$ rather than the full SU(N).

The action of the monopoles depends on the VEV of ϕ. Without loss of generality, consider $\langle\phi\rangle = \mathrm{diag}(v_1, v_2, \ldots, v_N)$ with $v_1 > v_2 > \ldots > v_N$. All other possible $\langle\phi\rangle$ are gauge equivalent. The action of each monopole is then given by

$$S_{\mathrm{cl.},i} = \frac{4\pi}{g^2}\frac{v_i - v_{i+1}}{2}\,, \qquad 1 \leq i \leq N-1\,. \tag{1.37}$$

The fermionic zero mode conditions follow from those for the embeded SU(2) monopole if we consider it in the background of the full adjoint VEV $\langle\phi\rangle$. Decomposing the adjoint VEV

[4]The Dirac string appears as a singularity along the z-axis in the gauge where $\lim_{x\to\infty}\phi(x) = v\sigma^3/2$ asymptotically.

for the n-th monopole, we have

$$\begin{aligned}\langle\phi\rangle =&\frac{v_n - v_{n+1}}{4}\,\mathrm{diag}(0,\ldots,1,-1,\ldots,0)\\ &+\frac{v_n + v_{n+1}}{4}\,\mathrm{diag}(0,\ldots,1,1,\ldots,0)\\ &+\frac{1}{2}\,\mathrm{diag}(v_1,\ldots,v_{n-1},0,0,v_{n+1},\ldots,v_N)\,.\end{aligned} \tag{1.38}$$

The $n, n+1$ components of a fundamental fermion form a doublet of the n-th monopole. Those doublet components have a real mass of $m_{\mathbb{R}} = m_{\mathbb{R}} + (v_n + v_{n+1})/4$. The condition for the fundamental fermion to have a zero mode in the n-th monopole is

$$\begin{aligned}|m_{\mathbb{R}} + \frac{v_n + v_{n+1}}{4}| &< \frac{v_n - v_{n+1}}{4}\,,\\ \rightarrow \frac{v_n}{2} > m_{\mathbb{R}} &> \frac{v_{n+1}}{2}\,.\end{aligned} \tag{1.39}$$

Due to the ordering $v_1 > \ldots > v_N$, this is only true for one of the monopoles. In particular, when $m_{\mathbb{R}} = 0$, only the monopole associated to the smallest positive eigenvalue carries fundamental zero modes. Adjoint fermions decompose as a triplet and $N-2$ doublets of the monopole SU(2). The triplet always has two zero modes, while the doublets have zero modes if

$$|\frac{v_n + v_{n+1}}{4} + \frac{v_i}{2}| < \frac{v_n - v_{n+1}}{4}\,, i \neq n, n+1 \tag{1.40}$$

$$\rightarrow v_n > v_i > v_{n+1} \tag{1.41}$$

which is impossible. Therefore each monopole carries two triplet zero modes for each adjoint fermion.

1.1.3 Instantons on $\mathcal{M} = \mathbb{R}^3 \times \mathbb{S}^1$ (Kaluza-Klein Monopoles)

The difference between $\mathbb{R}^3$ and $\mathbb{R}^3 \times \mathbb{S}^1$ is the ability for fields to wrap the compact dimension. For concreteness, let the compact dimension have coordinate x_4 and size $2\pi R$. Then the fields on $\mathbb{R}^3 \times \mathbb{S}^1$ decompose as

$$\phi(x) = \sum_n e^{\mathrm{i}n\frac{x_4}{R}} \phi_n(x) \,. \tag{1.42}$$

The components ϕ_n are called the KK tower. If we integrate out the compact dimension, the effective theory on $\mathbb{R}^3$ is described by the three dimensional KK tower states each with mass

$$m_n^2 = \frac{n^2}{R^2} \,. \tag{1.43}$$

For small radii, the extra states are very heavy and will not contribute to physics at long distances. In this sense, the theory on $\mathbb{R}^3 \times \mathbb{S}^1$ deforms into the $\mathbb{R}^3$ theory in the limit of a small compact dimension with the identifications

$$\phi_3(x) = \sqrt{2\pi R}\phi_4(x) \,. \tag{1.44}$$

$$g_3^2 = \frac{g_4^2}{2\pi R} \,. \tag{1.45}$$

Of course, this can only be exact if the tower of states is the only difference between the partition functions. While this is certainly true for the trivial vacuum, it may not be true for any instanton sectors of the theory.

As per usual, we need to consider the conditions for finite action to explore the instanton sectors of the theory. The conditions for finite action on the $\mathbb{R}^3$ factor of spacetime do not change with the existence of the $\mathbb{S}^1$. Therefore the same monopole-instantons of $\mathbb{R}^3$ are present on $\mathcal{M} = \mathbb{R}^3 \times \mathbb{S}^1$ as well. There is one additional instanton which comes about by

wrapping the monopole-instantons of $\mathbb{R}^3$ around the circle. This instanton is known as the KK monopole-instanton or the KK monopole for short.

For an SU(2) theory, the KK monopole can be generated by performing the gauge transformation

$$U(x) = \exp\left(-\mathrm{i}\frac{x_4}{2R}\sigma_3\right) \tag{1.46}$$

which is aperiodic over the compact dimension, but the gauge fields remain single-valued. The action of the configuration is given by

$$S_{\text{cl.,KK}} = \frac{4\pi}{g^2}\left(\frac{1}{R} - v\right) \tag{1.47}$$

where v is the asymptotic VEV of the adjoint scalar field.[5]

For general SU(N), the KK monopole is associated to the negative root of the root system or, in our convention, the diag$(-1, \ldots, 1)$ generator of the SU(N). The action of the configuration is

$$S_{\text{cl.,KK}} = \frac{4\pi}{g_3^2}\left(\frac{1}{R} - \frac{v_1 - v_N}{2}\right). \tag{1.48}$$

Note that $\frac{v_1 - v_N}{2} = \sum_{n=1}^{N-1} \frac{v_n - v_{n+1}}{2}$ such that

$$e^{-S_{\text{cl.,KK}}} = \exp\left(\frac{4\pi}{g_3^2 R}\right)\prod_{n=1}^{N-1} e^{S_{\text{cl.,n}}} \tag{1.49}$$

Thus the minimum action in the instanton sector with one KK monopole and each of the

[5]The adjoint scalar field could be the fourth component of the gauge field A_4 in which case the symmetry breaking is called Wilson loop breaking.

$N-1$ $\mathbb{R}^3$ monopoles is

$$S_{\text{cl.}} = \frac{4\pi}{g_3^2 R} = \frac{8\pi^2}{g_4^2} \tag{1.50}$$

which is precisely the action of an $\mathbb{R}^4$ instanton. The above multi-monopole-instanton configuration is known as the caloron and, in the limit of large compact dimension and small distances between the monopole-instantons, becomes the $\mathbb{R}^4$ instanton configuration. This correspondence goes further than the action and asymptotics of the fields; the caloron and the instanton have the same number of zero modes as well. Each monopole has 4 bosonic zero modes, totaling $4N$ bosonic zero modes, the same as for an $\mathbb{R}^4$ instanton. Similarly, each monopole has 2 adjoint fermion zero modes, totaling $2N$ adjoint fermion zero modes, the same as for an $\mathbb{R}^4$ instanton; and since only a single monopoles carries the fundamental zero modes, the number of fundamental zero modes matches between the caloron and $\mathbb{R}^4$ instanton as well.

In later chapters, we will revisit the correspondence between the caloron and $\mathbb{R}^4$ instanton in supersymmetric theories. In QCD- like theories, we find that the dynamics of an $\mathbb{R}^4$ instanton are reproduced from the $\mathbb{R}^3$ monopole-instanton when includes the effects of the KK monopole and takes the limit of large compact dimension. In many cases, one can explicitly derive nonperturbative dynamics in $\mathbb{R}^4$ which can only be calculated directly via this correspondence.

1.2 Exact Results in Supersymmetry

In this section, we review various exact results in SUSY. The fact that these results are exact is miraculous, since, even 30 years later, we are still not close to making similar statements about the non-supersymmetric variants of these theories. The key difference between the

supersymmetric and non-supersymmetric theories is the restriction of holomorphy which supersymmetric theories must obey.

To be more precise, any 4D $\mathcal{N} = 1$ SUSY Lagrangian can be written as a sum of three terms

$$\mathcal{L}_{\text{SUSY}} = \int d^2\theta d^2\bar{\theta} K + \int d^2\theta W + \int d^2\bar{\theta} W^\dagger \tag{1.51}$$

where K is the Kähler potential and W is the superpotential. While the Kähler potential is a function of all the fields in the theory, the superpotential is only a function of the chiral superfields Φ and not the anti-chiral superfields $\Phi^\dagger$. In other words, W is a holomorphic function of Φ. This significantly reduces the terms which are allowed in W and implies certain perturbative non-renormalization theorems for the couplings in W [93]. Terms in the superpotential can only be generated upon integrating out degrees of freedom or appear as a result of instanton corrections. Moreover, the superspace dependence of chiral superfields

$$\Phi(\theta) = \phi + \theta\psi + \theta^2 F \tag{1.52}$$

means that the superspace integral over W introduce terms in the Lagrangian with at most two left-handed Weyl fermions.[6] Therefore non-zero correlation functions between operators containing two left-handed Weyl fermions imply the existence of a superpotential. This presents a rather easy analysis of the role of instantons in SUSY QFTs. If the 't Hooft effective operator can be closed to a two-point fermion correlation function, it generates a superpotential where perturbative corrections are controlled and the instanton calculation remains valid at all strong coupling. Otherwise, the 't Hooft effective operator appears in the Kähler potential, and we have no control over the calculation.

Let us explore some relevant examples of instanton induced dynamics of various SUSY

[6]The equivalent term for the conjugate, right-handed Weyl fermions comes from the integral over $W^\dagger$.

theories. We begin by describing supersymmetric quantum chromodynamics (SQCD). The symmetries of the theory are given in Equation (1.53). The theory has an SU(N) gauge group with F chiral superfields Q in the fundamental representation and F chiral superfields $\bar{Q}$ in the anti-fundamental representation. The fermionic superpartner of the gauge bosons is called the gaugion, the fermionic components of the chiral superfields are called the quarks, and the scalar components of the chiral superfields are called the squarks. We will refer to this theory as SU(N) SQCD with F flavors. At the classical level, the theory has no superpotential.

	SU(N)	$\mathrm{U}(1)_\mathrm{R}$	$\mathrm{U}(1)_\mathrm{B}$	$\mathrm{U}(1)_\mathrm{A}$	$\mathrm{SU}(F)_\mathrm{L}$	$\mathrm{SU}(F)_\mathrm{R}$
Q	$\square$	0	1	1	$\square$	$\mathbf{1}$
$\bar{Q}$	$\overline{\square}$	0	-1	1	$\mathbf{1}$	$\overline{\square}$

(1.53)

The squarks of the theory may acquire VEVs which would break the gauge group and make some subset of the fields heavy. SUSY ensures a positive-definite vacuum energy, and SUSY is non broken if and only if the vacuum energy is zero. The set of VEVs which are compatible with SUSY is called the moduli space. The classical moduli space is derived from the so-called D-flatness conditions which arise from requiring that the auxillary D fields of the gauge multiplet vanish. In the case of SQCD, the D-flatness conditions are most easily stated for the gauge invariant composites. If $F < N$, the only gauge invariant composite is the meson $M_{\bar{i}j} = \bar{Q}^n_{\bar{i}} Q_{nj}$. The D-flatness condition is

$$\langle M_{\bar{i}j} \rangle = q_i^2 \delta_{\bar{i}j} \,. \tag{1.54}$$

For $F \geq N$, the gauge invariant composites are the mesons (as previously given) and the

baryons and anti-baryons

$$B^{i_1,\ldots,i_N} = \varepsilon^{n_1,\ldots,n_N} Q_{n_1,i_1} \ldots Q_{n_N,i_N} \,, \tag{1.55}$$

$$\bar{B}^{\bar{i}_1,\ldots,\bar{i}_N} = \varepsilon_{n_1,\ldots,n_N} \bar{Q}^{n_1}_{\bar{i}_1} \ldots \bar{Q}^{n_N}_{\bar{i}_N} \,. \tag{1.56}$$

The moduli space is described by the VEVs

$$\langle M_{\bar{i}j} \rangle = \bar{q}_i q_i \delta_{\bar{i}j} \qquad i \leq N \tag{1.57}$$

$$\langle M_{\bar{i}j} \rangle = 0 \delta_{\bar{i}j} \qquad i \geq N \tag{1.58}$$

$$\langle B^{i_1,\ldots,i_N} \rangle = q_1 \ldots q_N \,, \tag{1.59}$$

$$\langle \bar{B}^{\bar{i}_1,\ldots,\bar{i}_N} \rangle = \bar{q}_1 \ldots \bar{q}_N \,. \tag{1.60}$$

The maximal rank of M is N, and the composites obey the classical relation

$$B^{i_1,\ldots,i_N} \bar{B}^{\bar{i}_1,\ldots,\bar{i}_N} = M_{\bar{i}_1[i_1} \ldots M_{\bar{i}_N i_N]} \tag{1.61}$$

where the [ ] on the meson indices indicate antisymmetrization over the $\mathrm{SU}(F)_L$ indices. By symmetry, the $\mathrm{SU}(F)_R$ indices are also antisymmetrized.

Let us consider the theory with $F = N - 1$ flavors. In this case, the $\mathrm{SU}(N)$ instanton carries $2N + 2F$ fermion zero modes from the gaugino and quarks respectively. It would appear that the instanton has too many zero modes to contribute to the superpotential. However, there are Yukawa-like SUSY gauge couplings between the gaugino, squark, and quark which can be used to close the gaugino and quark zero modes in pairs in exchange for a squark. Pairing all of the quark zero mode legs, there are two gaugino legs leftover, and a non-zero correlation function will generate a superpotential. In principle, one could calculate the $2(N-1)$ squark, 2 gaugino correlation function described above. However, it is simpler to calculate the correlation function at a generic point in the moduli space

where all the squarks acquire VEVs. Then the squark legs end at VEV insertions and one simply calculates the gaugino-gaugino correlation function. The value can be calculated and interpetted as a dynamically generated superpotential

$$W_{\rm ADS}^{(F=N-1)} = \frac{\Lambda^{2N+1}}{\det M} \tag{1.62}$$

where $\Lambda^b = \exp(-\frac{8\pi^2}{g^2} + i\theta)$.

From here one can deform the theory by giving quarks large masses. Upon integrating out the quarks, one finds for general $F < N$

$$W_{\rm ADS}^{(N,F)} = (N-F)\left(\frac{\Lambda^{3N-F}}{\det M}\right)^{1/(N-F)} . \tag{1.63}$$

For $F \geq N$, the instanton carries too many zero modes, and the $\mathrm{U}(1)_R$ symmetry prohibits a superpotential term. When $F > N$, the theory has a dual description in terms of an $\mathrm{SU}(F-N)$ gauge theory. We will not go into detail for these theories. Let us, instead, focus on the case $F = N$. In this scenario, the gaugino and the quark have precisely the same number of zero modes. Thus when we close pairs of gaugino and quark zero modes with the squark, we arrive at a $2N$-squark correlation function. A precise analysis reveals that

$$\det M - \bar{B}B = \Lambda^{2N} . \tag{1.64}$$

However classically, we had that $\det M = \bar{B}B$, so how is this possible? The answer is that the quantum dynamics of the theory, i.e. the instantons in this scenario, deform the classical relations between the moduli. The space described by (**??**) is called the quantum moduli space. At first sight, this may seem insignificant, but in this scenario, it removes the point $\det M = \bar{B} = B = 0$ from the moduli space. Thus there is no SUSY vacuum where both $\mathrm{SU}(F)_{\rm L} \times \mathrm{SU}(F)_{\rm R}$ and $\mathrm{U}(1)_{\rm B}$ remain unbroken.

This completes our short overview of SQCD on $\mathbb{R}^4$. We will now discuss the dynamics of SQCD on $\mathbb{R}^3$.

1.3 Review of 3D $\mathcal{N} = 2$ SUSY gauge theories

This section is heavily based on work previously published in collaboration with Yuri Shirman [99].

In this section, we review basic properties of 3D SUSY QCD with four supercharges ($\mathcal{N} = 2$) (see, for example, [3, 39] for a more detailed introduction). We restrict our attention to SU(N) theories with $F < N$ massless flavors in the fundamental representation. The 3D action can be easily obtained by a dimensional reduction of the corresponding 4D theory:

$$S = \int d^3x \left[\int d^4\theta K(Q, \bar{Q}, V) + \int d^2\theta W(Q, \bar{Q}) + \frac{1}{g^2} \int d^2\theta \, \mathrm{Tr}(W_\alpha W^\alpha) + \mathrm{h.c.} \right] . \quad (1.65)$$

We use supersymmetric normalization with an explicit factor $1/g^2$ in front of the gauge kinetic term. In this normalization, the vector multiplet has the same mass dimension as in 4D, since the gauge coupling g^2 has mass dimension one in 3D. On the other hand, the chiral multiplet has mass dimension 1/2. Expanding in component fields, the vector multiplet is given by

$$V = -i\theta\bar{\theta}\sigma - \theta\gamma^i\bar{\theta}A_i + i\bar{\theta}^2\theta\lambda - i\theta^2\bar{\theta}\lambda^\dagger + \frac{1}{2}\theta^2\bar{\theta}^2 D \,, \quad (1.66)$$

where $\gamma^i = \{i\sigma^2, \sigma^1, \sigma^3\}$ and σ is the real scalar field in the adjoint representation, and the chiral multiplet is given by

$$Q = q + \psi\theta + \theta^2 F \,. \quad (1.67)$$

The classical moduli space of the pure $\mathcal{N} = 2$ SYM SU(N)) theory is described by the Coulomb branch parameterized by VEVs of the adjoint, $\langle\sigma\rangle = \text{diag}(v_1, \ldots, v_N)$, subject to the tracelessness condition, $\sum_i v_i = 0$. At a generic point on the Coulomb branch, the unbroken gauge symmetry is $\text{U}(1)^{N-1}$. The theory on the Coulomb branch retains the Weyl symmetry of SU(N) which interchanges the eigenvalues of σ. Without loss of generality we will restrict our attention to a positive Weyl chamber[7] defined by $v_i \geq v_{i+1}$. Quantum effects further divide the Weyl chamber into sub-wedges defined by the number of positive eigenvalues. We define the k^{th} sub-wedge by requiring there to be exactly k positive eigenvalues ($v_k > 0 > v_{k+1}$). The sub-wedge boundaries lie at the points where one of the eigenvalues of σ vanishes. We will call the boundary between the k^{th} and $(k+1)^{st}$ sub-wedges the k^{th} boundary. When $l = dim(ker(\langle\sigma\rangle)) > 1$, i.e. when several eigenvaues of σ vanish simultaneously, $l-1$ sub-wedges become degenerate, and the symmetry breaking pattern is $\text{SU}(N) \longrightarrow \text{U}(l) \times \text{U}(1)^{N-l-1}$.

As first realized by Polyakov [85], abelian gauge theories without charged matter fields have a dual description in terms of compact scalar fields. The compact scalar fields, γ, obey the relation,

$$\partial_i \gamma = \frac{\pi}{g^2} \epsilon_{ijk} F^{jk} \,, \tag{1.68}$$

where γ has a shift symmetry from its role as a Lagrange multiplier enforcing the Bianchi identity. In supersymmetric theories, this duality provides abelian vector superfields with a dual description in terms of chiral superfields, Φ, with scalar components, $\phi = 4\pi\sigma/g^2 + i\gamma$. The compactness of γ ensures that the low energy theory depends on chiral superfields $Y = \exp(\Phi)$ charged under the global symmetry $\text{U}(1)_J$ corresponding to the shift symmetry of γ.

[7]The Weyl chamber is a wedge subspace of $\mathbb{R}^r$ ($r = rank(G)$) given by $\mathbb{R}^r/\mathcal{W}$, where $\mathcal{W}$ is the Weyl group [3]. The equivalence class from modding out the Weyl symmetry can be represented by a choice of r positive, simple roots, $\{\alpha_i\}$, such that $\alpha_i \cdot \langle\sigma\rangle \geq 0$ or equivalently $v_i \geq v_{i+1}$. Sometimes this is referred to as the positive Weyl chamber [107].

The duality can be easily generalized to the Coulomb branch of non-abelian gauge theories. In the case of an SU(N) theory, the group is broken to a product of $N-1$ U(1)'s and each is dualized to a chiral superfield, obtaining a description in terms of $N-1$ chiral superfields Y_i defined as

$$Y_i = \exp\left[2\,\mathrm{Tr}(\phi T^i)\right] \,. \tag{1.69}$$

The $(T^i)_{ab} = \frac{1}{2}(\delta_{a,i} - \delta_{a,i+1})\delta_{ab}$ are the generators of the corresponding non-orthogonal U(1) subgroups of SU(N).[8] After the duality transformation, the theory has no gauge symmetry. Instead, the moduli Y_i are charged under topological global symmetries $\mathrm{U}(1)_{J_i}$ associated with each abelian factor in the original gauge theory. The topological symmetry is broken by non-perturbative dynamics and is not a symmetry of the low energy physics.

On the Coulomb branch of the 3D theory, there exist monopole solutions charged under the corresponding $\mathrm{U}(1)_{J_i}$ factors. All of the monopole and multi-monopole solutions on the Coulomb branch can be constructed out of $N-1$ fundamental monopoles. In the positive Weyl chamber, the fundamental monopoles are the monopoles charged under one of the $\mathrm{U}(1)_{J_i}$'s corresponding to the abelian factor generated by T^i. The action of the i^{th} fundamental monopole is given by

$$S_{i,cl} = \frac{4\pi(v_i - v_{i+1})}{g^2} \,. \tag{1.70}$$

Comparing the classical monopole action with the VEVs of the Coulomb branch moduli Y_i, we note that the monopole weights are given by[9] $1/Y_i$.

If we add F massless flavors of chiral superfields in the fundamental representation of SU(N),

[8] We chose to describe the low energy $\mathrm{U}(1)^{N-1}$ theory in terms of linearly independent but non-orthogonal U(1) factors so that Y_i are easily identified with fundamental monopoles of the positive Weyl chamber. One could also give a basis independent description of the Coulomb branch moduli in terms of the positive simple roots, $\{\alpha_i\}$, where $Y_i = \exp(\vec{\alpha}_i \cdot \phi)$.

[9] Thus we will refer to Y_i's as monopole moduli.

the theory possesses mixed Higgs-Coulomb branches of the moduli space (and a pure Higgs branch when $F \geq N-1$) in addition to the Coulomb branch. The mixed branch of the moduli space is not accessible from a generic point on the Coulomb branch – the flat directions parameterized by squark VEVs are lifted by the D-term potential. Squark VEVs are only classically allowed when one or more v_i's vanish.

First consider the case when only one adjoint VEV, say v_k, vanishes. The unbroken gauge symmetry is $\mathrm{U}(1)^{N-1}$. Of the $2NF$ chiral superfields, $2(N-1)F$ of them obtain large real masses, and the low energy effective theory is left with $2F$ massless chiral superfields. These fields are charged under one linear combination of the unbroken U(1)'s, and their VEVs must obey the D-flatness condition $\sum_f \left(|q_f^k|^2 - |\overline{q}_f^k|^2\right) = 0$. By flavor symmetry transformations, the squark VEVs can be rotated into a single flavor. Alternatively, we could parameterize the vacua by the VEV of the meson superfield, M, which is classically defined as $M = Q\bar{Q}$ and has maximal rank one in this region of the moduli space. Thus the space of physically inequivalent vacua on this branch is $N-1$ dimensional and can be parameterized by $N-2$ independent combinations of monopole moduli Y_i and a single eigenvalue of M.

Now consider the case when several adjoint VEVs, say $l \leq F$, vanish simultaneously. As discussed above, the unbroken gauge group in this region of the Coulomb branch is $U(l) \times \mathrm{U}(1)^{N-l-1}$. The low energy physics contains $2lF$ massless chiral multiplets, and D-flatness conditions allow squark VEVS which further break the gauge group to $\mathrm{U}(1)^{N-l-1}$. The meson matrix has rank l and once again coordinates along the Higgs direction of this mixed branch can be parameterized by the l eigenvalues of M. As before, the space of physically inequivalent vacua is $N-1$ dimensional.

It may also be useful to approach $\mathrm{U}(1)^{N-l-1}$ low energy theory from a different direction on the classical moduli space. If we start at the origin of the classical moduli space, the entire F^2-dimensional Higgs branch is accessible, and one can turn on $l \leq F$ meson eigenvalues breaking $\mathrm{SU}(N)$ to $\mathrm{SU}(N-l)$. At this point, a $N-l-1$ dimensional subspace of the Coulomb

branch is accessible, and the gauge symmetry is further broken to $\mathrm{U}(1)^{N-l-1}$. The space of physically inequivalent vacua remains $N-1$ dimensional. Of course, the superpotential of low energy theory in the $q \gg v$ limit should be the same as the superpotential in the $q \ll v$ limit. Considering the theory in different VEV limits can be used as a tool to both to derive and verify our results.

The introduction of matter fields into the theory has one more important consequence: the $N-1$ fundamental monopole moduli are no longer globally defined throughout the Weyl chamber because the quantum numbers of the moduli change as one crosses the boundary between different sub-wedges of the Weyl chamber. To understand this change of quantum numbers, we need to recall that quantum numbers of the monopole moduli depend on fermionic zero modes that exist in the background of the corresponding fundamental monopoles. Each fundamental monopole has two gaugino zero modes; however, only one fundamental monopole has matter fermion zero modes in any given sub-wedge of the Weyl chamber. For instance, in the k^{th} sub-wedge (denoted by a superscript), $Y_k^{(k)}$ has one zero mode for each massless fundamental (or anti-fundamental) fermion, while $Y_i^{(k)}$ $(i \neq k)$ has no matter fermion zero modes. The quantum numbers of mesons and fundamental monopoles in the k^{th} sub-wedge are:

	$\mathrm{U}(1)_\mathrm{R}$	$\mathrm{U}(1)_\mathrm{B}$	$\mathrm{U}(1)_\mathrm{A}$	$\mathrm{SU}(F)_\mathrm{L}$	$\mathrm{SU}(F)_\mathrm{R}$
Q	0	1	1	$\square$	$\mathbf{1}$
$\bar{Q}$	0	-1	1	$\mathbf{1}$	$\overline{\square}$
M	0	0	2	$\square$	$\overline{\square}$
$Y_k^{(k)}$	$2(F-1)$	0	$-2F$	$\mathbf{1}$	$\mathbf{1}$
$Y_{i\neq k}^{(k)}$	-2	0	0	$\mathbf{1}$	$\mathbf{1}$

(1.71)

We can see that the quantum numbers of $Y_k^{(k)}$ and $Y_{k+1}^{(k)}$ monopoles in the k^{th} sub-wedge are different from $Y_k^{(k+1)}$ and $Y_{k+1}^{(k+1)}$ in the $(k+1)^{st}$ sub-wedge despite the fact that both pairs

of coordinates correspond to the same semi-classical solutions in each sub-wedge. One can define a two-monopole modulus which is continuous across the k^{th} sub-wedge boundary,

$$Y_{k,2}^{(k)} = Y_k^{(k)} Y_{k+1}^{(k)} = Y_k^{(k+1)} Y_{k+1}^{(k+1)} = Y_{k,2}^{(k+1)} \,. \tag{1.72}$$

The introduction of the two-monopole modulus smooths out one combination of the two discontinous coordinates at each sub-wedge boundary. Specifically, the $Y_{k,2}^{(k)}$ modulus is still discontinuous at the $(k-1)^{st}$ sub-wedge boundary, but a different two-monopole modulus $Y_{k-1,2}^{(k)}$ is continuous at this boundary. It is possible to define a separate two-monopole modulus for each sub-wedge boundary that is continuous across that specific sub-wedge boundary.

One may hope to patch together the coordinate charts for each sub-wedge in this manner, but there are two technical issues which prevent such a construction. The first issue is the existence of a second modulus that is discontinuous at both sub-wedge boundaries. In other words, so far we have been able to define only one transition function for two discontinuous coordinates. A single continuous two-monopole modulus does not account for the two discontinuous monopole moduli.[10] The other issue is that the two adjacent sub-wedges of the classical Coulomb branch do not overlap, so the transition functions can not be properly defined. As we will see, the quantum deformations of the classical moduli space solve these issues by smoothing out the Higgs-Coulomb interface at each of the sub-wedge boundaries. The extension of disjoint sub-wedges onto the intermediate Higgs-Coulomb branch allows these extended sub-wedges to overlap, while implementation of the quantum deformation as a Lagrange multiplier term in the superpotential provides the second transition function.

[10] One could define the global modulus $Y = \prod_i Y_i$ which is continuous across all sub-wedge boundaries as has been done in previous studies [3, 4]. However, working only in terms of globally defined moduli does not allow one to investigate dynamics in the interior of the moduli space.

1.4 Magnetic monopoles

In this seciton, we briefly review properties of theories with magnetic monopoles. We begin with the Dirac construction for electromagnetism [41], then explain how it can be UV completed as the 't Hooft-Polyakov monopole [101, 84]. We then turn to explaining the difficulty of calculating in theories with both electric and magnetic charges. This sets up for the discussion in Chapter 4 where we develop a new formalism for studying these interactions.

Maxwell's equations have an apparent asymmetry between the role of the electric and magnetic field with is rather puzzling. A simple question which encapsulates this confusion is "Why aren't there magnetic charges?" One could presume that there is an issue with formulating a theory with both electric and magnetic charges. Here, and in Chapter 4, we will illustrate that this is not an issue.

A magnetic monopole is characterized by a magnetic field

$$\vec{B}(r) = g\frac{\hat{r}}{r^2} \tag{1.73}$$

where g is the magnetic charge of the monopole. The issue is that this violates $\nabla \cdot \vec{B} = 0$, and therefore $\vec{B} = \nabla \times \vec{A}$. The vector potential $\vec{A}$ is a necessary ingredient for quantization, so the magnetic monopole cannot be so simple. Dirac showed that there is a vector potential which reproduces (1.73)

$$\vec{A}_S = -\frac{g}{r}\frac{1+\cos\theta}{\sin\theta}\hat{\phi} \tag{1.74}$$

which has a singularity along the $+\hat{z}$ axis. The singularity induces an infinitesimal flux of magnetic field, called the Dirac string, which cancels the flux of magnetic field from the charge. The presence of the Dirac string is rather unsettling; however, the Dirac string's

location changes under gauge transformations

$$\vec{A}_N = \vec{A}_S - \frac{i}{e} e^{-2ieg\phi} \nabla e^{2ieg\phi} = \vec{A}_S + \frac{2g}{r \sin\theta} \hat{\phi} = \frac{g}{r} \frac{1 - \cos\theta}{\sin\theta} \hat{\phi} \,. \tag{1.75}$$

Therefore the Dirac string is not physical. To discuss physics in the volume with $z > 0$, we simply use $\vec{A}_N$, and for $z < 0$, we use $\vec{A}_S$. This construction may appear ad hoc, but it is natural from the point of view of mathematics. In mathematics, $\vec{A}$ is called a section of a principle bundle, and $\vec{A}_N$ and $\vec{A}_S$ are its values on local coordinate charts of the manifold. At the overlap of these two coordinate charts which we can take to be the equator of the monopole, these two coordinatizations of the bundle must agree up to a gauge transformation. The gauge transformation was already given as

$$U = \exp(2ieg\phi) \tag{1.76}$$

which when made periodic on the equator, gives the condition

$$2eg = n \in \mathbb{Z} \,. \tag{1.77}$$

The condition (1.77) is often called the Dirac quantization conditon and can be arrived at in a variety of different ways. From the above construction,[11] it is apparent that n somehow measures how 'wound' the gauge field is around the location of the monopole. Also noteworthy is the relationship between the electric and magnetic charges

$$g = \frac{n}{2e} \tag{1.78}$$

which ensures that if the electric charges are weakly-coupling ($e \ll 1$), the magnetic charges are strongly-coupled ($g \gg 1$). And any process which depends on the electromagnetic coupling will be a function of an order one coupling $eg = n/2$ without a reliable perturbative

[11] This construction is often called the Wu-Yang construction as it first appeared in [115, 116].

expansion.

From the above discussion, one should be convinced that there is a sensible way to combine electromagnetism, non-relativistic quantum mechanics, and magnetic monopoles. The question for relativistic electromagnetism turns out to be more difficult. Attempts to construct a fully relativistic Lagrangian make use of two vector potentials: the usual vector potential A_μ for electromagnetism and a 'magnetic' vector potential $\tilde{A}_\mu$. The two potentials are required to obey a constraint

$$e\tilde{A}_\mu - gA_\mu = 0 \tag{1.79}$$

such that only one remains dynamical. Dirac showed that a Lorentz invariant Lagrangian with both electric and magnetic charges must be non-local [40]. Zwanziger constructed a Lagrangian which is not Lorentz invariant due to the appearance of the Dirac string in the Lagrangian.[118] Surprisingly, the observables in Zwanziger's formalism are independent of the location of the Dirac string, and although the Lagrangians appear problematic, there are no inherent issues with the observables of the theories. In other words, although unsavory, they are fully relativistic, quantum mechanical theories of electromagnetism with both electric and magnetic charges. Additionally, these theories still have a strong-coupling problem due to the Dirac quantization condition (1.77). A natural question to ask is whether a theory with electric and magnetic charges can arise as the low-energy limit of a weakly-coupled QFT. The answer to this question is yes, as answered by 't Hooft and Polyakov where the magnetic monopole arises as a soliton of an SU(2) gauge theory broken to U(1).

As discussed perviously in Section 1.1, an SU(2) gauge theory which is spontaneously broken to U(1) admits an instanton field configuration on $\mathbb{R}^3$ which appears to carry magnetic charge. On $\mathbb{R}^4$, such a field configuration still exists, but it is attached to a line in $\mathbb{R}^4$. We can interpret this line as the world-line of the monopole. The derived monopole has

magnetic charge $Q = \frac{4\pi}{g_{\rm UV}}$ and mass $M = \frac{4\pi v}{g_{\rm UV}}$. Although the UV completion which arises from embedding electromagnetism in a non-abelian gauge group is compelling, it offers little in the realm of calculating the dynamics of the electric and magnetic charges of the low-energy theory. In Chapter 4, we develop a formalism inspired by the amplitudes program which can tackle the problem of electric-magnetic scattering.

1.5 Dark Matter and Cold Thermal Freeze Out

In this seciton, we briefly review cold thermal freeze out, following [70]. We consider it as a mechanism to explain the relic abundance of dark matter observed today and discuss the tension between the predictions from thermal freeze out and direct detection experiments. We provide a model which eases the tension in Chapter 5.

Dark matter is an unexplained phenomena where the gravitational force appears to behave as if there were more matter than is observed. It is estimated that dark matter makes up roughly 20% of the energy in the universe or roughly 4 times the matter energy of the universe. If this phenomena is explained by a particle which interacts with the Standard Model, then it must have been in thermal equilibrium with the rest of the known particles at some point in the early universe. Thermal freeze out details how particle species in the early universe decoupled from the rest of the known universe and could explain the origins of the observed dark matter abundance.

The thermal evolution of a species' number density n obeys the Bolztmann equation in an expanding universe

$$\frac{\mathrm{d}n}{\mathrm{d}t} + 3Hn = -\langle\sigma v\rangle(n^2 - n^{\mathrm{eq}\,2}) \tag{1.80}$$

where $H = (8\pi\rho/3M_{\rm Pl})^{1/2}$ is the expansion rate of the universe, $n^{\rm eq}$ is the number density at

thermal equilibrium, and $\langle \sigma v \rangle$ is the thermally averaged annihilation cross section times the relative velocity. The evolution of the species n is a competition of two terms, the expansion of the universe and the interaction rate of the particles $\Gamma \sim \langle \sigma v \rangle n$. The expanding universe wants the particle species to cool according to the expansion rate, while the interaction rate wants the particle species to remain in thermal equilibrium with the rest of the matter. When the universe is hot and dense, the interaction rate dominates the behavior of the equation, and the species remains in thermal equilibrium. However, as the universe cools, the interaction rate will drop below some threshold, and H will dominate. At this temperature, the particle species decouples from the thermal bath, leaving a relic in the universe today. Roughly speaking, this relic appears when $H \sim \langle \sigma v \rangle n$, i.e. the relic density at the time of freeze out is

$$n \sim \frac{H}{\langle \sigma v \rangle} \,, \tag{1.81}$$

which is a relationship between the freeze out temperature, the coupling strengths of the species, and the mass of the species. From the freeze out temperature and mass, one can determine how much energy there would be in the thermal relic today. Thus constructing a relationship between the observed relic abundance of a species, the mass of the species, and the couplings of the species. The question is therefore what predictions can we make about the qualities of the dark matter (mass and couplings) given that the relic abundance was produced from thermal freeze out. As will be explored later, there is a tension between the observed dark matter density and null observations at direct detection experiments.

Instead of using the heuristic given by (1.81), we should solve (1.80) systematically to make a concrete prediction for the relic density of the species. We begin by massaging (1.80) by defining new parameters $x = m/T$ and $Y = n/s$ where m is the mass of the species and s is

the entropy of the thermal bath. Then (1.80) becomes

$$\frac{\mathrm{d}Y}{\mathrm{d}x} = -\frac{\langle\sigma v\rangle}{Hx} s(Y^2 - Y^{\mathrm{eq}\,2}) \tag{1.82}$$

where $Y^{\mathrm{eq}} = n^{\mathrm{eq}}/s$. For a cold (non-relativistic) species, the equilibrium density is

$$n^{\mathrm{eq}} = g\left(\frac{mT}{2\pi}\right)^{3/2} e^{-m/T} \tag{1.83}$$

where m is the mass of the particle species in question and g is the number of degrees of freedom of the species (i.e. number of spin states or flavors). For non-relativistic interactions, $\langle\sigma v\rangle$ can be expanded

$$\langle\sigma v\rangle = a + b\langle v^2\rangle + \mathcal{O}(\langle v^4\rangle) \approx a + 6b/x\,. \tag{1.84}$$

The evolution in (1.80) is dominated by $a \neq 0$ or b for $a = 0$. If $a = b = 0$, one must expand $\langle\sigma v\rangle$ further. Using this expansion in (1.82), the equation can be integrated to find the relic energy density

$$\Omega h^2 \approx \frac{1.04 \times 10^9}{M_{\mathrm{Pl.}}} \frac{x_F}{\sqrt{g_*}} \frac{1}{a + 3b/x_F}\,, \tag{1.85}$$

where g_* is the number of relativistic degrees of freedom at the time of freeze out and $x_F = m/T_F$ is the dimensionless freeze out temperature. The freeze out temperature is determined from

$$x_F = \ln(c(c+2)\sqrt{\frac{45}{8}}\frac{g}{2\pi^3}\frac{mM_{\mathrm{Pl}}(a + 6b/x_F)}{g_*^{1/2} x_F^{1/2}}) \tag{1.86}$$

which can be solved iteratively and c is a value determined numerically. We take $c = 1/2$, but the exact value of c does not change the value of x_F dramatically.

From the above relations, one can deduce what the energy density of dark matter would be from $\langle \sigma v \rangle$ and the mass of the particle. Direct detection experiments like XENON1T look for interactions between matter and $\langle \sigma v \rangle$. These experiments have yet to see any signals for dark matter interactions. From the null observations, one can exclude certain models which would produce the entire dark matter abundance. This was done systematically in 2008 [11]. At the time, direct detection experiments were able to rule out dark matter masses up to ~ 200 GeV for fermionic dark matter interacting via a scalar mediator with Standard Model matter and dark matter masses up to ~ 1 TeV for fermionic dark matter interacting via a vector mediator with Standard Model matter. Modern experiments push these limits higher with more models rules out. In Chapter 5, we explore how much higher these limits are and show how these limits can be evaded if the universe has a non-standard cosmological history with an early QCD phase transition.

Chapter 2

Kaluza-Klein Monopoles and Their Zero Modes

This chapter is heavily based on work previously published in collaboration with Csaba Csàki, Yuri Shirman, and John Terning [35].

2.1 Introduction

As discussed in Sections 1.1 and 1.2, the essential property of monopoles that largely determines the structure of the induced superpotential terms is the number of fermionic zero modes in a given monopole background. The Callias index theorem [20, 81, 87] specifies the number of fermionic zero modes in different gauge group representations for a given monopole background. However, for the compactified theory, there is a twisted embedding of the monopole solution called the KK monopole. This KK monopole is obtained by performing an anti-periodic gauge transformation along the compactified circle. The effects of the KK monopole are crucial for obtaining the correct interpolation between the 4D and 3D

theories. Thus it is essential to understand how the number of fermionic zero modes of the KK monopole can change. The goal of this chapter is to give a simple intuitive accounting for fermion zero modes in a KK monopole background. KK monopoles were first introduced by Lee and Yi [76], though their contribution to the superpotential was anticipated by Seiberg and Witten [95]. Using the Nahm construction, KK monopole configurations were found explicitly in [75, 74, 37]. Aharony et. al [3] already contains a brief comment on the number of fermionic zero modes. The number of fermionic zero modes was also inferred in [81, 87] using the fact that all the independent monopoles together make up a 4D instanton in the large radius limit [75]. The analogs of the KK monopoles for finite temperature field theories were introduced in [72], while an analysis of the zero modes of the finite temperature version was presented in [17]. Here we give a detailed explanation of why a fermion in the fundamental representation has a zero mode in a KK monopole background only when the real mass m satisfies $|m| > \frac{v}{2}$, where v is the asymptotic adjoint scalar vacuum expectation value (VEV) of the monopole background. This is the exact opposite of the condition for the existence of a zero mode in the ordinary monopole background: $|m| < \frac{v}{2}$. On the other hand the condition for the existence of an adjoint fermion (gaugino) zero mode is the same for both the ordinary monopole and the KK monopole. The root cause for the unusual behavior of the fundamental zero modes is the fact that the fundamental carries a single gauge index, and hence the usual zero mode would become anti-periodic under the large gauge transformation that connects the KK monopole to the ordinary monopole. The true KK zero mode originates in a configuration that is anti-periodic around the circle before the gauge transformation is performed. Since the adjoint carries two indices, its zero mode is periodic in either case, so there is no difference in the conditions for gaugino zero modes. Our results provide an intuitive explanation of KK monopole decoupling in the limit of a large real mass: for a sufficiently large real mass the KK monopole *acquires* additional fundamental fermion zero modes, and as a result the KK monopole cannot correspond to a superpotential term.

The chapter is organized as follows. First we briefly review the construction of the KK

monopole solution, and then remind the reader of the form of the fermionic zero modes in ordinary monopole backgrounds. Rather than relying on index theorems [20, 81, 87] we analyze the properties of the solutions of the Dirac equation in the monopole background à la Jackiw and Rebbi [66], while allowing for a real mass term. Next we present our main result: the condition for the existence of fermionic zero modes in the fundamental representation in the KK monopole background. We apply our result to explain the decoupling of the effects of the KK monopole in $\mathcal{N} = 1$ SUSY (4 supercharges) theories on $\mathbb{R}^3 \times \mathbb{S}^1$. Finally we show a neat example based on the SU(2) $\times$ SU(2) theory with a bifundamental where the interplay between the fundamental fermion zero modes of the KK monopole and the ordinary monopoles exactly reproduces the answers expected from the 4D analysis of [63].

2.2 BPS vs. KK Monopoles

The fundamental BPS monopole is nothing but the usual 't Hooft Polyakov monopole of the Georgi-Glashow model. For simplicity we will only consider the SU(2) case, but all results can be readily generalized to SU(N) by the embedding of SU(2) subgroups. Since we have the application to SUSY gauge theories in mind we will use the holomorphic normalization of the gauge fields (where the gauge coupling g appears only in the gauge kinetic terms). The explicit expression of the monopole background is

$$A_i^a(\vec{x}) = \epsilon_{ija}\,\hat{x}^j \frac{f(r)}{r}\,,\ \phi^a(\vec{x}) = v\,\hat{x}^a h(r) \tag{2.1}$$

where v is the asymptotic adjoint scalar VEV, $r = |\vec{x}|$, and (since there is no scalar potential) the functions h, f are $f(r) = \left(1 - \frac{vr}{\sinh(vr)}\right)$, $h(r) = \left(\coth(vr)\frac{1}{vr}\right)$, where both $f, h \to 1$ for $r \to \infty$. In the compactified Euclidean theory the scalar ϕ can be thought of as the fourth component of the gauge field $A_4 = \phi$. In the following we use σ^i to denote the Pauli matrices.

The construction of the KK monopole on the interval $0 \leq x_4 \leq 2\pi R$ requires three steps [75]. First, one replaces the asymptotic adjoint VEV v with $v' = 1/R - v$. Then one performs a large gauge transformation $\sim e^{-i\frac{x_4}{2R}\sigma^3}$, which is anti-periodic along the compact x_4 dimension. This transformation shifts the VEV by $1/R$. Finally, one can restore the original VEV v by a Weyl transform that takes $v \to -v$. The result of the combined transformations takes the form [75]

$$A_\mu = U^\dagger A_\mu(\vec{x}, v')U + iU^\dagger \partial_\mu U \,, \tag{2.2}$$

where A_μ is the gauge field (with $A_4 = \phi$) of the BPS monopole and the gauge transformation U is given by [75]

$$U = U_h \sigma^2 e^{-i\frac{x_4\sigma^3}{2R}} U_h^\dagger \,, \tag{2.3}$$

where

$$U_h = \frac{\sigma^3 \cosh\frac{v'r}{2} + \vec{\sigma}\cdot\vec{x}\sinh\frac{v'r}{2}}{\sqrt{\cosh v'r + \hat{x}_3 \sinh v'r}} \,. \tag{2.4}$$

In (2.3) U_h is trivial at the origin while implementing a transformation between hedgehog and singular gauges at infinity. It is only needed to make sure that the behavior of ϕ^a at infinity is the same for both KK and BPS monopoles. The global transformation σ^2 implements Weyl reflection. Finally, $\sim e^{-i\frac{x_4}{2R}\sigma^3}$ is the anti-periodic gauge transformation that flips the magnetic charge of the monopole.

2.3 Zero modes of the BPS monopole

According to the Callias index theorem a chiral fermion in the fundamental representation has one zero mode in the background of the BPS monopole. To explicitly find this zero mode we need to solve the Dirac equation à la Jackiw and Rebbi. We are taking the 3D theory obtained by compactifying the theory on a circle in the timelike direction, and Wick-rotated to Euclidean space with $x_4 = -ix_0, A_4 = -iA_0$. The equation is given by

$$\left(\vec{\nabla}\cdot\vec{\sigma}^{\,\alpha\beta}\delta^m_n + i\vec{A}^a\cdot\vec{\sigma}^{\,\alpha\beta}T^{am}_{\ \ n} - \phi^a\,\delta^{\alpha\beta}T^{am}_{\ \ n} - m\,\delta^{\alpha\beta}\delta^m_n\right)\psi_{\beta m} = 0\,, \tag{2.5}$$

where m is the real mass of the fundamental, obtained from the time component of a four-dimensional background gauge field, which weakly gauges "baryon" number (implying that it is SU(2) color invariant, hence the additional color Kronecker delta).

We will look for solutions of the form

$$\psi_{\alpha m}(\vec{x}) = \begin{pmatrix} u \\ d \end{pmatrix} = \sigma^2_{\alpha m}X(x) + (\hat{x}^a\sigma^a\sigma^2)_{\alpha m}Y(x)\,. \tag{2.6}$$

With this ansatz, the zero mode must satisfy the equations

$$\begin{aligned} Y' + \frac{2-f}{r}Y + \frac{v}{2}hY &= mX \\ X' + \frac{f}{r}X + \frac{v}{2}hX &= mY \end{aligned} \tag{2.7}$$

For $m = 0$ the two equations are decoupled and can be integrated. The requirement that the solution is normalizable implies that $Y = 0$. The single zero mode in this case is then

given by [66]

$$X(r) = Ce^{-\int_0^r \left(\frac{v}{2}h(r') + \frac{f(r')}{r'}\right)dr'} \tag{2.8}$$

which is normalizable since $h(r) \to 1, \frac{f(r)}{r} \to 0$ as $r \to \infty$. For the case with a real mass m we need to solve the second order differential equation

$$\left(\frac{d}{dr} + \frac{2-f}{r} + \frac{v}{2}h\right)\left(\frac{d}{dr} + \frac{f}{r} + \frac{v}{2}h\right)X = m^2 X \ . \tag{2.9}$$

When X is normalizable the asymptotic behavior is $X \sim e^{-\lambda r}$, with $\lambda > 0$. Eq. (2.9) then implies $(\frac{v}{2} - \lambda)^2 = m^2$. There is a positive solution for λ provided that

$$-\frac{v}{2} < m < \frac{v}{2} \tag{2.10}$$

which exactly agrees with the Callias index theorem [20, 81, 87].

2.4 Zero modes of the KK monopole

It is well-known that for a vanishing real mass, the KK-monopole does not have a normalizable zero mode for fermions in the fundamental representation. Next we explain why this is so and show that for sufficiently large real masses normalizable zero modes do exist. The essential physics insight is the fact that a fundamental fermion behaves differently under an anti-periodic gauge transformation than an adjoint fermion due to the fact that it carries only a single SU(2) index. A large gauge transformation on adjoints introduces a periodic dependence on the coordinate along the compactified circle. However fields in the fundamental pick up an additional sign and thus would become anti-periodic. Thus, the expectation is that while gaugino zero modes in the KK monopole background exist and can be obtained by

a large gauge transformation (2.3), the fundamental fermion has no zero modes. However, a careful examination of the properties of the anti-periodic solution suggests that a new, twisted, zero mode of the fundamental fermion exists for sufficiently large mass. Since the large gauge transformation introduces an additional anti-periodic phase for the fundamental fermion, we need to look for an *anti periodic* solution to the Dirac equation in the BPS monopole background, with the VEV shifted to $v' = \frac{1}{R} - v$. Thus we look for an ansatz of the form

$$\psi(x, x_4) = e^{\pm \frac{ix_4}{2R}} \psi(x) \tag{2.11}$$

which is anti-periodic for both sign choices. For this ansatz, the ∂_4 derivative shifts the fermion mass by $\pm 1/(2R)$; thus the 3-dimensional part of the Dirac equation has an effective mass

$$m_{\text{eff}} = m \mp \frac{1}{2R} \,. \tag{2.12}$$

The condition for the existence of a normalizable zero mode solution $|m_{\text{eff}}| < \frac{v'}{2}$ is translated to $|m \mp \frac{1}{2R}| < \frac{1}{2R} - \frac{v}{2}$, which can be satisfied provided

$$m > \frac{v}{2} \quad \text{or} \quad m < -\frac{v}{2} \,. \tag{2.13}$$

While this solution is anti-periodic and not physical in the BPS monopole background, after the application of the large gauge transformation it becomes periodic and provides the proper zero mode in the KK monopole background. Note that the final form of the solution will be

$$\psi(x, x_4) = \begin{pmatrix} e^{in\frac{x_4}{R}} u \\ e^{i(n+1)\frac{x_4}{R}} d \end{pmatrix} \,, \tag{2.14}$$

where $n = 0$ corresponds to the choice of the + sign in (2.11) and $n = -1$ to the - sign. It is easy to generalize this result to the case of a fundamental representation of SU(N). In this case there is a monopole solution for each simple root α_i, where $i = 1, \ldots, N-1$. Writing an adjoint VEV as $\text{diag}(v_1, v_2, \ldots, v_N)$ with $\sum_i v_i = 0$ and $v_i > v_{i+1}$, the fundamental zero mode lives on the monopole associated with α_i if $v_{i+1}/2 < m < v_i/2$, and on the KK monopole for $m > v_1/2$ or $m < v_N/2$. We note finally that the KK monopole acquires a zero mode exactly as the zero mode disappears from the BPS monopole. This means that the total number of zero modes in N-monopole backgrounds is independent of the real mass and always matches the number of fermionic zero modes of the 4D instanton.

2.5 KK monopole decoupling

The physical importance of KK monopole zero modes becomes obvious if we consider[1] gauge theories with $\mathcal{N} = 1$ SUSY (4 supercharges) on $\mathbb{R}^3 \times \mathbb{S}^1$. This theory can be used to interpolate between the 4D theory (taking the radius of the circle $R \to \infty$) and the 3D theory (by taking R very small). However, the $R \to 0$ limit is not sufficient to obtain a truly 3D theory since, as noted in [3], rather than reproducing a truly 3D SUSY gauge theory, one arrives at the theory deformed by a tree level superpotential ηY, where Y is the KK monopole operator parametrizing the Coulomb branch. While η vanishes in the $R \to 0$ limit, the presence of such an operator is problematic for 3D duality since KK monopole operators appear on both sides of the duality and force the duality scale to zero. The appearance of KK monopole zero modes resolves the problem and allows for the derivation of 3D dualities. Generically, there are several monopole operators Y_i corresponding to the simple roots of the gauge group. Semiclassically these monopole operators are given by $Y_i \sim e^{4\pi(v_{i+1}-v_i)/g_3^2}$, where the v_i's are the adjoint VEVs (which can be promoted to chiral superfields), and g_3

[1] Another interesting case was recently studied in [22] where KK monopoles were shown to play a role in chiral symmetry breaking.

is the 3D gauge coupling. Whenever there are exactly two fermionic zero modes for a BPS monopole a superpotential term of the form $1Y_i$ is generated. On the other hand, the action of a KK monopole is proportional to $4\pi[1/R - (v_i - v_N)]/g_3^2$, thus giving a contribution $\sim e^{-4\pi/Rg_3^2}\prod_i Y_i$. The first factor $\eta = e^{-4\pi/Rg_3^2}$ can be thought of as the analog of the 4D instanton factor Λ_4^b if one matches the 3D and 4D gauge couplings: $2\pi R\, g_3^2 = g_4^2$. It is conventional to define $Y \equiv \prod_i Y_i$. It is the presence of the additional ηY term upon compactification that enforces some of the 4D properties on the 3D theory, and therefore it is essential that one properly decouple this term in order to arrive at a true 3D theory without deformations.

The proposal of [4] was to add a large real mass to one of the quark flavors. Naively one could think that decoupling a single flavor would just change the ηY term of the KK monopole to an effective $\tilde{\eta}\tilde{Y}$ of the theory with the number of quark flavors reduced by one. Aharony *et* al. however argued [4] that a large real mass for a single flavor completely removes the ηY term: an effective $\tilde{\eta}\tilde{Y}$ would necessarily depend upon the real mass of the flavor that was decoupled, but the real mass can not appear in a holomorphic quantity and hence there can be no $\tilde{\eta}\tilde{Y}$ in the effective superpotential. However the dynamical origin of the KK monopole decoupling from the superpotential is not intuitively clear from this argument. Indeed, the KK monopole itself obviously still exists even when one flavor becomes heavy. Thus it can only decouple if the number of fermion zero modes changes. Since gaugino zero modes exist independently of the real mass for the fundamental flavor, the decoupling would require an appearance of new zero modes and this is precisely what we found. Once the real mass is raised above $v/2$ the KK monopole no longer contributes to a chiral fermionic two-point correlation function and thus does not generate a superpotential term. This provides a dynamical explanation for the decoupling of the effects of the KK monopole and hence the explanation of how the undeformed 3D theory is approached in this limit.

2.6 $\mathrm{SU}(2) \times \mathrm{SU}(2)$ with a bifundamental

In this section we illustrate the importance of KK monopole zero modes by considering a supersymmetric $\mathrm{SU}(2) \times \mathrm{SU}(2)$ theory with four supercharges and matter Q in the bifundamental representation.[2] The superpotential of this theory was found to be [63]:

$$W = \frac{\left(\Lambda_1^{5/2} \pm \Lambda_2^{5/2}\right)^2}{Q^2}, \tag{2.15}$$

where Q^2 is a gauge invariant meson constructed out of the bifundamental. In 4D the origin of this superpotential can be understood as follows: both SU(2) factors have the right number of flavors to produce an instanton generated ADS superpotential term. Along the Higgs branch parametrized by the meson VEV Q^2 the gauge group is broken to a diagonal $\mathrm{SU}(2)_D$ and there are no charged light fields remaining. Gaugino condensation in the low-energy gauge group contributes another $\pm 2\Lambda_D^3$ term to the superpotential. The superpotential (2.15) arises as a combination of these three effects.

Let us now consider the dynamics of this model on $\mathbb{R}^3 \times \mathbb{S}^1$ and then recover 4D physics by taking $R \to \infty$. The classical moduli space contains a Coulomb branch parametrized by the adjoint VEVs v_1, v_2 as well as a Higgs branch parametrized by the squark VEV Q. The adjoint VEVs break $\mathrm{SU}(2)_1 \times \mathrm{SU}(2)_2$ to $\mathrm{U}(1)_1 \times \mathrm{U}(1)_2$, while the squark VEV breaks $\mathrm{SU}(2)_1 \times \mathrm{SU}(2)_2$ to the diagonal subgroup $\mathrm{SU}(2)_D$. For concreteness we will assume that $v_1 > v_2 \gg Q$. It is important to note that from the point of view of the $\mathrm{SU}(2)_1$ dynamics, the v_2 VEV serves as a real mass term for the $\mathrm{SU}(2)_1$ doublets. Similarly, the v_1 VEV serves as a real mass for the $\mathrm{SU}(2)_2$ doublets. We can see that the BPS monopole of $\mathrm{SU}(2)_1$ and the KK monopole of $\mathrm{SU}(2)_2$ have two gaugino and two quark zero modes, while the KK monopole of $\mathrm{SU}(2)_1$ and the BPS monopole of $\mathrm{SU}(2)_2$ only have two gaugino zero modes.

[2] A non-supersymmetric theory with similar matter content has been analyzed in [97].

At first sight one might conclude that there is a superpotential contribution from the first KK monopole and the second BPS monopole, but the actual dynamics is somewhat more intricate. Since there is a squark VEV turned on, it will break the two U(1)'s to the diagonal, $\mathrm{U}(1)_1 \times \mathrm{U}(1)_2 \to \mathrm{U}(1)_D$, and monopoles which carry the broken U(1) charge are confined. Thus only multi-monopole configurations neutral under the broken U(1) will contribute to the superpotential. There are four such multi-monopole configurations made out of two confined monopoles: the first BPS and the first KK monopoles, the second BPS and the second KK monopoles, the two BPS monopoles, and the two KK monopoles. While these multi-monopole solutions each have several zero modes, some of them can be soaked up using the squark VEV each eventually yielding contributions to the superpotential. Which zero modes are lifted is determined by the pattern of U(1) breaking since the corresponding gaugino gets a mass with a quark via the squark VEV as required by SUSY.

For example, the double monopole made of the first BPS and first KK monopoles generates the expected ADS term in the superpotential,

$$W_1 = \frac{\eta_1}{Q^2}\,. \tag{2.16}$$

In fact, this two monopole configuration is equivalent [75] to a periodic instanton on $\mathbb{R}^3 \times \mathbb{S}^1$. Similarly, the configuration made up of the second BPS and KK monopoles leads to the instanton-generated ADS superpotential in $\mathrm{SU}(2)_2$ even though the distribution of fermion zero modes between BPS and KK monopoles is different here:

$$W_2 = \frac{\eta_2}{Q^2}\,. \tag{2.17}$$

Finally, the configurations with the two BPS and the two KK monopoles (which act as the

monopoles of $\mathrm{SU}(2)_D$) produce the superpotential

$$W_{1,2} = \frac{1}{Q^2}\left(\eta_1\eta_2 Y_1 Y_2 + \frac{1}{Y_1 Y_2}\right) . \tag{2.18}$$

Solving the equations of motion for the composite monopole $Y_1 Y_2$ we find that (2.18) will contribute $\pm\frac{2\sqrt{\eta_1\eta_2}}{Q^2}$, which together with (2.16) and (2.17) results in the correct superpotential (2.15).

2.7 Conclusions

Fermionic zero modes of monopoles largely determine the structure of the dynamical monopole-induced effects in supersymmetric theories. We have found the condition for the existence of fermionic zero modes in the fundamental representation in the KK monopole background, and showed that such zero modes will be present for a sufficiently large real mass term. This explains the previously mysterious decoupling of the effects of KK monopoles in theories with four supercharges in the presence of a large real mass, which allows one to explore the dynamics of a truly 3D theory. We have applied our results to the $\mathrm{SU}(2) \times \mathrm{SU}(2)$ model with a bifundamental and shown that the terms attributed to gaugino condensation in 4D originate from multi monopole terms in the 3D theory.

Chapter 3

Deformations of the moduli space and superpotential flows in 3D SUSY QCD

This chapter is heavily based on work previously published in collaboration with Yuri Shirman [99].

3.1 Introduction

In this chapter, we calculate quantum deformations of the classical moduli spaces in 3D SUSY QCD with $F < N$ flavors and investigate their role in the origin of the pre-ADS superpotentials as well as their role in the flow of superpotentials in the theory space as one adds holomorphic mass terms and decouples heavy flavors. It has long been known [3] that the classical moduli space is deformed quantum mechanically in a 3D SU(N) theory with $F = N - 1$ flavors, taking the form $Y \det M = g^{2F}$, where Y is a globally defined

monopole modulus and g^2 is a 3-dimensional coupling. We will derive this constraint by following the approach of [48] and calculating the two-point holomorphic scalar correlation function in an SU(2) theory with one flavor. In fact, the physics behind such a modification is clearer in 3D. An SU(2) theory with 4 supercharges has a Coulomb branch along which the gauge group is broken to U(1). On the Coulomb branch, the Higgs direction is lifted, and the squark VEVs are not allowed. Thus, the meson VEV $M = q\overline{q}$ must vanish classically. Nevertheless, the holomorphic two-point squark correlation function receives non vanishing contributions in a single monopole background. Indeed, the fundamental monopole of the SU(2) theory has two gaugino and two doublet zero modes. Thus it generates a four-fermion vertex in the low energy effective theory. When this 't Hooft operator is combined with supersymmetric gauge couplings, one can construct a two loop diagram contributing to the two-point scalar correlation function. Such a diagram is naively UV divergent, but this divergence is cutoff by the finite size of the monopole. We perform a full calculation of this two-point correlation function in Section 3.2. Then we generalize the result to SU(N) theories with $F = N-1$ flavors and arbitrary N. In Section 3.3, we observe that the classical moduli space is also deformed in theories with an arbitrary number of flavors, $F \leq N-1$. When $F = N-1$ the deformation is global (constraining the global moduli Y and M), while in the case of $F < N-1$, the deformations exist in locally defined coordinate charts of the moduli space. These local deformations lead to several important consequences. They guarantee the equivalence of the Coulomb branch superpotential discussed in [3, 4] and the multi monopole generated superpotential on the mixed Higgs-Coulomb branch of the theory found in [33]. Furthermore, the constraints ensure that the superpotential is valid in all coordinate charts on the moduli space. In Section 3.3.1, we present detailed analysis of the quantum moduli space of an SU(3) model with $F = 1$. In Section 3.3.2, we extend our results to all SU(N) models with $F = 1$. Finally, in Section 3.3.3, we generalize our discussions to arbitrary $F < N$ and show how the existence of such local deformations explains the superpotential flow between theories with different numbers of flavors as mass terms are

added. We finish with a summary of our results in Section 3.4.

3.2 $F = N - 1$: Quantum Deformed Moduli Space

In this section, we derive the 3D quantum constraint by calculating two-point holomorphic squark correlation function in SU(2) theory with one flavor and generalizing the result to SU(N) with $F = N - 1$ flavors. As discussed in the previous section, the classical moduli space of the SU(2) theory has two one-dimensional branches: a Higgs branch parameterized by a squark VEV $q = \bar{q}$ (or, in a gauge invariant language, by the meson $M \sim q\bar{q}$) and a Coulomb branch parameterized by the VEV of the adjoint scalar component of the gauge multiplet. Along the Coulomb branch, the gauge symmetry is broken to U(1), and it is convenient to describe the physics in terms of the monopole modulus Y. Classical Higgs and Coulomb branches only intersect at the origin of the moduli space. Therefore, on the Coulomb branch, the holomorphic squark-anti-squark correlation function must vanish clasically. However, as we explicitly show below, this correlation function obtains a non-vanishing contribution $\langle M \rangle = \langle q\bar{q} \rangle = g^2/Y$ in the monopole background on the Coulomb branch. The corresponding semi-classical calculation is weakly coupled and under control for sufficiently large v. Holomorphy guarantees that this result remains valid everywhere on the Coulomb branch, implying a well known 3D quantum constraint $YM = g^2$.

Our calculation is similar to 4D calculations of quantum constraints in [48]. The instanton-monopole of the SU(2) theory with 1 flavor has two gaugino and two fundamental zero modes and contributes to chiral four fermion correlation function. This correlation function can be converted to holomorphic two point squark correlation function by the insertion of two supersymmetric gauge couplings. The resulting contribution can be visualized in Figure 3.1.

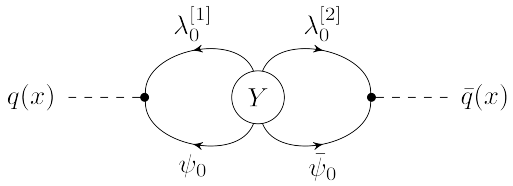

Figure 3.1: Diagram illustrating the monopole contribution to squark correlation functions

In the language of the path integral, we must evaluate

$$\langle \bar{q}^i(x) q_i(x) \rangle = \int [\mathcal{D}\phi]_{qu} \left(\bar{q}^i(x) q_i(x) \right) e^{-S_{cl.} - S[\phi_{qu}]} \,, \tag{3.1}$$

where $[\phi_{qu}]$ is short-hand for all quantum field fluctuations around the monopole background. We present the details of the calculation in the Appendix. The resulting correlation function is

$$\langle \bar{q}^i(x) q_i(x) \rangle = \frac{v^2}{g^4} e^{-\frac{4\pi v}{g^2}} g^2 I \,, \tag{3.2}$$

where I is a positive definite integral. At first sight, this is non-holomorphic, but as explained in [44, 86], the non-holomorphic pre-factor v^2/g^4 can be absorbed into redefinition of the Kähler potential. The required field redefinition leads to a finite renormalization of the gauge coupling

$$\frac{1}{g^2} \longrightarrow \frac{1}{g^2} - \frac{2}{v} \,. \tag{3.3}$$

In terms of the rescaled modulus Y the two point scalar correlation function becomes

$$\langle M \rangle = \frac{g^2}{Y} \,. \tag{3.4}$$

The generalization to SU(N) theories with $F = N - 1$ flavors is reasonably straightforward. Consider the theory on the mixed Higgs-Coulomb branch where the rank of the meson M is

$N-2$, and the low energy physics is described by an $F=1$ SU(2) theory. The calculation of the two-point holomorphic scalar correlation function is illustrated in Figure 3.2 where crosses represent VEV insertions. As before, the coupling constant of the low energy theory is renormalized due to the contributions of non-zero modes and is shifted by terms of the form $1/v$. The fundamental monopole of the low energy SU(2) can be written in terms of the fundamental monopoles and mesons of the high energy theory $Y_L = \prod_i Y_i \det' M/g^{2(F-1)}$ where prime denotes the determinant over $N-2$ flavors with non-vanishing VEVs. The scalar correlation function for the remaining massless flavor of the low energy SU(2) follows from our earlier calculation and gives the quantum constraint $Y \det M = g^{2F}$. One could also derive the constraint by calculating the $2(N-1)$-point scalar correlation function at a generic point on the Coulomb branch in the background of $N-1$ fundamental monopoles, but this calculation would be difficult in practice.

The existence of quantum deformations of the classical moduli space for an arbitrary number of flavors implies that the rank of the meson superfield is maximal ($rank(M) = N-1$). We will later see that M will have maximal rank ($rank(M) = F$) for any number of flavors. This means that, quantum mechanically, the gauge symmetry is always maximally broken and some fundamental monopoles can not contribute to the superpotential despite the fact that, at a generic point on a pure Coulomb branch, these monopoles have exactly the two fermion zero modes necessary to generate two fermion correlation function and the corresponding superpotential terms.

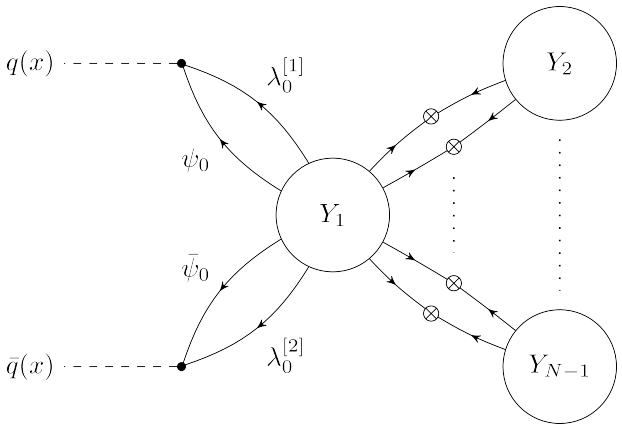

Figure 3.2: Diagram illustrating the multimonopole contribution to a $2F$ squark correlation function

3.3 $F < N - 1$: Quantum Constraints as Transition Functions

As discussed in Section 1.3, the space of physically inequivalent classical vacua consists of several distinct $(N-1)$-dimensional branches. One might expect that the moduli space becomes a smooth, locally connected manifold in the quantum theory. We could attempt to describe such a manifold in terms of globally defined moduli Y and M. However, M has maximal rank F, and there are an insufficient number of globally defined moduli $(F+1)$ to parameterize the entire $N-1$ dimensional moduli space when $F < N-1$. The fundamental monopoles can not serve as additional coordinates on the moduli space, since they are discontinous at sub-wedge boundaries. To resolve the problem, one would need to introduce new composite coordinates valid in two or more sub-wedges and transition functions between the composite coordinates that are valid on overlapping sets of sub-wedges. For example, one could use the two-monopole modulus $Y_{k,2}^{(k)}$ discussed earlier. However, this is not sufficient, because there are two discontinous coordinates at each sub-wedge boundary. One of these coordinates can be replaced by the two-monopole modulus, but the existence of a second discontinous coordinate will prevent us from patching together disjoint sub-wedges.

As we will show below, quantum effects deform the classical moduli space even in theories with $F < N-1$, but such deformations are local (i.e. they are only valid in specific sub-wedges of the classical moduli space). Moreover, these deformations smooth out the interface between the sub-wedges and make the mixed Higgs-Coulomb branch accessible from either adjacent sub-wedge. These quantum deformations also provide necessary transition functions to cover the entire quantum moduli space with overlapping coordinate charts. The quantum deformed moduli space is further lifted by monopoles, and the exact superpotential of the theory can be written down in terms of the appropriate coordinates in all coordinate patches.

In Section 3.3.1, we will show how this plays out in the case of an SU(3) theory with $F = 1$. While the SU(3) example is illuminating, it is not sufficiently general. In this case. there are two globally defined moduli $Y = Y_1 Y_2$ and M which can describe dynamics everywhere on the moduli space. In Section 3.3.2, we extend these results to all SU(N) theories with $F = 1$. We show that once again quantum effects deform the classical moduli space, relating monopole and meson moduli at each boundary. This deformation allows us to cover the moduli space by a set of overlapping coordinate charts, with each patch covering two neighboring sub-wedges. We will demonstrate that calculations of the pre-ADS superpotential generated by single monopole contributions in any sub-wedge of the Coulomb branch lead to the same result, and this is the same superpotential that can be found by considering monopole and multi-monopole contributions on mixed Higgs-Coulomb branches emanating from the boundaries between sub-wedges. In Section 3.3.3, we further generalize the results to SU(N) models with $F < N-1$ flavors. Here the quantum deformation relates the mesons to F-monopole composite operators

$$Y_{k,F} \det M = \left(\prod_{i=k}^{k+F-1} Y_i^{(k)} \right) \det M = g^{2F} \,. \tag{3.5}$$

This local deformation allows us to introduce the $(F+1)$-monopole modulus $Y_{k,F+1} = \prod_{i=k}^{k+F+1} Y_i^{(k)}$ which is continuous across the intermediary boundaries $Y_{k,F+1}^{(k)} = Y_{k,F+1}^{(k+1)} =$

$\ldots = Y_{k,F+1}^{(k+F)}$. We can then cover the moduli space by a set of overlapping coordinate charts with well defined transition functions and show that superpotentials calculated on all of the quantum-mechanically accessible branches of the moduli space are equivalent.

3.3.1 SU(3) theory with $F = 1$

Consider a one flavor SU(3) model on the Coulomb branch in the positive Weyl chamber. Classically, the Weyl chamber is split into two sub-wedges depending on the sign of v_2, while at $v_2 = 0$, the Higgs branch is accessible. In the $v_2 < 0$ sub-wedge, it is convenient to parameterize the Coulomb branch coordinate by monopole moduli Y_1 and Y_2 which in a semiclassical regime are approximated by $Y_1 \sim \exp[4\pi(v_1 - v_2)/g^2]$ and $Y_2 \sim \exp[4\pi(v_2 - v_3)/g^2]$. In the $v_2 > 0$ sub-wedge, we need to choose different Coulomb branch moduli Y_1' and Y_2'. As explained earlier, despite similar behavior in the semi-classical regime, the quantum numbers of Y_1' and Y_2' differ from those of Y_1 and Y_2 respectively and do not represent the same degrees of freedom in the quantum theory.

Consider the first sub-wedge of the Weyl chamber defined by $v_1 > 0 > v_2 > v_3$. Here the first fundamental monopole Y_1 has four (two gaugino and two matter) fermion zero modes, while the second fundamental monopole Y_2 has two gaugino zero modes. Only the second fundamental monopole contributes to the superpotential, and we find $W = Y_2^{-1}$. In addition, we can calculate two-point scalar correlation function in Y_1 background. Since the fields of the Y_1 monopole (including the fermion zero modes) can be embedded in an SU(2) subgroup of SU(3), the calculation is nearly identical to the one we performed in the previous section. There are two new features that must be taken into account. First, the contributions of non-zero modes of the matter doublets are modified since, from the point of view of Y_1 monopole, the matter fermions have real mass $(v_1 + v_2)/2$. Second, the gaugino contains components that transform as doublets in the Y_1 monopole background. These

components of the gaugino do not have zero modes, but their non-zero modes contribute to the path integral just like matter doublets with a real mass $3(v_1 + v_2)/2$ would. Similar to the non-holomorphic prefactor in the SU(2) theory, these effects can be understood as finite renormalization of the U(1) gauge coupling of the low energy theory, and we find $Y_1 M \sim g^2$. This result can be enforced in the first sub-wedge of the Weyl chamber through a Lagrange multiplier term in the superpotential,

$$W = \frac{g^4}{Y_2} + \lambda_1 (Y_1 M - g^2) \,. \tag{3.6}$$

In the $v_1 > v_2 > 0 > v_3$ sub-wedge, we similarly find

$$W = \frac{g^4}{Y_1'} + \lambda_2 (Y_2' M - g^2) \,. \tag{3.7}$$

To verify that these two expressions are consistent with each other we must compare them at a jumping point where $v_2 = 0$. Integrating out the Lagrange multiplier terms, both forms of the superpotential lead to the same result

$$W = \frac{g^6}{Y_1 Y_2 M} = \frac{g^6}{Y_1' Y_2' M} \,, \tag{3.8}$$

where the composite two-monopole modulus $Y = Y_1 Y_2 = Y_1' Y_2'$ is continous across the boundary between the two sub-wedges as explained in Section 1.3. It is tempting to interpret the superpotential (3.8) as a two-monopole contribution to the superpotential, and indeed it agrees with the results of the two monopole superpotential calculation on the mixed Higgs-Coulomb branch of the theory [33]. We conclude that Y and M are valid in both coordinate charts of the $F = 1$ SU(3) theory and are related to moduli of the two coordinate charts by $\{Y_1 = g^2/M, Y_2 = YM/g^2\}$ and $\{Y_1' = YM/g^2, Y_2' = g^2/M\}$.

Note that the above procedure is precisely that described at the beginning of this section. The quantum constraints enforced by λ_1 and λ_2 provided a transition functions from the

two sets of Coulomb branch coordinates to the mixed Higgs-Coulomb branch coordinates, while the continuity of the two-monopole modulus ensures that the two Coulomb branch coordinate charts overlap on the Higgs branch. Together, these effects guarantee agreement between all three expressions for the superpotential.

Let us consider some standard checks of ADS and pre-ADS superpotentials. Specifically, we can study the theory on a Higgs branch where the low energy physics is described by a pure SYM SU(2) as well as deform the theory by a large holomorphic mass term, m, so that the low energy description is given in terms of a pure SYM SU(3) theory. In the former case, the low energy superpotential is given by $1/Y_L$, and by comparing with (3.8), we conclude that the matching of high and low energy theories requires a rescaling of chiral superfields to absorb M into the definition of $Y_L = Y_1 Y_2 (M/g^2)$. Similarly to non-holomorphic rescaling discussed in [86], this field redefinition affects the matching relation between the coupling constants of the high and low energy theories and should reproduce the finite renormalization of the low energy U(1) coupling constant. When the theory is deformed by a mass term, the low energy superpotential must be

$$W = \frac{g_L^4}{Y_{1L}} + \frac{g_L^4}{Y_{2L}} \,. \tag{3.9}$$

We can obtain this superpotential by starting either with (3.6) or (3.7) and adding a mass term. For example in the $v_2 < 0$ sub-wedge of the Weyl chamber, the superpotential is

$$W = \frac{g^4}{Y_2} + \lambda_1 (Y_1 M - g^2) + mM \,. \tag{3.10}$$

Integrating out both the Lagrange multiplier and the meson superfield, we find the low energy superpotential,

$$W = \frac{g^2 m}{Y_1} + \frac{g^4}{Y_2} \,, \tag{3.11}$$

which agrees with (3.9) if we identify[1] $g_L^2 = g^2$, $Y_{1L} = Y_1 g^2/m$, and $Y_{2L} = Y_2$. Once again, the rescaling required to absorb the mass into the Y_L monopole of the low energy theory determines the coupling constant matching and correctly reproduces the renormalization of the $\mathrm{U}(1)_1$ coupling constant. We stress that the local deformation of the moduli space, implemented through the Lagrange multiplier term in (3.10), plays an essential role in reproducing the superpotential of the SYM low energy theory when the matter fields are decoupled by taking the superpotential mass term, m, to infinity.

3.3.2 $\mathrm{SU}(N)$ with $F = 1$

The generalization to $\mathrm{SU}(N)$ theories with an arbitrary number of colors and one massless flavor is straightforward. We will denote monopole moduli in the k^{th} sub-wedge by $Y_i^{(k)}$, $i = 1, \ldots, N-1$. With the exception of $Y_k^{(k)}$, all the fundamental monopoles in this sub-wedge have two gaugino zero modes and no matter zero modes. Thus they contribute to the superpotential. Calculating the two point scalar correlation function, we find a local constraint applicable to the k^{th} sub-wedge, $Y_k^{(k)} M = g^2$. Thus within this sub-wedge of the Coulomb branch, the physics is described by the superpotential

$$W = \sum_{i \neq k} \frac{g^4}{Y_i^{(k)}} + \lambda_k (Y_k^{(k)} M - g^2)\,. \tag{3.12}$$

Although this superpotential is calculated in the k^{th} sub-wedge, it can be extended into the $(k+1)^{st}$ (or $(k-1)^{st}$) sub-wedges by using the constraint as a transition function and replacing $Y_{k+1}^{(k)}$ (or $Y_{k-1}^{(k)}$) by the composite two-monopole modulus that is continuous in the appropriate regions. Let us explicitly carry this out for the $(k+1)^{st}$ sub-wedge. Integrating

[1] Here we neglect finite non-holomorphic shifts in the coupling discussed earlier.

out the Lagrange multiplier, the superpotential can be written as

$$W = \sum_{i \neq k,k+1} \frac{g^4}{Y_i^{(k)}} + \frac{g^6}{Y_k^{(k)} Y_{k+1}^{(k)} M} \,. \tag{3.13}$$

The last term can be interpreted as arising from the two monopole contribution considered in [33]. In this form, the superpotential is valid both in the k^{th} and $(k+1)^{st}$ sub-wedges due to their overlap at the mixed Higgs-Coulomb boundary. However, in the $(k+1)^{st}$ sub-wedge, the same superpotential can be written in two more forms. First, it can be written in terms of the monopole moduli of the $(k+1)^{st}$ sub-wedge, $Y_i^{(k+1)}$, and the local constraint, $\lambda_{k+1}\left(Y_{k+1}^{(k+1)} M - g^2\right)$, valid in this sub-wedge:

$$W = \sum_{i \neq k+1} \frac{g^4}{Y_i^{(k+1)}} + \lambda_{k+1}(Y_{k+1}^{(k+1)} M - g^2) \,. \tag{3.14}$$

Second, it can be written in terms of the composite monopole moduli $Y_{k+1}^{(k+1)} Y_{k+2}^{(k+1)} M/g^2$. Recall that this term in the superpotential can be interpreted as a two monopole contribution generated on the mixed Higgs-Coulomb branch accessible from the boundary between the $(k+1)^{st}$ or $(k+2)^{nd}$ sub-wedges. This procedure can be used to recursively generate the sets of coordinate charts and transition functions required to cover the entire quantum moduli space of the theory and to define it as a smooth, locally connected manifold. Moreover, the calculations on all accessible branches of the moduli space lead to the same results. It is easy to see that, just like in the case of the SU(3) theory, the deformation of the theory by the mass term correctly leads to the low energy physics described by a pure $\mathcal{N} = 2$ SYM SU(N) theory.

3.3.3 SU(N) with $F < N-1$

We conclude our study of the pre-ADS superpotentials and quantum deformations of the moduli space by considering a general case of an SU(N) theory with F massless flavors. We will consider the first sub-wedge of the Weyl chamber, $v_1 > 0 \geq v_2 \geq \ldots \geq v_N$. By calculating $2F$ scalar correlation function in the F-monopole background, one finds there exists a local constraint given by $\left(\prod_{i=1}^{F} Y_i\right) \det M = g^{2F}$.[2] This is easiest to see by performing a calculation on the mixed Higgs-Coulomb branch where the rank $F-1$ meson VEV is allowed. This is the region where $v_i = 0$ for $i = 2 \ldots F-1$. In the presence of VEVs, the multi-monopole $Y^{(1)}_{1,F} = \prod_{i=1}^{F} Y^{(1)}_i$ will collapse into a single fundamental monopole of the low energy SU($N-F+1$) theory $Y_{1L} = Y^{(1)}_{1,F} \det' M / g^{2(F-1)}$ where $\det' M$ denotes determinant taken over $F-1$ flavors with large VEV. As discussed earlier, the rescaling used in the definition of Y_{1L} shifts the coupling of the low energy theory. We can calculate the two scalar correlation function for the remaining squark flavor in the low energy effective theory and find

$$\langle M_{FF} \rangle = \frac{g_L^2}{Y_{1L}} = \frac{g^{2F}}{Y^{(1)}_{1,F} \det' M} \,. \tag{3.15}$$

One can then write the full nonperturbative superpotential in the form,

$$W = \sum_{i=F+1}^{N-1} \frac{g^4}{Y^{(1)}_i} + \lambda_1 \left(Y^{(1)}_{1,F} \det M - g^{2F} \right) \,. \tag{3.16}$$

As expected, integrating out the Lagrange multiplier term, we find the multi-monopole generated superpotential found in [33]

$$W = \sum_{i=F+2}^{N-1} \frac{g^4}{Y^{(1)}_i} + \frac{g^{2F+4}}{Y^{(1)}_{1,F+1} \det M} \,, \tag{3.17}$$

[2] Similar to the SU(N) with $F = N-1$ case described in Section 3.2, the constraint enforces $rank(M) = F$ and prohibits the superpotential of F individual fundamental monopoles.

where $Y^{(1)}_{1,F+1} = \prod_{i=1}^{F+1} Y^{(1)}_i$.

Alternatively, we can consider the second sub-wedge, $v_1 > v_2 > 0 \geq \ldots \geq v_N$ where the rank of M is $F-1$. Here we find the superpotential

$$W = \frac{1}{Y^{(2)}_1} + \sum_{i=F+2}^{N-1} \frac{g^4}{Y^{(2)}_i} + \lambda_2 \left(Y^{(2)}_{2,F} \det M - g^{2F} \right) . \tag{3.18}$$

The valid coordinate patches for (3.16) and (3.18) overlap on the mixed Higgs-Coulomb branch where both superpotentials are

$$W = \sum_{i=F+2}^{N-1} \frac{g^4}{Y^{(1/2)}_i} + \frac{g^{2F+4}}{Y^{(1/2)}_{1,F+1} \det M} . \tag{3.19}$$

With the help of the constraints, we can construct transition functions that allow us to cover the full moduli space with coordinate charts and verify that superpotentials calculated in any of these charts are equivalent.

Finally, we deform the theory by adding the mass term mM_{FF} to the last flavor. Integrating out the heavy flavor we find the superpotential of low energy SU(N) theory with $F-1$ flavors

$$W = \sum_{i=F+1}^{N-1} \frac{g^4}{Y^{(1)}_i} + \frac{mg^{2F}}{Y^{(1)}_{1,F} \det' M} . \tag{3.20}$$

This is precisely the superpotential of the $F-1$ flavor theory calculated in [33]. In addition, we need to compliment this superpotential by a new local constraint $Y^{(1)}_{1,F-1} \det' M = g^{2(F-1)}$. This superpotential can then be extended to other regions of the $F-1$ flavor theory moduli space or reduced to the superpotential of the $F-2$ flavor theory by adding another large mass term.

3.4 Conclusions

In this chapter, we explicitly calculated quantum constraint $YM = g^2$ in the 3D SU(2) theory with one massless flavor and showed how to generalize the calculation to an $F = N - 1$ theory with an arbitrary N. We also showed that a local version of such a constraint exists in 3D SU(N) theories with an arbitrary number of flavors, $F < N - 1$ flavors. The existence of local constraints allowed us to construct a set of coordinate charts that cover the entire moduli space and show that the superpotential calculations in different charts are equivalent. Additionally, the existence of local constraints ensures the agreement between the superpotentials generated by fundamental monopoles on the pure Coulomb branch of an SU(N) theory [3] with the superpotentials arising from fundamental monopoles and multi-monopole contributions on the mixed Higgs-Coulomb branch of the theory [33]. The validity of the superpotential throughout the entire moduli space implies that the physics is fully described by a single Coulomb branch of the low energy pure SYM SU($N-F$) theory coupled to dilaton-like moduli M. We also showed that constraints play an essential role in the flow of the superpotential between theories with different numbers of flavors. When a superpotential mass term for one flavor is added to the theory and the heavy flavor is decoupled, the local constraint guarantees that the low energy superpotential reproduces the one expected in a theory with $F - 1$ flavors. To continue the flow in flavor space as additional mass terms are added, one must include new local constraints that are generated whenever new mass terms are added to the superpotential. We expect that our analysis of SU(N) gauge theories by considering deformations of the classical moduli space will be useful in understanding gauge theories with more general gauge groups and matter content.

Chapter 4

Scattering Amplitudes for Monopoles: Pairwise Little Group and Pairwise Helicity

This chapter is heavily based on work previously published in collaboration with Csaba Csáki, Sungwoo Hong, Yuri Shirman, Ofri Telem, and John Terning [31].

4.1 Introduction

Unitary representations of the Poincaré group, classified by Wigner [113] in the 1930s, provide the foundation of the quantum mechanical (QM) description of particle physics and quantum field theory. The essential elements in Wigner's construction are one-particle states — representations of the Poincaré group associated with a single asymptotic particle, in an irreducible representation of its little group (LG) [112]. While this satisfying picture provides the full classification of one-particle states, the general construction of multi-particle

states has rarely been addressed: they are simply assumed to be direct products of one-particle states. However, in a beautiful, under-appreciated paper in 1972 Zwanziger [119] found that quantum states with both electric and magnetic charges transform in non-trivial multi-particle representations of the Poincaré group. In the first part of this chapter, we address the general construction of multi-particle states and introduce the concept of the pairwise LG, which is necessary to fully classify the multi-particle representations of the Poincaré group. In addition to the one-particle LGs introduced by Wigner, the pairwise LG completes the characterization of the transformation properties of the multi-particle system as a whole [30]. In particular, it may yield an additional phase under Lorentz transformations on top of the one-particle LG transformations, as in the first specific realization found by Zwanziger [119]. The pairwise LG is always just a U(1), and in the most commonly considered scattering processes the corresponding helicity q_{12} simply vanishes, confirming the expectation that the asymptotic multi-particle state is simply a direct product of the one-particle states. However, for charge-monopole scattering the pairwise U(1) helicity is the quantized "cross product" of charges

$$q_{12} = e_1 g_2 - e_2 g_1 \ , \tag{4.1}$$

where $e_{1,2}$ ($g_{1,2}$) are the electric (magnetic) charges of the two particles. This implies modified transformation properties for scattering amplitudes involving both electrically and magnetically charged particles. We note that three-particle and higher LGs are always trivial, and so the general classification of multi-particle states in 4D will be given in terms of the momenta, spins/helicities and *pairwise* LG helicities [30]

$$|p_1, \ldots, p_n \ ; \ \sigma_1, \ldots, \sigma_n \ ; \ q_{12}, q_{13}, \ldots, q_{n-1,n}\rangle \ . \tag{4.2}$$

In the second half of this chapter, we use our refined understanding of the pairwise LG to

construct scattering amplitudes of electrically and magnetically charged states. Understanding the interactions of magnetically charged states has been a long standing issue in particle physics. Dirac showed that a Lorentz invariant Lagrangian with both electric and magnetic charges must be non-local [40], and such interactions are often referred to as being "mutually non-local." Alternatively, Zwanziger showed [118] that one can write a local Lagrangian, but manifest Lorentz invariance is lost. These problems seem to be an artifact of the unphysical, gauge-variant Dirac string. For some time it was not even clear that the scattering of electrically and magnetically charged particles makes sense. Paradoxically, Weinberg found [111] that the amplitude for one photon exchange between an electric charge and a magnetic monopole is not Lorentz invariant (and implicitly not gauge invariant [104]). However, recently it was shown by Terning and Verhaaren [104] that an all orders resummation of soft photons can restore both Lorentz and gauge invariance if Dirac charge quantization [41] is satisfied. Hence it is believed that the electric-magnetic S-matrix is both local and Lorentz invariant, but Lagrangian formulations cannot make both properties manifest at the same time, leading, unsurprisingly, to seemingly unending difficulties in calculating scattering amplitudes [73, 51, 18, 34, 53, 26, 61, 103].

Thus we can see that electric-magnetic scattering is an ideal proving ground for on-shell methods. In this chapter we indeed find that electric-magnetic scattering demonstrates a success for the on-shell program in theories where Lagrangian methods fall short. We should note that in our formulation we never need to introduce a Dirac string. This is in contrast to previous attempts to apply on-shell methods to electric-magnetic scattering [21, 62, 80] which have been only partially successful in eliminating the unphysical Dirac string, thus suffering from a Lorentz violating sign ambiguity.

The bulk of this chapter is devoted to extending on-shell amplitude methods to calculations of electric-magnetic S-matrix elements while maintaining manifest Lorentz invariance and locality. Thus we see that "mutually non-local" scattering is, in fact, local aside from the

angular momentum carried in the Coulomb fields of the particles. The key is to ensure that the full action of the Poincaré group, including the one-particle and pairwise LGs, is properly incorporated. We find a beautiful and simple implementation of this scheme in the spinor-helicity framework, allowing us to go far beyond Zwanziger's special case of pairwise helicities equal to one. To capture the effect of the pairwise LG, we define *null* "pairwise" momenta $p_{ij}^{\flat\pm}$ which are linear combinations of the momenta of each electric-magnetic pair. The pairwise momenta are then naturally expressed using pairwise spinor-helicity variables

$$|p_{ij}^{\flat\pm}\rangle, \left[p_{ij}^{\flat\pm}\right|, \tag{4.3}$$

which are constructed such that under Lorentz transformations they pick up exactly the phase dictated by the pairwise LG. Along with the standard massless and massive spinor-helicity variables, the pairwise spinor-helicity variables serve as the fundamental building blocks for the construction of the S-matrix for magnetic scattering[1].

We utilize our newly defined pairwise spinors to construct all 3-point electric-magnetic amplitudes, as a direct generalization of Arkani-Hamed, Huang, and Huang [7]; our derivation implies a non-trivial generalization of the selection rules derived in [7]. For example in the decay of a massive spin s to two massless particles, we get the selection rule $|\Delta h - q| \leq s$, which reduces to the standard $|\Delta h| \leq s$ in the non-magnetic case with $q = 0$. Another non-trivial selection rule we derive is for the decay of a massive spin s_1 into two massive particles with spins s_2 and s_3. In this case we get $s_1 + s_2 + s_3 \geq |q_{23}|$, indicating, as a special case, that a scalar dyon cannot decay into two other scalar dyons with $q_{23} \neq 0$. Armed with our general classification of 3-point magnetic amplitudes, we move on to address the $2 \to 2$ scattering of a fermion and a monopole, making use of the fully relativistic partial wave decomposition, adapted to the magnetic case. Using minimal dynamical information about the phase shifts

[1]Note that we will use the term magnetic scattering or magnetic S-matrix to emphasize that there is at least one magnetically charged object among the scattered states, but our discussion is fully general and applicable to generic multi-dyon scattering.

of the higher partial wave amplitudes, we are able to fully reproduce the results of the non-relativistic quantum mechanics (NRQM) calculation of Kazama, Yang and Goldhaber [68]. In particular, our selection rules immediately tell us that in the lowest partial wave only the helicity-flip amplitudes are non-zero while forward scattering is not allowed. Furthermore, we are able to determine the full expression for the helicity flip amplitude. For the higher partial waves our formalism allows us to fix the full angular dependence of the amplitudes, while the overall magnitude of all partial waves can be fixed using unitarity and the phase shifts.

The chapter is organized as follows. Section 4.2 contains our discussion of the general transformation properties of multi-particle states under the Poincaré group. We introduce the concept of pairwise LG here. We also give a basic introduction into the unusual properties of the charge-monopole system, rooted in the asymptotic angular momentum contained in the electromagnetic field. In section 4.3 we define our main objects of interest — the pairwise spinor-helicity variables which transform covariantly under the pairwise LG. These new spinor-helicity variables, together with the standard spinors for massless and massive particles, serve as a complete set of building blocks for the magnetic (and non-magnetic) S-matrix. We put our new building blocks to use in section 4.4, in which we demonstrate how to construct the magnetic S-matrix and derive concrete expressions for all magnetic 3-point amplitudes in the spirit of ref. [7]. In section 4.5 we take a further step and derive the general partial wave expansion for magnetic $2 \to 2$ matrix elements. Finally, in sections 4.6-4.7, we apply our formalism to the case of fermion-monopole scattering, effortlessly reproducing the non-trivial results of Kazama, Yang, and Goldhaber [68], including the helicity-flip of the lowest partial wave and the full angular dependence of the higher partial waves. Finally, in section 4.8 we discuss partial wave unitarity in the context of the magnetic S-matrix, knowledge of which is required to obtain the magnitude of higher partial wave processes.

4.2 Representations of the Poincaré Group for Charge-Monopole System: Pairwise LG

It has long been known that the simultaneous presence of a magnetic monopole and an electric charge results in unusual rotational properties. The first explicit statement of this came from J.J. Thomson [106] who found that the EM field of a system containing an electric charge e and magnetic charge g carries an angular momentum even when both charges are at rest:[2]

$$\vec{J}^{\,\text{field}} = \frac{1}{4\pi}\int d^3x\ \vec{x}\times\left(\vec{E}\times\vec{B}\right) = -eg\,\hat{r} \equiv -q\hat{r} \tag{4.4}$$

where $\hat{r}$ is a unit vector pointing from the magnetic monopole to the charge. Quantum mechanically, angular momentum is quantized in half integer units, and so we get yet another derivation of the Dirac quantization condition [41] $eg = n/2$.

The angular momentum of the electromagnetic field Eq. (4.4) was generalized to the case of dyons by Schwinger [91] and Zwanziger [117]

$$\vec{J}^{\,\text{field}} = \sum q_{ij}\,\hat{r}_{ij} \tag{4.5}$$

with the sum taken over all dyon pairs and

$$q_{ij} = e_i\,g_j - e_j\,g_i = \frac{n}{2}\,, \tag{4.6}$$

where the Dirac-Schwinger-Zwanziger quantization condition[3] for q_{ij} is once again implied

[2]Due to the appearance of E and B the field angular momentum must be proportional to eg. It is also a dimensionless vector for which the only candidate is $\hat{r}$, hence the result must be proportional to $eg\hat{r}$ which can be verified by explicit calculation [106].

[3]Sometimes this condition is given as $(e_i\,g_j - e_j\,g_i)/4\pi = \frac{n}{2}$. Here and throughout we normalize the magnetic charge such that Eq. (4.6) holds, and there is never a $(4\pi)^{-1}$ factor in the quantization condition.

by angular momentum quantization.

Zwanziger [119] further showed how to write the angular momentum for scattering dyons in a Lorentz covariant fashion

$$M^{\nu\rho}_{\text{field};\,\pm} \quad = \quad \pm \sum_{i>j} q_{ij} \, \frac{\epsilon^{\nu\rho\alpha\beta} \, p_{i\alpha} \, p_{j\beta}}{\sqrt{(p_i \cdot p_j)^2 - m_i^2 \, m_j^2}} \, , \tag{4.7}$$

where the sum is taken over all distinct dyon pairs in the initial state (final state) with a $+(-)$ sign. The origin of the unusual $\pm$ sign is the appearance of a $t/|t|$ in the asymptotic expression for M. In the non-relativistic limit, this expression reduces to $\vec{J}_{\pm}^{\,\text{field}} = \pm \sum q_{ij} \, \hat{p}_{ij}$, where $\hat{p}_{ij}$ is the relative 3-momentum between the dyons in each pair. Since asymptotically $\hat{p} \cdot \hat{r} = \mp 1$, this exactly reproduces Eq. (4.5).

The physical implications of (4.4)-(4.5) are hard to overstate. They imply the following unusual properties of charge-monopole (or general dyonic) systems:

- The conserved angular momentum for the interacting theory is different from the angular momentum of the free theory
- As a consequence, the asymptotic quantum states representing dyon pairs do not completely factorize into single-particle states
- In general there is no crossing symmetry for the electric-magnetic S-matrix

The first and second points can be immediately understood. Since the angular momentum of the EM field depends only on q_{ij} and does not depend on the relative distance (just orientation) this term does not vanish no matter how far the charge and the monopole are separated, hence the direct product of two single-particle states never captures this additional

contribution to the angular momentum. The third point will be elaborated below once we consider the LG transformation of the magnetic S-matrix.

4.2.1 Electric-Magnetic angular momentum: the NRQM case

Before jumping into our main topic, which is the representation of the Poincaré group and quantization of theories with magnetic charges, let us briefly remark on the NRQM case. Rather than defining the non-relativistic S-matrix in full generality, we show here how the conserved angular momentum operator $\vec{L}$ is modified in the presence of magnetic charges [77].

The Hamiltonian of a charged particle in the background field of a stationary monopole is given by

$$H = -\frac{1}{2m}\left(\vec{\nabla} - ie\vec{A}\right)^2 + V(r) = -\frac{1}{2m}\vec{D}^2 + V(r) \tag{4.8}$$

where $\vec{D} = \vec{\nabla} - ie\vec{A}$ and $\vec{A}$ is the vector potential for the monopole, defined most conveniently using two coordinate-patches in [115]. Specifically, with the monopole at the origin, $A_\phi = \frac{\pm g}{r\sin\theta}(1 \mp \cos\theta)$ on each of the patches, usually chosen to be the upper (lower) hemisphere in the monopole rest frame. One can easily check that the usual particle definition of the angular momentum $\vec{L} = -i\vec{r} \times \vec{D}$ does not satisfy the angular momentum algebra

$$[L_i, L_j] = i\epsilon_{ijk}L_k \tag{4.9}$$

$$[L_i, H] = 0\,. \tag{4.10}$$

This algebra, however, is satisfied once the angular momentum operator is generalized to include a term that depends both on electric and magnetic charges

$$\vec{L} = -i\vec{r} \times \vec{D} - eg\hat{r} = m\vec{r} \times \dot{\vec{r}} - eg\hat{r} \tag{4.11}$$

where $\hat{r} = \vec{r}/r$ is a unit vector pointing radially outward and we used the Heisenberg equation of motion $\dot{\vec{r}} = -i\vec{D}/m$ in the second equality. Hence for a charged particle moving in a monopole background, angular momentum must be supplemented with an additional term proportional to q corresponding to the contribution of the EM field. Importantly, the contribution of the EM field, as well as the total angular momentum, is non-vanishing even when $\dot{\vec{r}} = 0$ (i.e. in a situation where both the charged particle and the monopole are at rest).

This expression can be generalized to a quantum field theory in the the case of a 't Hooft-Polyakov monopole background. The 't Hooft-Polyakov monopole solution in an SU(2) gauge theory is not invariant either under spatial rotations or gauge transformations, however, it is invariant under a combined transformation generated by $\vec{L} + \frac{\vec{\tau}}{2}$ (recall that the solution for the scalar field is $\Phi_{\text{cl}} \propto \tau^a \hat{r}^a$). For a particle of spin S in a representation R of SU(2) and moving in the monopole background, the conserved angular momentum is given by

$$\vec{J} = \vec{L} + \vec{T}_R + \vec{S}\,, \tag{4.12}$$

where $\vec{T}_R$ are the SU(2) generators in the representation R. This expression is especially instructive for a particle in a doublet representation of the SU(2) (so that the electric charges under the unbroken U(1) are minimal). In the singular gauge where the magnetic field of the monopole points in the τ_3 direction in group space and the field contribution to the

angular momentum is $\pm 1/2$, we find an exact match to the NRQM result. In the relativistic quantum theory, this extra contribution gives rise to the additional LG phase, as we discuss below.

4.2.2 Pairwise LG

In order to properly understand the effect of the modified angular momentum operator on the construction of the quantum mechanical Hilbert space we first need to go back and understand the properties of multi-particle representations of the Poincaré group. It is well-known that for single particles one needs to define a reference momentum k, which may be chosen as $(M, 0, 0, 0)$ for massive particles or $(E, 0, 0, E)$ for massless particles. The LG is then the set of Lorentz transformations that leave the reference momenta invariant. For massive particles the LG is $SO(3) \sim \mathrm{SU}(2)$, while for massless particles it is ISO(2) the two dimensional Euclidean group. The nature of the particle we are describing thus determines the required representation of the LG. For example, given a massive particle the representation is specified by the mass and the spin, s, and the state in the Hilbert space is just $|k, s\rangle$. For the case of massless particles, while interesting non-trivial representations of ISO(2) are in principle allowed by the kinematics of the Lorentz group [90], the models needed to match experiment do not take advantage of the additional quantum number offered by using the entire ISO(2) group rather than just the $\mathrm{SO}(2) \sim \mathrm{U}(1)$ subgroup corresponding to ordinary helicity.

When considering the representations of the Poincaré group one usually stops here and assumes that multi-particle states transform as products of single particle states. However a closer examination of the Poincaré group shows that this is not the only possibility: as first pointed out by Zwanziger [119], there are rotations that leave the momenta of a pair of particles invariant. To see this, we can consider a two-particle state $|p_1, p_2\rangle$ and again

consider some reference momenta for this multi-particle state. The simplest choice is to go into the center of momentum (COM) frame

$$\begin{aligned} (k_1)_\mu &= (E_1^c, 0, 0, +p_c) \\ (k_2)_\mu &= (E_2^c, 0, 0, -p_c) \ , \end{aligned} \tag{4.13}$$

where

$$p_c = \sqrt{\frac{(p_1 \cdot p_2)^2 - m_1^2 m_2^2}{s}} \quad , \quad E_{1,2}^c = \sqrt{m_{1,2}^2 + p_{\rm c}^2} \, , \tag{4.14}$$

are Lorentz invariant, and $s = (E_1^c + E_2^c)^2$. A Lorentz boost L_p brings the reference momenta back into the arbitrary pair of original momenta $p_1 = L_p \, k_1, \ p_2 = L_p \, k_2$. The important observation is that there exists a non-trivial two-particle or pairwise LG which leaves these reference momenta unchanged — it is simply a rotation around the z-axis, corresponding to a U(1) pairwise LG. We would like to emphasize that this pairwise LG is independent of the usual one-particle LG: it describes the relative transformation of the two particle state compared to the product of the one-particle states. Hence the general two-particle state is characterized by the representations of the individual particles under the one-particle LG, as well as the additional U(1) charge, q_{12}, corresponding to the representation of the two-particle state under the pairwise LG. We call this charge the "pairwise helicity". Thus the state is $| \, p_1, p_2 \ ; \ \sigma_1, \sigma_2 \ ; \ q_{12} \, \rangle$. The p_1, p_2 are simply the individual momenta for each particle, and the σ_i are collective indices denoting the individual s_i^2, s_i^z for massive particles or the helicity h_i for massless ones. The novelty here is the additional quantum number q_{12}, which is associated with the particle *pair* rather than an individual particle. Under a Lorentz

transformation, this quantum state transforms as

$$U(\Lambda)\,|\,p_1,p_2\;;\;\sigma_1,\sigma_2\;;\;q_{12}\,\rangle\;=\;e^{i\,q_{12}\,\phi}\;\mathcal{D}_{\sigma_1'\,\sigma_1}\;\mathcal{D}_{\sigma_2'\,\sigma_2}\,|\,\Lambda p_1,\Lambda p_2\;;\;\sigma_1',\sigma_2'\;;\;q_{12}\,\rangle \tag{4.15}$$

where ϕ is the U(1) rotation angle corresponding to the pairwise LG, while the $\mathcal{D}$s' are representations of one-particle LG rotations for each of the two particles. For massive particles, the LG is just SU(2) and the $\mathcal{D}$ matrices are in the spin s_i representation of SU(2). For massless particles, the LG is U(1) and the $\mathcal{D}$s are the ordinary helicity phases $e^{ih_i\phi_i}$. We will show that this is indeed the right transformation for the spinless case. A construction valid for particle with arbitrary spin and state for any number of particles is presented in [30], showing that general multi-particle states are indeed charaterized by pairwise helicities in addition to the standard spin/helicity, and they transform according to Eq. (4.16).

This transformation rule can be derived in the usual way by applying Wigner's method of induced representations [113] , which we briefly summarize at the end of this subsection. But first we would like to ask what happens for the case of more than two particles. To that end it is sufficient to consider a three particle state. Clearly, its transformation includes a product of three representations of the one-particle LG. Each one-particle LG transformation leaves the momentum of the corresponding particle invariant. The three particle state also transforms as a product of representations under three pairwise LGs, each leaving the momenta of the corresponding pair invariant. However, there is no non-trivial subgroup of the Poincaré group that leaves invariant an arbitrary set of three momenta. Hence the three-particle LG is trivial and the Lorentz transformations of three particle states are fully characterized by their transformations under three single particle LGs and three pairwise LGs. This conclusion easily generalizes to all n-particle states: such states are characterized by n masses and spins, as well as $\binom{n}{2}$ pairwise U(1) helicities q_{ij}, $|\,p_1,p_2,\ldots,p_n\;;\;\sigma_1,\sigma_2,\ldots,\sigma_n\;;\;q_{12},q_{13},\ldots,q_{n-1,n}\,\rangle$

with Lorentz transformations given by

$$U(\Lambda)\,|\,p_1,\ldots,p_n\;;\;\sigma_1,\ldots,\sigma_n\;;\;q_{12},q_{13},\ldots q_{n-1,n}\,\rangle = \\ e^{i\sum_{i<j}q_{ij}\phi(p_i,p_j,\Lambda)}\;\prod_{i=1}^{n}\;\mathcal{D}^{i}_{\sigma_i'\sigma_i}|\,\Lambda p_1,\ldots,\Lambda p_n\;;\;\sigma_1',\ldots,\sigma_n'\;;\;q_{12},q_{13},\ldots,q_{n-1,n}\,\rangle \quad . \tag{4.16}$$

The exact representations of the pairwise LGs for multi-particle states, i.e. the helicities q_{ij}, depend on the dynamics of the theory. In most cases only trivial representations of the pairwise LGs arise and $q_{ij}=0$. The one known exception is a state containing both electric and magnetic charges. As we will see below, the action of the angular momentum operator requires in this case the identification $q_{ij}=e_ig_j-e_jg_i$, corresponding to the Dirac-Schwinger-Zwanziger quantization condition; the existence of EM field angular momentum implies that multi-particle states do not fully factorize into products of single particle states.

We conclude this subsection by reviewing the Wigner method of induced representations to derive Eq. (4.16) for the spinless case with two particles, following [113, 112, 119]. This also provides us with an explicit formula for the pairwise LG phase $\phi(p_i,p_j,\Lambda)$. We define our reference quantum states as

$$|\,k_1,k_2\;;\;q_{12}\,\rangle\,. \tag{4.17}$$

Having identified the effect of the pairwise LG on the reference states with a rotation around z-axis we have

$$J_z\;|\,k_1,k_2\;;\;q_{12}\,\rangle = q_{12}\,|\,k_1,k_2\;;\;q_{12}\,\rangle\,. \tag{4.18}$$

This equality correctly reproduces the EM field contribution to the angular momentum in Eqs. (4.5)-(4.7) provided that $q_{ij} = e_i g_j - e_j g_i$. Interestingly, this identification also directly implies the Dirac-Schwinger-Zwanziger condition for q_{12}, simply from the properties of the Lorentz group. To see this, note that due to the spinorial double coverings of the Lorentz group, any 4π rotation (rather than 2π) around $\hat{z}$ must be the identity,

$$e^{i4\pi q_{12}} = 1 \;\; \Rightarrow \;\; q_{12} \;\equiv\; e_1\, g_2 \,-\, e_2\, g_1 \;=\; \frac{n}{2},\; n \in \mathbb{Z}. \tag{4.19}$$

The quantum states for general momenta p_1, p_2 can be obtained from the reference pairwise state with a Lorentz boost

$$|\, p_1, p_2 \;;\; q_{12} \,\rangle \equiv U\,(L_p)\,|\, k_1, k_2 \;;\; q_{12} \,\rangle\,, \tag{4.20}$$

where $U(L_p)$ is a unitary operator representing the Lorentz boost L_p. We now wish to learn how a generic Lorentz transformation Λ acts on the states $|\, p_1, p_2 \,;\, q_{12} \,\rangle$. Proceeding as in the standard method of induced representations, we have

$$\begin{aligned} U(\Lambda)|\, p_1, p_2 \;;\; q_{12} \,\rangle \;&=\; U\,(L_{\Lambda p})\; U\left(L_{\Lambda p}^{-1} \Lambda L_p\right) |\, k_1, k_2 \;;\; q_{12} \,\rangle \\ &=\; U\,(L_{\Lambda p})\; U\,(W_{k_1,k_2})\,|\, k_1, k_2 \;;\; q_{12} \,\rangle, \end{aligned} \tag{4.21}$$

where $W_{k_1,k_2}(p_1, p_2, \Lambda) \equiv L_{\Lambda p}^{-1} \Lambda L_p = R_z\,[\phi(p_1, p_2, \Lambda)]$ is a LG transformation, which is nothing but a rotation around the z-axis with an angle $\phi(p_1, p_2, \Lambda)$. By definition, this LG

transformation acts on $|k_1, k_2\ ;\ q_{12}\rangle$ as $\exp\left[iq_{12}\phi(p_1, p_2, \Lambda)\right]$, so that

$$U(\Lambda)|\, p_1, p_2\ ;\ q_{12}\,\rangle = e^{iq_{12}\phi(p_1,p_2,\Lambda)}\ |\,\Lambda p_1, \Lambda p_2\ ;\ q_{12}\,\rangle. \tag{4.22}$$

We can easily see that the transformation rule for general multi-particle states in Eq. (4.16) is unitary and indeed forms a representation of the Lorentz group. First, since Eq. (4.16) only differs from the standard Lorentz transformation by a phase $e^{i\Sigma}$, this transformation is clearly unitary. Second, because the phase angles $\phi(p_i, p_j, \Lambda)$ are identical to the ones that arose as LG phases for the two-scalar case, and since they furnish a representation, we know that

$$\phi(p_i, p_j, \Lambda_2\Lambda_1) \ = \ \phi(\Lambda_1 p_i, \Lambda_1 p_j, \Lambda_2) + \phi(p_i, p_j, \Lambda_1)\,. \tag{4.23}$$

This proves that $U(\Lambda_2\Lambda_1) = U(\Lambda_2)\,U(\Lambda_1)$ and so our transformation rule is indeed a representation of the Lorentz group.

4.2.3 In- and Out-states for the Electric-Magnetic S-matrix

Now that we understand the general transformation properties of dyonic multi-particle states, we are ready to define the relativistic S-matrix for electric-magnetic scattering processes. To do this we have to first properly define the multi-particle *in*- and *out*- states. As usual, we separate the full Hamiltonian of the system into a free Hamiltonian, H_0, and an interaction:

$$H \ = \ H_0 \ + \ V\,. \tag{4.24}$$

In the standard definition, due to Weinberg [112], we can choose our quantum in/out states to be eigenstates of the full interacting Hamiltonian that approach free states[4] as $t \to \pm\infty$. However, in the case of electric-magnetic scattering, this definition has to be modified. This is because H_0 and H have *different* conserved angular momentum operators,

$$\left[H, \vec{J}\right] \;=\; \left[H_0, \vec{J}_0\right] \;=\; 0, \quad \vec{J} \;\neq\; \vec{J}_0\,. \tag{4.25}$$

The operator J_0 represents the total orbital and spin angular momentum of different particles, while J also includes the contribution of the EM field, as is evident from Eq. (4.7). The inequality of J and J_0 seems, so far, to be unique to electric-magnetic scattering. As a consequence the Lorentz group is represented differently[5] on the *in*- and *out*- eigenstates of H. This is simply a reflection of the fact that q_{ij} can be non-vanishing for the *in*- and *out* states, while the eigenstates of H_0 are simply the direct product states of the free one-particle states with all $q_{ij} = 0$.

In accordance with our discussion in section 4.2.2, we identify the multi-particle *in*- and *out*-states as the states transforming with definite values of q_{ij}:

$$U(\Lambda)\,|p_1, \ldots, p_n\,;\,\pm\rangle \quad = \quad \prod_i \mathcal{D}(W_i)\;|\Lambda p_1, \ldots, \Lambda p_n\,;\,\pm\rangle\, e^{\pm i\,\Sigma}\,, \tag{4.26}$$

where $\Sigma \equiv \sum_{i>j}^{n} q_{ij}\,\phi(p_i, p_j, \Lambda)$. Here, and below, '+' stands for 'in', and '−' stands for 'out', the $\mathcal{D}(W_i)$ are the one-particle LG transformations, while the $e^{\pm i\,\Sigma}$ is the additional phase factor corresponding to the pairwise LGs. Note that we need to choose opposite signs for

[4]Actually this language is not completely accurate since the in/out- states are conventionally defined in the Heisenberg picture and are time independent. For a rigorous definition of our S-matrix, see appendix D.

[5]The generator of boosts K is always represented on the *in*/*out* states differently from its representation on free states. The surprise here is the difference between *in*- and *out*- states, which is a unique consequence of $J \neq J_0$.

the pairwise LG phases for the *in*- and *out*- sates, in accordance with the extra sign showing up in the asymptotic expression (4.7). We see that the transformation rule Eq. (4.26) is a departure from Weinberg's standard definition of the S-matrix, in the sense that the Lorentz group is represented *differently* on *in*- and *out*- states.

4.2.4 Lorentz transformation of the electric-magnetic S-matrix

In the previous section, we presented the Lorentz transformation, Eq. (4.26), of multi-particle quantum states involving electric and magnetic charges. The general LG transformation for the S-matrix readily follows,

$$\begin{aligned} S\,(p'_1,\ldots,p'_m\,|\,p_1,\ldots,p_n) \;&\equiv\; \langle p'_1,\ldots,p'_m;\,-\,|\,p_1,\ldots,p_n;\,+\,\rangle \\ &=\; \big\langle p'_1,\ldots,p'_m;\,-\,|U(\Lambda)^\dagger\;U(\Lambda)|\,p_1,\ldots,p_n;\,+\,\big\rangle \\ &=\; e^{i(\Sigma_+ + \Sigma_-)}\;\prod_{i=1}^{m}\mathcal{D}(W_i)^\dagger\;\;\prod_{j=1}^{n}\mathcal{D}(W_j),\;\; S\,(\Lambda\,p'_1,\ldots,\Lambda\,p'_m\,|\,\Lambda\,p_1,\ldots,\Lambda\,p_n) \end{aligned} \tag{4.27}$$

where [6]

$$\Sigma_+ \equiv \sum_{i>j}^{n} q_{ij}\,\phi(p_i,p_j,\Lambda) \quad , \quad \Sigma_- \equiv \sum_{i>j}^{m} q_{ij}\,\phi(p'_i,p'_j,\Lambda)\,. \tag{4.28}$$

and W_i are the LG rotations for one-particle states in the *in*- and *out*- states. To go from the second to the third line, we used the fact that the extra U(1) LG factor has the same sign for $\langle out|$ and $|in\rangle$ states. Note that since $\Sigma_\pm$ pairs particles within the *in*- and *out*- states but doesn't involve in-out pairs, this is a manifest violation of crossing symmetry. Inverting

[6] Below we use the notation $\phi_{ij} = \phi(p_i,p_j,\Lambda)$ when it's clear whether we are talking about the *in*- or *out*-state.

Eq. (4.27), we have

$$\begin{aligned} &S\left(\Lambda\, p_1', \ldots, \Lambda\, p_m' \,|\, \Lambda\, p_1, \ldots, \Lambda\, p_n\right) \;\; = \\ &e^{-i\,(\Sigma_+ + \Sigma_-)} \prod_{i=1}^{m} \mathcal{D}(W_i) \prod_{j=1}^{n} \mathcal{D}(W_j)^\dagger \;\; S\left(p_1', \ldots, p_m' \,|\, p_1, \ldots, p_n\right) \end{aligned} \tag{4.29}$$

This transformation rule was first derived in [119]. If all $q_{ij} = 0$ (in particular, if none of the scattering particles have magnetic charge), the transformation rule Eq. (4.29) reduces to the standard LG transformation with $\Sigma_\pm = 0$. To construct the electric-magnetic S-matrix elements that satisfy the transformation rule given in Eq. (4.29) using on-shell methods we need to introduce a new kind of spinor-helicity variable that enables us to saturate the extra "electric-magnetic" U(1) phase in Eq. (4.29).

4.3 Pairwise Spinor-Helicity Variables for the Electric-Magnetic S-matrix

4.3.1 Standard spinor-helicity variables for the standard LG

In the spinor-helicity formalism without magnetic charges, we can directly write down the amplitude that transforms by construction as in Eq. (4.29) with $q = 0$. To do this, we construct the amplitude from contractions of the spinor-helicity variables. For a massless particle i, we use the spinor-helicity variables $|p_i\rangle_\alpha$ $[p_i|_{\dot\alpha}$, which transform under Lorentz transformations as

$$\Lambda_\alpha{}^\beta |p_i\rangle_\beta \;\; = \;\; e^{+\frac{i}{2}\phi(p_i,\Lambda)}\; |\Lambda p_i\rangle_\beta, \quad [p_i|_{\dot\beta}\; \tilde\Lambda^{\dot\beta}{}_{\dot\alpha} \;=\; e^{-\frac{i}{2}\phi(p_i,\Lambda)}\; [\Lambda p_i|_{\dot\alpha}\;, \tag{4.30}$$

where the phase $\phi(p_i, \Lambda)$ corresponds to the action of the one-particle LG for massless particles. For a derivation of this transformation rule, see for example [46, 59, 23]. In many cases we simply drop the p_i from the spinors and just use the notation $|i\rangle_\alpha \equiv |p_i\rangle_\alpha$ and $[i|_{\dot\alpha} \equiv [p_i|_{\dot\alpha}$. An S-matrix involving an outgoing massless particle i with helicity h_i has the correct LG phase for the i^{th} particle if we construct it from n_i copies of $|i\rangle_\alpha$ and $\tilde{n}_i$ copies of $[i|_{\dot\alpha}$, such that $\tilde{n}_i - n_i = 2\,h_i$.[7]

Similarly, an amplitude involving a massive particle j of spin s_j is constructed from $2s_j$ insertions of the *massive* spinor-helicity variables $|\mathbf{i}\rangle^I{}_\alpha$, with their spinor indices symmetrized. The indices I on the massive spinors indicate that they transform as doublets of the LG SU(2) for massive particles. These indices are usually suppressed, as they are only needed when taking the massless limit (specifying a value for the I index is like choosing a particular helicity in the massless limit). Note that the I indices are automatically symmetrized when one symmetrizes over the spinor indices α or $\dot\alpha$. We refer the reader to ref. [7] for a detailed discussion of the spinor-helicity formalism for massive particles.

4.3.2 Pairwise momenta

As we argued in the previous section, in the case of the electric-magnetic S-matrix[8], the transformation rule involves an additional pairwise LG phase associated with the angular momentum in the EM field, as can be seen in Eq. (4.29). Since this extra phase is associated with pairs of momenta p_i, p_j, it is not possible to reproduce the correct transformation rule using only the standard spinor-helicity variables $|i\rangle_\alpha$ and $[i|_{\dot\alpha}$ (or $|\mathbf{i}\rangle^I{}_\alpha$ and $[\mathbf{i}|^I_{\dot\alpha}$). This motivates us to the define a new kind of spinor-helicity variable associated with pairs of

[7]Notice that while $|p\rangle$ ($|p]$) carries a helicity weight $\pm 1/2$, as is evident from Eq. (4.29), for checking LG scaling of the S-matrix, we need to do $|p\rangle \to |\Lambda p\rangle \propto \omega^{-1}|p\rangle$ and $|p] \to |\Lambda p] \propto \omega|p]$, where ω is a helicity $+1/2$ factor.

[8]In our construction for electric-magnetic scattering we refer to the "S-matrix" rather than the usual scattering amplitude. The reason behind this is that in the magnetic case, selection rules sometimes forbid the appearance of the δ function in the standard relation $S_{\alpha\beta} = \delta(\alpha - \beta) - 2i\pi\delta^{(4)}(p_\alpha - p_\beta)\,\mathcal{A}_{\alpha\beta}$.

momenta p_i, p_j, which transform with the pairwise LG phase ϕ_{ij}. Importantly, the pairwise LG transformation of the S-matrix is always a U(1) phase, and so we need the new spinors to be *massless*, and associated with *null* momenta.

Since the extra LG factor for the electric-magnetic S-matrix is associated with the momenta p_i, p_j of each pair in the in/out- state, it is natural to define two null linear combinations of p_i, p_j, which we call the pairwise momenta[9] $p_{ij}^{\flat\pm}$. Below, we will define pairwise spinor-helicity variables associated with these pairwise momenta, and show that they have the correct pairwise LG weight to be used as building blocks for the electric-magnetic S-matrix. We first define the "reference" pairwise (null) momenta in the COM frame as

$$\left(k_{ij}^{\flat\pm}\right)_\mu \;=\; p_c\,(1,0,0,\pm 1)\;, \tag{4.31}$$

where p_c is the COM momentum of the ij pair, as in Eq. (4.14). The pairwise momenta $p_{ij}^{\flat\pm}$ in any other frame can be obtained by boosting $k_{ij}^{\flat\pm}$ into that frame. Clearly $k_{ij}^{\flat\pm}\cdot k_{ij}^{\flat\pm}=0$ and $k_{ij}^{\flat+}\cdot k_{ij}^{\flat-}=2p_c^2$, and these relations obviously hold in any other frame.

For reference, we also present the Lorentz covariant definition of $p_{ij}^{\flat\pm}$,

$$\begin{aligned} p_{ij}^{\flat+} &= \frac{1}{E_i^c+E_j^c}\left[\left(E_j^c+p_c\right)p_i-\left(E_i^c-p_c\right)p_j\right] \\ p_{ij}^{\flat-} &= \frac{1}{E_i^c+E_j^c}\left[\left(E_i^c+p_c\right)p_j-\left(E_j^c-p_c\right)p_i\right]\;. \end{aligned} \tag{4.32}$$

In the $m_i\to 0$ limit, we have $E_i^c\to p_c$ and so $p_{ij}^{\flat+}\to p_i$ and $p_{ij}^{\flat-}$ becomes Parity-conjugate

[9]The use of the label $\flat$ to denote null linear combinations of timelike momenta is inspired by the notation of [71] and of the OPP reduction [82] in the context of generalized unitarity [13, 49]. There, null combinations of external momenta were used in order to construct a null basis to span the internal loop momenta that have been put on shell.

of p_i. Similarly, in the $m_j \to 0$ limit, we have $E_j^c \to p_c$ and so $p_{ij}^{\flat -} \to p_j$ and $p_{ij}^{\flat +}$ becomes Parity-conjugate of p_j. By inverting these equations, we can express the massive momenta using the null momenta as

$$\begin{aligned} p_i &= \frac{1}{2p_c}\left[(E_i^c + p_c)\, p_{ij}^{\flat +} + (E_i^c - p_c)\, p_{ij}^{\flat -}\right] \\ p_j &= \frac{1}{2p_c}\left[\left(E_j^c + p_c\right) p_{ij}^{\flat -} + \left(E_j^c - p_c\right) p_{ij}^{\flat +}\right] . \end{aligned} \tag{4.33}$$

4.3.3 Pairwise spinor-helicity variables

We are now in a position to define spinor-helicity variables related to the pairwise momenta $p_{ij}^{\flat \pm}$. As we will show, these pairwise spinor-helicity variables transform with a U(1) LG phase directly related to the pairwise LG phase of the *in*- and *out*- states in Eq. (4.26). This makes them natural building blocks for the electric-magnetic S-matrix.

As a first step, note that linearity implies that the canonical Lorentz transformation L_p defined in Eq. (4.20) that takes $k_i \to p_i$ also gives

$$L_p\, k_{ij}^{\flat \pm} \quad = \quad p_{ij}^{\flat \pm} . \tag{4.34}$$

This is instrumental in proving that the pairwise spinor-helicity variables defined below transform with the same LG phase as the two-particle states in Eq. (4.22). The next step is

to define the reference pairwise spinor-helicity variables,

$$
\begin{aligned}
|k_{ij}^{\flat+}\rangle_\alpha &= \sqrt{2\,p_c}\begin{pmatrix}1\\0\end{pmatrix} \quad , \quad |k_{ij}^{\flat-}\rangle_\alpha = \sqrt{2\,p_c}\begin{pmatrix}0\\1\end{pmatrix} \\
\left[k_{ij}^{\flat+}\right|_{\dot\alpha} &= \sqrt{2\,p_c}\,(1\ \ 0) \quad , \quad \left[k_{ij}^{\flat-}\right|_{\dot\alpha} = \sqrt{2\,p_c}\,(0\ \ 1)\ .
\end{aligned}
\tag{4.35}
$$

These spinors are the "square roots" of the null reference momenta

$$
k_{ij}^{\flat\pm}\cdot\sigma_{\alpha\dot\alpha} \quad = \quad |k_{ij}^{\flat\pm}\rangle_\alpha\left[k_{ij}^{\flat\pm}\right|_{\dot\alpha}\ . \tag{4.36}
$$

The above relation is a standard mapping of a bi-spinor into a vector. Multiplying both sides by $\bar\sigma_\nu^{\dot\alpha\alpha}$ and taking the trace we can also write it in the form

$$
2\left(k_{ij}^{\flat\pm}\right)^\nu = \langle k_{ij}^{\flat\pm}|^\alpha\sigma^\nu_{\alpha\dot\alpha}\left|k_{ij}^{\flat\pm}\right]^{\dot\alpha}\ . \tag{4.37}
$$

While the LHS of this relation transforms with L_p under a Lorentz transformation, the helicity variables on the RHS transform with $(\mathcal{L}_p)_\alpha^{\ \beta}$ and $\left(\tilde{\mathcal{L}}_p\right)_{\ \dot\alpha}^{\dot\beta}$ appropriate for spinorial representation. Thus up to a LG invariant factor the pairwise spinors $p_{ij}^{\flat\pm}$ are defined by

$$
\begin{aligned}
|p_{ij}^{\flat\pm}\rangle_\alpha &= (\mathcal{L}_p)_\alpha^{\ \beta}\,|k_{ij}^{\flat\pm}\rangle_\beta \quad , \quad \left[p_{ij}^{\flat\pm}\right|_{\dot\alpha} = \left[k_{ij}^{\flat\pm}\right|_{\dot\beta}\left(\tilde{\mathcal{L}}_p\right)_{\ \dot\alpha}^{\dot\beta} \\
&.
\end{aligned}
\tag{4.38}
$$

This guarantees the relation

$$p_{ij}^{\flat\pm}\cdot\sigma_{\alpha\dot{\alpha}} \quad = \quad |p_{ij}^{\flat\pm}\rangle_{\alpha}\,\big[p_{ij}^{\flat\pm}\big|_{\dot{\alpha}}\,. \tag{4.39}$$

Following the same procedure as in the standard definition of spinor-helicity variables, it is straightforward to show that they transform with a U(1) LG factor as required, since

$$\Lambda_{\alpha}{}^{\beta}|p_{ij}^{\flat\pm}\rangle_{\beta} \quad = \quad e^{\pm\frac{i}{2}\phi(p_i,p_j,\Lambda)}\,|\Lambda p_{ij}^{\flat\pm}\rangle_{\alpha} \quad , \quad \big[p_{ij}^{\flat\pm}\big|_{\dot{\beta}}\,\tilde{\Lambda}^{\dot{\beta}}{}_{\dot{\alpha}} \;=\; e^{\mp\frac{i}{2}\phi(p_i,p_j,\Lambda)}\,\big[\Lambda p_{ij}^{\flat\pm}\big|_{\dot{\alpha}}\,. \tag{4.40}$$

Where $\Lambda_{\alpha}{}^{\beta}$ and $\tilde{\Lambda}^{\dot{\beta}}{}_{\dot{\alpha}}$ are the spinor versions of the Lorentz transformation Λ. Note that $|p_{ij}^{\flat+}\rangle_{\alpha}$ and $|p_{ij}^{\flat-}\rangle_{\beta}$ have *opposite* pairwise helicities $\pm 1/2$. Importantly, the LG phase $\phi(p_i,p_j,\Lambda)$ in Eq. (4.40) is defined with respect to the canonical Lorentz transformation L_p, which is the same as the one we used to derive the transformation rule of the quantum states in section 4.22. This proves that $\phi(p_i,p_j,\Lambda)$ is exactly the same phase as the one in Eq. (4.22). Consequently, we are free to use our pairwise spinor-helicity variables to construct an S-matrix that transforms correctly under the pairwise (and also one particle) LGs. Explicit expressions for spinor-helicity variables in the COM frame are given in appendix C. Here we simply present the main results in the $m_i \to 0$ limit:

$$\begin{aligned}
\big[p_{ij}^{\flat+}\,i\big] \;&=\; \big\langle i\,p_{ij}^{\flat+}\big\rangle \;=\; \big[\hat{\eta}_i\,p_{ij}^{\flat-}\big] \;=\; \big\langle p_{ij}^{\flat-}\,\hat{\eta}_i\big\rangle \;=\; 0 \\
\big[p_{ij}^{\flat-}\,i\big] \;&=\; \big\langle i\,p_{ij}^{\flat-}\big\rangle \;=\; \sqrt{2p_c}\,\big[\hat{\eta}_i\,p_{ij}^{\flat+}\big] \;=\; \sqrt{2p_c}\,\big\langle p_{ij}^{\flat+}\,\hat{\eta}_i\big\rangle \;=\; 2p_c\,,
\end{aligned} \tag{4.41}$$

where $|i\rangle_{\alpha}$, $[i|_{\dot{\alpha}}$ are the standard massless spinor-helicity variables, and $|\hat{\eta}_i\rangle_{\alpha}$, $[\hat{\eta}_i|_{\dot{\alpha}}$ are the

(dimensionless) Parity-conjugate massless spinors that appear in the massless limit of the massive spinors $|\mathbf{i}\rangle^I_\alpha$, $[\mathbf{i}|^I_{\dot\alpha}$ (see ref. [7] for their definition). Note that the above equations are Lorentz *and* LG invariant, and so hold in any other reference frame as well.

4.4 Constructing Electric-Magnetic S-matrices

In section 4.2.4 we derived the transformations of electric-magnetic S-matrices under the pairwise and one-particle LGs:

$$\begin{aligned} &S\left(\Lambda\, p'_1,\ldots,\Lambda\, p'_m\,|\,\Lambda\, p_1,\ldots,\Lambda\, p_n\right) \;=\\ &e^{-i\,(\Sigma_-+\Sigma_+)}\,\prod_{i=1}^{m}\mathcal{D}(W_i)\,\prod_{j=1}^{n}\mathcal{D}(W_j)^\dagger\;\; S\left(p'_1,\ldots,p'_m\,|\,p_1,\ldots,p_n\right) \end{aligned} \tag{4.42}$$

To make use of this transformation for constructing electric-magnetic S-matrix elements, we defined the pairwise spinor-helicity variables in section 4.3.3. Now we can use the pairwise and regular spinor-helicity variables to construct S-matrices that respect Eq. (4.42). This enables us to fix electric-magnetic S-matrix elements up to a LG invariant.

We also reiterate here that we are constructing electric-magnetic *S-matrix elements* rather than *amplitudes*. This is because by using the word "amplitude" we are implicitly assuming the possibility of forward scattering, as encoded in the standard relation

$$S_{\alpha\beta} \;=\; \delta(\alpha-\beta) \;-\; 2i\pi\delta^{(4)}(p_\alpha-p_\beta)\,\mathcal{A}_{\alpha\beta}\,. \tag{4.43}$$

However, in our very peculiar case of electric-magnetic scattering, the decomposition of Eq. (4.43) may not actually hold. In fact, we will see below that selection rules generically

forbid forward scattering for the lowest partial wave, which makes the relation Eq. (4.43) inadequate for electric-magnetic scattering. Rather than trying to adapt it to our case, we opt to never use this relation at all and just construct the S-matrix itself directly. Energy and momentum conservation are implicitly assumed.

In constructing the S-matrix we use an all-outgoing convention common in the amplitudes literature. However, the use of this convention in the study of magnetic S-matrix elements is non-trivial due to lack of crossing symmetry in electric-magnetic scattering. Thus we begin by reviewing the subtleties associated with the all-outgoing convention.

4.4.1 The all-outgoing convention

In section 4.2.4, we described how general electric-magnetic S-matrices transform under Lorentz transformations. In that section, the discussion was in terms of *in*- and *out*-states. In the spinor-helicity formalism it is however customary to use a notation where all particles are outgoing which we call the *out-out* formalism. In the standard cases without magnetic charges this is achieved using the crossing symmetry of the S-matrix. To define crossing symmetry, we first assume analyticity, namely, that the S-matrix is an analytic function of its complexified external momenta. Crossing symmetry is then the condition that the scattering S-matrix for a process with an in-state that includes particle A, and some out-state, has *the same* analytic form as the "crossed" versions of the original process, with an outgoing anti-particle $\bar{A}$. While in the original process, the particle appearing in the in-state carries positive energy, in the crossed process, the anti-particle $\bar{A}$ appearing in the out-state carries negative energy. However, crossing symmetry allows one to use the same analytic S-matrix element to also calculate the process with an outgoing anti-particle $\bar{A}$ in its physical kinematic regime. In the presence of crossing symmetry, a single analytic function provides the S-matrix for several different processes in different regions of complexified momentum

space. For massless particles, under crossing,

$$\begin{aligned} \text{particle} &\leftrightarrow \text{antiparticle} \\ \text{incoming} &\leftrightarrow \text{outgoing} \\ \text{helicity } h &\leftrightarrow -h \\ p^\mu &\leftrightarrow -p^\mu \end{aligned}$$

Since the S-matrix for electric-magnetic scattering processes does not obey crossing symmetry, one can not describe different processes using the same S-matrix element. Nevertheless, we can still use a *crossing transformation* to translate the problem formulated in *in-out* language into the *out-out* language, which is the conventional choice of the spinor-helicity community. This is possible because, as can be seen from Eq. (4.42), the LG transformation of an S-matrix involving incoming states with helicities h_i and pairwise helicities q_{ij} is the *same* as that of an S-matrix with outgoing states with helicities $-h_i$ and pairwise helicities q_{ij}.

Consequently, we are free to construct S-matrices in the *out-out* formalism, as long as we keep working in the same kinematic regime of the original *in-out* S-matrix. Furthermore, even in the *out-out* formalism, we consider pairwise helicities q_{ij} only for pairs of states which are both in the initial state or both in the final state for a given physical process.

4.4.2 Constructing the electric-magnetic S-matrix: spinor-helicity cheat sheet

We are now ready to formulate general rules for constructing electric-magnetic S-matrix elements. As usual in the amplitudes program, the spinor-helicity variables are the basic

building blocks. The main novelty is the appearance of the pairwise spinor-helicity variables, needed to capture the additional pairwise LG phase in the S-matrix, in addition to the ordinary ones. As usual, we will assign helicity weights (or for massive particles SU(2) quantum numbers) to each spinor-helicity variable, as well as a *separate* pairwise helicity weights to each pairwise spinor-helicity variable. We will require that the helicity weights under each individual particle as well as the pairwise helicity weights are matched for both the initial and the final states. Of course only the diagonal Lorentz transformation (where each particle and each pair of particles are transformed simultaneously) is physical. However, as is common in the amplitudes approach, as a book-keeping tool we can pretend that helicity and pairwise helicity transformations can be performed independently on each particle/pair of particles, which will make the construction of the properly transforming S-matrix particularly easy. Hence for the pairwise helicity variable we assign *only* the pairwise helicity (and no ordinary helicities), even though these pairwise spinor-helicity variables are constructed as a function of the ordinary helicity variables, and in some limits they even coincide with one of the ordinary spinor-helicity variables.[10]

These rules are summarized by the following equations.

$$S\left(\omega^{-1}|i\rangle, \omega|i]\right) = \omega^{2h_i} S\left(|i\rangle, |i]\right), \quad \text{for } \forall i \tag{4.44}$$

$$S\left(\omega^{-1}|p_{ij}^{\flat+}\rangle, \omega|p_{ij}^{\flat+}], \omega|p_{ij}^{\flat-}\rangle, \omega^{-1}|p_{ij}^{\flat-}]\right) = \omega^{-2q_{ij}} S\left(|p_{ij}^{\flat+}\rangle, |p_{ij}^{\flat+}], |p_{ij}^{\flat-}\rangle, |p_{ij}^{\flat-}]\right) \quad \text{for } \forall \text{ pair } \{i,j\}, \tag{4.45}$$

where ω represents the LG weight $+1/2$. The resulting rules for the full set of charge assignments of the spinor-helicity variables are presented in Table 4.1, which summarizes

[10] In the massless limit, the regular LG phase coincides with the pairwise phase, and LG weights of some of the regular variables are used to match the regular LG weights, while the rest are used to saturate the pairwise LG weight.

the different LG weights of the regular and pairwise spinor-helicity variables, as well as the overall weights of the amplitude implied from Eq. (4.44) and (4.45).

	$\mathrm{U}(1)_i$	$\mathrm{SU}(2)_i$	$\mathrm{U}(1)_{ij}$
Required weight	h_i	$\mathbf{S}_i$	$-q_{ij}$
$\lvert i\rangle_\alpha,\ [i]_{\dot\alpha}$	$-\frac{1}{2}\,,\ \frac{1}{2}$	–	–
$\langle \mathbf{i}\rvert^{I;\alpha}$	–	$\square$	–
$\lvert p_{ij}^{\flat+}\rangle_\alpha,\ \big[p_{ij}^{\flat+}\big]_{\dot\alpha}$	–	–	$-\frac{1}{2}\,,\ \frac{1}{2}$
$\lvert p_{ij}^{\flat-}\rangle_\alpha,\ \big[p_{ij}^{\flat-}\big]_{\dot\alpha}$	–	–	$\frac{1}{2}\,,\ -\frac{1}{2}$

Table 4.1: LG weights of the standard and pairwise spinor-helicity variables, as well as the overall weight required by Eq. (4.44) and (4.45).

4.4.3 First examples

To illustrate the construction of electric-magnetic S-matrix elements, let us work out a few examples.

(1) Massive fermion decaying to massive fermion + massless scalar, $q = -1$.
In this case we need to use one massive spinor for the decaying fermion and one massive spinor for the final fermion. This gives us two spinor indices that should be contracted with pairwise spinors. Note that in general, the number of pairwise spinors is not completely fixed by the LG: only the difference $n_{23}^- - n_{23}^+$ between the number of pairwise spinors with weight $\frac{1}{2}$ and $-\frac{1}{2}$ is fixed to be $-2q_{23}$. In our case we need a total of 2 spinor indices and so $n_{23}^+ = 2$, $n_{23}^- = 0$. The S-matrix is then

$$S\left(\mathbf{1}^{s=1/2}\,|\,\mathbf{2}^{s=1/2}, 3^0\right)_{q_{23}=-1} \quad\sim\quad \left\langle p_{23}^{\flat-}\,\mathbf{1}\right\rangle \left\langle p_{23}^{\flat-}\,\mathbf{2}\right\rangle\,, \tag{4.46}$$

up to a LG invariant.[11]

(2) Massive scalar decaying to massive scalar + massless vector, $q = -1$.

In this case we need to use two regular spinor-helicity variables for the helicity of the vector, as well as two pairwise spinors for the $q_{23} = -1$ of the final state. The S-matrix elements for helicity ± 1 vectors are then

$$S\left(\mathbf{1}^{s=0} \,|\, \mathbf{2}^{s=0}, 3^{+1}\right)_{q_{23}=-1} \quad \sim \quad \left[p_{23}^{\flat+}\, 3\right]^2 \sim \left\langle p_{23}^{\flat-}|2|3\right]^2 , \tag{4.47}$$

up to a LG invariant. On the other hand, there is no way to write a LG covariant expression for $S\left(\mathbf{1}^{s=0} \,|\, \mathbf{2}^{s=0}, 3^{-1}\right)_{q_{23}=-1}$. We will see later that this is a particular example of a more general LG *selection rule*.

(3) Massive vector decaying to two different massless fermions, $q = -2$.

In this case we need to use 2 massive spinors for the vector and one regular spinor-helicity variable for each fermion, as well as four pairwise spinors for the $q_{23} = -2$ of the out state. The S-matrix for opposite helicity fermions is then

$$S\left(\mathbf{1}^{s=1} \,|\, 2^{-1/2}, 3^{+1/2}\right)_{q_{23}=-2} \quad \sim \quad \left\langle 2 p_{23}^{\flat-}\right\rangle \left[p_{23}^{\flat+}\, 3\right] \left\langle \mathbf{1}\, p_{23}^{\flat-}\right\rangle^2 . \tag{4.48}$$

up to a LG invariant. Note that the S-matrix for same helicity fermions[12] is forbidden in this case, due to the fact that $\left\langle p_{23}^{\flat-} 3\right\rangle = \left[p_{23}^{\flat+} 2\right] = 0$. This is our second encounter with a LG

[11] In principle, there are other "legally" acceptable expressions such as $\left[p_{23}^{\flat+}\mathbf{1}\right]\left[p_{23}^{\flat+}\mathbf{2}\right]$ or $\left[p_{23}^{\flat+}\mathbf{1}\right]\left\langle p_{23}^{\flat-}\mathbf{2}\right\rangle$ or $\left\langle p_{23}^{\flat-}\mathbf{1}\right\rangle\left[p_{23}^{\flat+}\mathbf{2}\right]$. However, using the Dirac equations for the massive variable, $p_{\alpha\dot\alpha}\tilde\lambda^{\dot\alpha I} = m\lambda_\alpha^I$ and $p_{\alpha\dot\alpha}\lambda_{\alpha I} = -m\tilde\lambda_{\dot\alpha}^I$, one can check that these are equivalent to Eq. (4.46) up to LG invariants.

[12] In the all-*outgoing* sense.

selection rule.

(4) Massive vector decaying to two different massless fermions, $q = -1$.
In this case we need to use 2 massive spinors for the vector and one regular spinor-helicity variable for each fermion, as well as four pairwise spinors for the $q_{23} = -1$ of the out state. Note that unlike the previous examples, here the total number of pairwise spinors is *not* given by $-2q_{23}$. This is because there are four spinor indices from the standard spinors that need to be contracted, so that $n_{23}^{+} + n_{23}^{-} = 4$. Pairwise LG, on the other hand, implies $n_{23}^{+} - n_{23}^{-} = -2q_{23} = 2$, and so we have $n_{23}^{+} = 3$, $n_{23}^{-} = 1$. The S-matrix for positive helicity fermions is then

$$S\left(\mathbf{1}^{s=1} \,|\, 2^{-1/2}, 3^{-1/2}\right)_{q_{23}=-1} \quad \sim \quad \left\langle 2 p_{23}^{\flat -} \right\rangle \left\langle p_{23}^{\flat +}\, 3 \right\rangle \left\langle \mathbf{1}\, p_{23}^{\flat -} \right\rangle^2 . \tag{4.49}$$

up to a LG invariant. Note that the S-matrix for $h_2 = -h_3 = 1/2$ is forbidden in this case, due to the fact that $\left[p_{23}^{\flat -} 3\right] = 0$.

4.4.4 All electric-magnetic 3-point S-matrix elements

The examples above give us a flavor of how to construct electric-magnetic S-matrix elements up to LG invariants. In the case of 3-point S-matrix elements, we can make the discussion even more concrete and write down systematic expressions and selection rules for electric-magnetic S-matrix elements. These are modifications of the general 3-point amplitudes derived in [7], when the three scattering particles can have magnetic charge. Without loss of generality, we choose one massive particle (that may be a dyon) in the incoming state, and two particles (that may also be dyons) in the outgoing state. Note that our expressions extend the ones presented in [7] to the case of electric-magnetic scattering, and reduce to

them when $q = 0$ for the outgoing states. Below, whenever we call a particle "dyon", we mean that it may, or may not, have a magnetic charge. In all our cases, the decaying particle may be any kind of "dyon".

• *Incoming massive particle, two outgoing massive particles*

In this case the S-matrix is the contraction of the massive part (in the notation of [7])

$$\left(\langle \mathbf{1}|^{2s_1}\right)^{\{\alpha_1 \ldots \alpha_{2s_1}\}} \left(\langle \mathbf{2}|^{2s_2}\right)^{\{\beta_1 \ldots \beta_{2s_2}\}} \left(\langle \mathbf{3}|^{2s_3}\right)^{\{\gamma_1 \ldots \gamma_{2s_3}\}} \tag{4.50}$$

with a massless part involving the pairwise spinors $|w\rangle_\alpha \equiv |p_{23}^{\flat -}\rangle_\alpha$ and $|r\rangle_\alpha \equiv |p_{23}^{\flat +}\rangle_\alpha$ (with pairwise helicities $\pm\frac{1}{2}$), which saturates the pairwise LG transformation. The most general expression is

$$S^q_{\{\alpha_1,\ldots,\alpha_{2s_1}\}\{\beta_1,\ldots,\beta_{2s_2}\}\{\gamma_1,\ldots,\gamma_{2s_3}\}} \;=\; \sum_{i=1}^{C} a_i \left(|w\rangle^{\hat{s}-q} |r\rangle^{\hat{s}+q}\right)_{\{\alpha_1,\ldots,\alpha_{2s_1}\}\{\beta_1,\ldots,\beta_{2s_2}\}\{\gamma_1,\ldots,\gamma_{2s_3}\}}, \tag{4.51}$$

where $\hat{s} = s_1 + s_2 + s_3$, C counts all the possible ways to group the spinors into α, β and γ indices, and $q = q_{23} = e_2 g_3 - e_3 g_2$. Since both exponents have to be non-negative integers, we get a *selection rule*:

$$|q| \leq \hat{s} \ . \tag{4.52}$$

We can also check that Eq. (4.51) reduces to the standard expression from [7] for $q = 0$. To

see this, note that

$$\begin{aligned}
(\,|w\rangle\,|r\rangle\,)_{\{\alpha\beta\}} &\sim \mathcal{O}_{\{\alpha\beta\}} \equiv (p_2)_{\{\alpha\dot{\gamma}}\,(p_3)_{\beta\}}{}^{\dot{\gamma}} \\
(\,|w\rangle\,|r\rangle\,)_{[\alpha\beta]} &\sim \varepsilon_{\alpha\beta}\,.
\end{aligned} \tag{4.53}$$

where the two index tensors $\mathcal{O}_{\{\alpha\beta\}}$ were defined in [7]. This can be seen from Eq. (4.33), i.e.

$$(p_2)_{\{\alpha\dot{\gamma}}\,(p_3)_{\beta\}}{}^{\dot{\gamma}} = \frac{E_2^c + E_3^c}{2p_c}\,\left(p_{23}^{\flat+}\right)_{\{\alpha\dot{\gamma}}\,\left(p_{23}^{\flat-}\right)_{\beta\}}{}^{\dot{\gamma}} = (E_2^c + E_3^c)\,(\,|w\rangle\,|r\rangle\,)_{\{\alpha\beta\}}\,. \tag{4.54}$$

When $q = 0$, we get Eq. (4.27) of [7],

$$S^0_{\{\alpha_1,\ldots,\alpha_{2s_1}\}\{\beta_1,\ldots,\beta_{2s_2}\}\{\gamma_1,\ldots,\gamma_{2s_3}\}} = \sum_{i=0}^{1} \tilde{a}_i\,\left(\mathcal{O}^{\hat{s}-i}\varepsilon^i\right)_{\{\alpha_1,\ldots,\alpha_{2s_1}\}\{\beta_1,\ldots,\beta_{2s_2}\}\{\gamma_1,\ldots,\gamma_{2s_3}\}}. \tag{4.55}$$

• *Incoming massive particle, outgoing massive particle + massless particle; unequal mass case.*

This is the electric-magnetic version of the two massive, one massless S-matrix from [7]. In this case the S-matrix is the contraction of the massive part

$$\left(\langle\mathbf{1}|^{2s_1}\right)^{\{\alpha_1\ldots\alpha_{2s_1}\}}\left(\langle\mathbf{2}|^{2s_2}\right)^{\{\beta_1\ldots\beta_{2s_2}\}}, \tag{4.56}$$

with the massless part constructed from two "regular" spinors:

$$(|u\rangle_\alpha, |v\rangle_\alpha) \;=\; (|3\rangle_\alpha, |\,2\,|3]_\alpha)\;, \tag{4.57}$$

with regular LG weights $\mp\frac{1}{2}$, as well as the pairwise spinors

$$(|w\rangle_\alpha, |r\rangle_\alpha) \;=\; \left(|p_{23}^{\flat-}\rangle_\alpha, |p_{23}^{\flat+}\rangle_\alpha\right)\;, \tag{4.58}$$

with pairwise LG weights $\pm\frac{1}{2}$. Note that $|\,2\,|p_{23}^{\flat-}]_\alpha$ is nothing but a LG invariant times $|p_{23}^{\flat+}\rangle_\alpha$.

The general massive 3-point S-matrix for an initial spin s_1 particle and an final spin s_2 particle is then

$$\begin{aligned} S^{h,q,\text{ unequal}}_{\{\alpha_1,\ldots,\alpha_{2s_1}\}\{\beta_1,\ldots,\beta_{2s_2}\}} \;=\; & \sum_{i=1}^{C}\sum_{j,k} a_{ijk}\,\langle ur\rangle^{\max(j+k,0)}\,\langle vw\rangle^{\max(-j-k,0)} \\ & \left(|u\rangle^{\frac{\hat{s}}{2}-h-j}|v\rangle^{\frac{\hat{s}}{2}+h+k}|w\rangle^{\frac{\hat{s}}{2}-q+j}|r\rangle^{\frac{\hat{s}}{2}+q-k}\right)_{\{\alpha_1,\ldots,\alpha_{2s_1}\}\{\beta_1,\ldots,\beta_{2s_2}\}}\,, \end{aligned} \tag{4.59}$$

where $\hat{s} = s_1 + s_2$, and $q = q_{23} = e_2g_3 - e_3g_2$. Again C is the number of distinct tensor structures. The j and k sums are over values that give non-negative exponents. In particular, they are in the intervals $-\frac{\hat{s}}{2}+q \le j \le \frac{\hat{s}}{2}-h$ and $-\frac{\hat{s}}{2}-h \le k \le \frac{\hat{s}}{2}+q$. These intervals exist only if $|h+q| \le \hat{s}$, which gives us a *selection rule*. In particular,

$$s_1 \;=\; s_2 \;=\; 0 \;\;\rightarrow\;\; h \;=\; -\,q\,. \tag{4.60}$$

• *Incoming massive particle, outgoing massive particle + massless particle; equal mass case.*

When the two masses are equal, we know that $\langle uv\rangle \propto p_2 \cdot p_3 = 0$, hence, u and v are parallel. For constructing the S-matrix, therefore, we use only one of the two, say $|u\rangle$. However, the ratio x of the two is defined via[13]

$$m\, x|u\rangle \;=\; |v\rangle\,, \tag{4.62}$$

and carries regular helicity of +1 for the particle 3, and can be used to satisfy the regular helicity weight of the S-matrix. Similarly, $\langle wr\rangle = 0$ and we have the relation

$$\langle ur\rangle^2\; x|w\rangle \;\sim\; |r\rangle\,, \tag{4.63}$$

up to an overall LG invariant. Overall, the S-matrix is then constructed using $x, |u\rangle_\alpha, |w\rangle_\alpha$ and $\epsilon_{\alpha\beta}$. A solution consistent with the regular/pairwise helicity weight and the number of required spinor indices is found to be

$$\begin{aligned} S^{h,q,\text{equl}}_{\{\alpha_1\ldots\alpha_{2s_1}\}\{\beta_1\ldots\beta_{2s_2}\}} \quad = \quad & \sum_{i=1}^{C}\sum_{j}\sum_{k=-j}^{j} x^{h+q+j}\; \langle ur\rangle^{\max[2q+j-k,0]}\; \langle vw\rangle^{\max[-2q-j+k,0]}\;\cdot \\ & \big(|u\rangle^{j+k}|w\rangle^{j-k}\epsilon^{\hat{s}-j}\big)_{\{\alpha_1\ldots\alpha_{2s_1}\}\{\beta_1\ldots\beta_{2s_2}\}}\,, \end{aligned} \tag{4.64}$$

[13] An alternative expression for this x-factor can be written as [7]

$$x \;=\; \frac{\langle\zeta|2|3]}{m\,\langle\zeta 3\rangle}\,, \tag{4.61}$$

where $\langle\zeta|$ is an arbitrary spinor which drops out of any physical calculation.

where the j sum extends over $0 \leq j \leq \hat{s}$. Note that while the powers of u, w, ϵ have to be non-negative integers, there is no such requirement for the power of x.

• *Incoming massive particle, two outgoing massless particles*

In this case the S-matrix is the contraction of the massive part

$$\left(\langle \mathbf{1}|^{2s}\right)^{\{\alpha_1 \ldots \alpha_{2s}\}} \tag{4.65}$$

with a massless part involving the regular spinors $|u\rangle_\alpha = |2\rangle_\alpha$, $|v\rangle_\alpha = |3\rangle_\alpha$ and the pairwise spinors $|w\rangle_\alpha = |p_{23}^{\flat -}\rangle_\alpha$ and $|r\rangle_\alpha = |p_{23}^{\flat +}\rangle_\alpha$. The most general expression is

$$\begin{aligned} S^q_{\{\alpha_1,\ldots,\alpha_{2s}\}} \;=\; \sum_{ij}\; a_{ij}\; \left(|u\rangle^{s/2-i-\Delta}\; |v\rangle^{s/2-j+\Delta}\; |w\rangle^{s/2+j-q}\; |r\rangle^{s/2+i+q}\right)_{\{\alpha_1,\ldots,\alpha_{2s}\}} \cdot \\ [uv]^{\max[\Sigma+(s-i-j)/2\,,0]}\; \langle uv\rangle^{\max[-\Sigma-(s+i+j)/2\,,0]}\; \left(\langle uw\rangle\,[vr]\right)^{\frac{1}{2}\max[i-j\,,0]}\; \left([uw]\,\langle vr\rangle\right)^{\frac{1}{2}\max[j-i\,,0]}\,, \end{aligned} \tag{4.66}$$

with $\Sigma = h_2 + h_3$, $\Delta = h_2 - h_3$. Again $q = q_{23} = e_2 g_3 - e_3 g_2$, and the i and j sums are over values in the intervals $-s/2 - q \leq\; i \;\leq s/2 - \Delta$ and $-s/2 + q \leq\; j \;\leq s/2 + \Delta$, such that all of the exponents are non-negative integers. These intervals exists only when $|\Delta - q| \leq s$, which gives us another *selection rule*. In the non-magnetic $q = 0$ case, this gives us the same

selection rule as [7]. In particular, for a spin s coupling to $h_2 = -h_3$, we have

$$\begin{aligned}
&\text{For } q = 0 \ : \\
&s \ = \ 0 \ \ \rightarrow \ \ h_2 \ = \ h_3 \ = \ 0 \\
&s \ = \ 1 \ \ \rightarrow \ \ |h_2 \, - \, h_3| \ \leq \ 1 \ \ \rightarrow \ \ |h_2| = |h_3| \leq 1/2 \\
&s \ = \ 2 \ \ \rightarrow \ \ |h_2 \, - \, h_3| \ \leq \ 2 \ \ \rightarrow \ \ |h_2| = |h_3| \leq 1
\end{aligned} \tag{4.67}$$

in other words, massless particles with $|h| > \frac{1}{2}$ cannot couple to a Lorentz covariant conserved current, and massless particles with $|h| > 1$ cannot couple to a conserved stress tensor. For $q \neq 0$, the situation is even more restrictive. For example, when $|q| = \frac{1}{2}$ we have

$$\begin{aligned}
&\text{For } q = \pm 1/2 \ : \\
&s \ = \ 0 \ \ \rightarrow \ \ \text{forbidden} \\
&s \ = \ 1 \ \ \rightarrow \ \ |h_2 \, - \, h_3 \mp 1/2| \ \leq \ 1 \ \ \rightarrow \ \ |h_2| \ = \ |h_3| \ = \ 0 \quad \text{or} \ \ h_2 = -h_3 = \pm 1/2 \\
&s \ = \ 2 \ \ \rightarrow \ \ |h_2 \, - \, h_3 \mp 1/2| \ \leq \ 2 \ \ \rightarrow \ \ |h_2| \ = \ |h_3| \ \leq \ 1/2 \ \ \text{or} \ \ h_2 = -h_3 = \pm 1 \, .
\end{aligned} \tag{4.68}$$

We see that for $|q| = 1/2$ the selection rule is more restrictive than in the $q = 0$ case, since it discards the $h_2 = -h_3 = -qs$ option.

4.5 Partial Wave Decomposition for $2 \to 2$ Electric-Magnetic S-matrix

Following [7] and [67], we can now perform a relativistic partial wave decomposition for $2 \to 2$ electric-magnetic S-matrix elements[14]. In a Poincaré invariant setting, the partial wave decomposition is nothing but the expansion in a complete eigenbasis of the Casimir operator W^2, where W^μ is the Pauli-Lubanski operator defined by

$$W^\mu \equiv \frac{1}{2}\,\epsilon_{\mu\nu\rho\sigma}\,P^\nu\,M^{\rho\sigma}\,. \tag{4.69}$$

In the above expression P^ν is the momentum operator and $M^{\rho\sigma}$ is the Lorentz generator. The eigenvalues of W^2 are given by $-P^2\,J\,(J+1)$ where J is the total angular momentum, so clearly this is the relativistic version of a partial wave decomposition. The operators P^μ, $M^{\mu\nu}$ and W_μ act on the *amplitude* or parts of it. In particular, we will make use of their representation as differential operators acting in spinor-helicity space [114]. In the non-magnetic case and for massless particles, these are given by [114, 27]

$$\begin{aligned}
(\sigma_\mu)_{\alpha\dot\alpha}\;P^\mu \quad &\equiv \quad P_{\alpha\dot\alpha} \;=\; \sum_i |i\rangle_\alpha\,[i|_{\dot\alpha} \\
(\sigma_{\mu\nu})_{\alpha\beta}\;M^{\mu\nu} \quad &\equiv \quad M_{\alpha\beta} \;=\; i\sum_i |i\rangle_{\{\alpha}\,\frac{\partial}{\partial\langle i|^{\beta\}}} \\
(\bar\sigma_{\mu\nu})_{\dot\alpha\dot\beta}\;M^{\mu\nu} \quad &\equiv \quad \tilde M_{\dot\alpha\dot\beta} \;=\; i\sum_i [i|_{\{\dot\alpha}\,\frac{\partial}{\partial\,|i]^{\dot\beta\}}}\,,
\end{aligned} \tag{4.70}$$

[14]For a complementary approach to mapping all possible spinor structures for 4-point non-magnetic amplitudes, see [45]

where the sum i is over a collection of particles. In the $2 \to 2$ case we are interested in the total angular momentum of particles 1 and 2, and so the sum will be over $i = 1, 2$. The generalization of Eq. (4.70) for massive particles is straightforward [27, 56]: we bold the spinors and contract their SU(2) LG indices. The Casimir operator W^2 is then expressible as [27, 67]

$$W^2 \;=\; \frac{P^2}{8}\,\left[\mathrm{Tr}\left(M^2\right) \,+\, \mathrm{Tr}\left(\tilde{M}^2\right)\right] \,-\, \frac{1}{4}\,\mathrm{Tr}\left(M\,P\,\tilde{M}\,P^{\mathrm{T}}\right)\,. \tag{4.71}$$

Eq. (4.70) can be straightforwardly generalized to our electric-magnetic case by treating the regular and pairwise spinors on the same footing:

$$\begin{aligned}
(\sigma_{\mu\nu})_{\alpha\beta}\; M^{\mu\nu} \quad &\equiv \quad M_{\alpha\beta} \;=\; i\,\left[\sum_i |i\rangle_{\{\alpha}\,\frac{\partial}{\partial\langle i|^{\beta\}}} \,+\, \sum_{i>j,\pm} |p_{ij}^{\flat\pm}\rangle_{\{\alpha}\,\frac{\partial}{\partial\langle p_{ij}^{\flat\pm}|^{\beta\}}}\right] \\
(\bar{\sigma}_{\mu\nu})_{\dot{\alpha}\dot{\beta}}\; M^{\mu\nu} \quad &\equiv \quad \tilde{M}_{\dot{\alpha}\dot{\beta}} \;=\; i\,\left[\sum_i [i|_{\{\dot{\alpha}}\,\frac{\partial}{\partial\,|i]^{\dot{\beta}\}}} \,+\, \sum_{i>j,\pm} \left[p_{ij}^{\flat\pm}\right|_{\{\dot{\alpha}}\,\frac{\partial}{\partial\left|p_{ij}^{\flat\pm}\right]^{\dot{\beta}\}}}\right]\,,
\end{aligned} \tag{4.72}$$

where the sum is now over all pairs as well as individual particles in the state. It is easy to see that

$$W^2\,\langle 12\rangle \;=\; W^2\,\left\langle p_{12}^{\flat\pm} 2\right\rangle \;=\; W^2\,\left\langle p_{12}^{\flat\pm} 1\right\rangle \;=\; W^2\,\left\langle p_{12}^{\flat\pm} p_{12}^{\flat\mp}\right\rangle \;=\; 0\,, \tag{4.73}$$

with W^2 the Casimir associated with particles 1 and 2 and defined via Eq. (4.72). Similarly,

$$W^2\,|\,1\,\rangle_{\{\alpha}\,|p_{12}^{\flat-}\rangle_{\beta\}} \;=\; -\,s\,1(1+1)\,|\,1\,\rangle_{\{\alpha}\,|p_{12}^{\flat-}\rangle_{\beta\}}\,. \tag{4.74}$$

In other words, the eigenfunctions of W^2 are combinations of regular and pairwise spinors with symmetrized spinor indices. The eigenvalues are $-s\,j\,(j+1)$ where j is just the number of uncontracted spinor indices, divided by 2. This is the same conclusion as in ref. [67], only with the inclusion of of pairwise spinors in the definition of W^2. It is now natural to expand the S-matrix in a complete eigenbasis of W^2 with eigenfunctions

$$W^2\ \mathcal{B}^J \ = \ -\,s\,J\,(J+1)\ \mathcal{B}^J\,. \tag{4.75}$$

Following [67], we call the $\mathcal{B}^J$ *basis amplitudes*. The most general expansion then reads

$$S_{12\to 34} \ = \ \mathcal{N}\sum_J (2J+1)\,\mathcal{M}^J(p_c)\,\mathcal{B}^J\,, \tag{4.76}$$

where $\mathcal{N}\equiv\sqrt{8\pi s}$ is a normalization factor and $\mathcal{M}^J(p_c)$ are coefficients[15] satisfying

$$W_{12}^2\ \mathcal{M}^J(p_c) \quad = \quad W_{34}^2\ \mathcal{M}^J(p_c) \ = \ 0\,. \tag{4.77}$$

The eigenfunctions $\mathcal{B}^J$ are then nothing but symmetrized products of spinors,

$$\mathcal{B}^J \ = \ C^{J;\,\text{in}}_{\{\alpha_1,\ldots,\alpha_{2j}\}}\,C^{J;\,\text{out};\ \{\alpha_1,\ldots,\alpha_{2j}\}}\,, \tag{4.78}$$

[15]We also added the factor $(2J+1)$ as part of normalization so that the partial wave unitarity equation is expressed in a simple form in terms of $\mathcal{M}^J(p_c)$ Eq. (4.111).

where

$$\begin{aligned} W_{12}^2\; C^{J;\,\text{in}}_{\{\alpha_1,\ldots,\alpha_{2J}\}} &= -\,s\,J\,(J+1)\,C^{J;\,\text{in}}_{\{\alpha_1,\ldots,\alpha_{2J}\}} \\ W_{34}^2\; C^{J;\,\text{out};\;\{\alpha_1,\ldots,\alpha_{2J}\}} &= -\,s\,J\,(J+1)\,C^{J;\,\text{out};\;\{\alpha_1,\ldots,\alpha_{2J}\}}\,. \end{aligned} \tag{4.79}$$

In the above expression W_{12}^2 and W_{34}^2 are the Casimir operators associated with particles 1,2 and 3,4, respectively. The coefficient functions $\mathcal{M}^J(p_c)$ are angular momentum singlets, and so they can only depend on the energy scale of the scattering, given by the COM momentum p_c. Inspired by the Wigner-Eckart theorem, we call them "reduced matrix elements". They contain the dynamical information of the scattering process, as opposed to the angular dependence that is fixed for every partial wave. The coefficients $C^{J;\,\text{in/out}}$, on the other hand, are generalized Clebsch-Gordan coefficients [67].[16] These coefficients are completely fixed by group theory, and we can easily find them using an elegant trick from [7, 67]. Simply put, the Clebsch-Gordan coefficient connecting the particles i and j to the total angular momentum J is directly extracted from the 3-point S-matrix element with the particles i and j and a massive, spin J particle. For example, if 1 and 2 are two massive scalar dyons with $q_{12} = -1$, the corresponding 3-point S-matrix element is

$$S\left(1^0, 2^0 \,|\, \mathbf{3}^J\right)_{q_{12}=-1} \;=\; a\,\left\langle \mathbf{3}\, p_{12}^{\flat -}\right\rangle^{J+1}\,\left\langle \mathbf{3}\, p_{12}^{\flat +}\right\rangle^{J-1}\,. \tag{4.80}$$

Since there is only one relevant tensor structure for this S-matrix (see Eq. (4.51)), we have only one coefficient a. This will change when we include non-scalar particles — for example with a massive fermion f and a scalar there are two possible tensor structures, depending

[16] To be more precise, our $C^{J;\,\text{in/out}}$ are not really *coefficients*, they are $SL(2,\mathbb{C})$ tensors. The generalized Clebsch-Gordan coefficients defined in [67] is given in terms of our $C^{J;\,\text{in/out}}$ by $C^{J;\,\text{in/out};\{\alpha_1\ldots,\alpha_{2J}\}}\lambda^{I_1}_{\alpha_1}\cdots\lambda^{I_{2J}}_{\alpha_{2J}}$.

on which spinor is contracted with $|\mathbf{f}]$. The corresponding generalized Clebsch-Gordan part can be directly read off from this 3-point S-matrix element by stripping off the spinors $\langle \mathbf{3}|^{\alpha}$ corresponding to the massive spin J,

$$\left(C^{J;\,\mathrm{in}}_{0,0,-1}\right)_{\{\alpha_1,\ldots,\alpha_{2J}\}} \;=\; \left(|p_{12}^{\flat -}\rangle^{J+1}\,|p_{12}^{\flat +}\rangle^{J-1}\right)_{\{\alpha_1,\ldots,\alpha_{2J}\}}\,, \tag{4.81}$$

where the subscript $(0,0,-1)$ indicates (s_1, s_2, q_{12}) and we have normalized away the a coefficient.

4.6 Fermion-Monopole Scattering: Lowest Partial Wave and Helicity Flip

As an illustrative application of our generalized amplitude formalism we now consider scattering of an electrically charged fermion with charge e off a massive magnetic monopole with magnetic charge g (with $q = eg$), reproducing the well known results of ref. [68]. In this section we eamine the lowest partial wave process, ($J = |q| - \frac{1}{2}$), and derive the celebrated helicity flip amplitude. In section 4.7 we apply our formalism to higher partial wave processes.

4.6.1 Massive Fermion

It is convenient to start with a massive Dirac fermion denoted by

$$\psi \;=\; \begin{pmatrix} f \\ \bar{f}^{\dagger} \end{pmatrix} , \tag{4.82}$$

where f, $\bar{f}$ are both LH Weyl fermions with opposite charges e and $-e$.

The $J = |q| - \frac{1}{2}$ Clebsch-Gordan coefficient for the in state can be obtained by taking $s_1 \equiv s_f = 1/2$, $s_2 \equiv s_M = 0$ and $s_3 \equiv s_J = J = |q| - 1/2$ in Eq. (4.51). That means that $\hat{s} = |q|$, and for $q > 0$ the only valid 3-point S-matrix element is

$$S^{\text{3-pt,in}}_{q>0} \quad = \quad a \, \langle \mathbf{f} \, p^{\flat+}_{fM} \rangle \, \langle \mathbf{J} \, p^{\flat+}_{fM} \rangle^{2|q|-1} \; . \tag{4.83}$$

As explained in the previous section there is only one a coefficient, which we absorb in the reduced matrix element $\mathcal{M}^{J=|q|-1/2}$. Stripping away the $\langle \mathbf{J}|^{\alpha}$ part, we find

$$C^{|q|-1/2;\,\text{in}}_{q>0} \quad = \quad \langle \mathbf{f} \, p^{\flat+}_{fM} \rangle \, \left(|p^{\flat+}_{fM}\rangle^{2|q|-1} \right)_{\{\alpha_1,\ldots,\alpha_{2|q|-1}\}} , \tag{4.84}$$

and a similar one for the out state. Contracting the generalized Clebsch-Gordan factors for

the *in*- and *out*-states, we find the *basis amplitude*[17]

$$\mathcal{B}^{|q|-1/2}_{q>0} \;=\; \frac{\langle \mathbf{f}\, p^{\flat+}_{fM}\rangle \langle \mathbf{f}'\, p^{\flat+}_{f'M'}\rangle}{4p_c^2}\left(\frac{\langle p^{\flat+}_{fM} p^{\flat+}_{f'M'}\rangle}{2p_c}\right)^{2|q|-1}. \tag{4.85}$$

We can repeat the exercises for $q<0$, obtaining

$$\mathcal{B}^{|q|-1/2}_{q<0} \;=\; \frac{\langle \mathbf{f}\, p^{\flat-}_{fM}\rangle \langle \mathbf{f}'\, p^{\flat-}_{f'M'}\rangle}{4p_c^2}\left(\frac{\langle p^{\flat-}_{fM} p^{\flat-}_{f'M'}\rangle}{2p_c}\right)^{2|q|-1}. \tag{4.86}$$

4.6.2 The massless limit

In the massless fermion limit the particles are labeled by their helicity. Overall there are four possible choices, namely helicity $\pm\frac{1}{2}$ for the initial fermion (particle 1) and helicity $\pm\frac{1}{2}$ for the final fermion (particle 3). In our all-outgoing convention, the helicity flip process involves the same helicity for the initial state and the final state fermions, while in the non-flip process they have opposite helicity.

The allowed processes for external fermions of charge e are

$$\begin{aligned}
&\text{Helicity non-flip :} && f + M \to f + M \quad , \quad \bar{f}^{\,\dagger} + M \to \bar{f}^{\,\dagger} + M \\
&\text{Helicity flip :} && f + M \to \bar{f}^{\,\dagger} + M \quad , \quad \bar{f}^{\,\dagger} + M \to f + M\,.
\end{aligned} \tag{4.87}$$

We first consider the last process in Eq. (4.87), the right-handed incoming fermion (helicity

[17]Since we aim to determine the S-matrix up to reduced matrix element $\mathcal{M}^J(p_c)$ we rescale our expression by powers of p_c to make the basis amplitude dimensionless.

$+1/2$) and the left-handed outgoing fermion (helicity $-1/2$). In the *out-out* formalism this corresponds to both fermions having helicity $-1/2$. We can take the massless limit of Eqs (4.85) and (4.86) by simply unbolding $\langle \mathbf{f}|$, $\langle \mathbf{f}'|$ spinors [7].

$$\mathcal{B}^{|q|-\frac{1}{2}} \;=\; \frac{\left\langle f\, p^{\flat\pm}_{fM}\right\rangle \left\langle f'\, p^{\flat\pm}_{f'M'}\right\rangle}{4p_c^2} \left(\frac{\left\langle p^{\flat\pm}_{fM} p^{\flat\pm}_{f'M'}\right\rangle}{2p_c}\right)^{2|q|-1} \quad \text{for } \operatorname{sgn}(q) = \pm 1 \tag{4.88}$$

We further note that the helicity flip amplitude Eq. (4.88) is only non-trivial for $q < 0$. Indeed, in the $m_i \to 0$ limit the spinor $|p^{\flat+}_{ij}\rangle$ is parallel to $|i\rangle$ and, according to Eq. (4.41), $\left\langle f\, p^{\flat+}_{fM}\right\rangle = \left\langle f'\, p^{\flat+}_{f'M'}\right\rangle = 0$. The vanishing of the S-matrix element for $q > 0$ has a simple intuitive physical explanation. When $q > 0$ the EM field component of the magnetically modified angular momentum operator (4.11) points towards the monopole and has eigenvalues $q, q+1, q+2, \ldots$ Since we are considering the right-handed incoming fermion the minimal value of the z-component of the total angular momentum will be $q + 1/2$ which is not part of the lowest partial wave state corresponding to $J = |q| - 1/2$. One can similarly see that the outgoing left-handed particle can not be a part of the lowest partial wave when $q > 0$.

Similarly, let us consider the helicity-flip amplitude where the incoming fermion is left-handed while the outgoing fermion is right-handed. In the *out-out* formalism this corresponds to both massless fermions having helicity $+\frac{1}{2}$. In this case we can't simply *unbold* the $\langle \mathbf{f}|$, $\langle \mathbf{f}'|$ spinors, but instead have to replace them with the Parity-conjugates[18] of $\langle f|$ and $\langle f'|$, denoted by $\langle \hat{\eta}_f|$, $\langle \hat{\eta}_{f'}|$,

$$\mathcal{B}^{|q|-\frac{1}{2}} \;=\; \frac{\left\langle \hat{\eta}_f\, p^{\flat\pm}_{fM}\right\rangle \left\langle \hat{\eta}_{f'}\, p^{\flat\pm}_{f'M'}\right\rangle}{4p_c^2} \left(\frac{\left\langle p^{\flat\pm}_{fM} p^{\flat\pm}_{f'M'}\right\rangle}{2p_c}\right)^{2|q|-1} \quad \text{for } \operatorname{sgn}(q) = \pm 1 \tag{4.89}$$

[18]We use the properly normalized $\langle \hat{\eta}_i|$ instead of $\langle \eta_i| = m_i \langle \hat{\eta}_i|$ and absorb the normalization in our reduced matrix element.

This time, Eq. (4.41) tells us that $\langle \hat{\eta}_f \, p^{\flat -}_{fM} \rangle = \langle \hat{\eta}_{f'} \, p^{\flat -}_{f'M'} \rangle = 0$, and so the S-matrix vanishes for $q < 0$. Once again, there is a simple physical explanation of this fact: neither a left-handed incoming particle nor a right-handed outgoing particle can be a be part of the $J = |q| - \frac{1}{2}$ partial wave when $q < 0$. Therefore, we find that the only non-vanishing amplitude basis for the helicity-flip process is given by

$$\mathcal{B}^{|q|-\frac{1}{2}}_{q<0} = \frac{\langle f \, p^{\flat -}_{fM} \rangle \langle f' \, p^{\flat -}_{f'M'} \rangle}{4p_c^2} \left(\frac{\langle p^{\flat -}_{fM} p^{\flat -}_{f'M'} \rangle}{2p_c} \right)^{2|q|-1} \tag{4.90}$$

$$\mathcal{B}^{|q|-\frac{1}{2}}_{q>0} \sim \frac{[f \, p^{\flat -}_{fM}] \, [f' \, p^{\flat -}_{f'M'}]}{4p_c^2} \left(\frac{\langle p^{\flat +}_{fM} p^{\flat +}_{f'M'} \rangle}{2p_c} \right)^{2|q|-1} \tag{4.91}$$

where once again we used Eq. (4.41).

One can similarly show that, regardless of the sign of q, the S-matrix element vanishes for the two remaining helicity choices: $\left(\pm\frac{1}{2}, \mp\frac{1}{2}\right)$. Mathematically, this is the consequence of the fact that now the amplitude basis is proportional to a factor of the form $\langle f \, p^{\flat \pm}_{fM} \rangle \langle \hat{\eta}_{f'} \, p^{\flat \pm}_{f'M'} \rangle$, and this vanishes for either choice of $\mathrm{sgn}(q)$. Physically, this happens because for the helicity-non-flip process either incoming or outgoing fermion can not be a part of the lowest partial wave. In other words, at the lowest partial wave helicity-non-flip process can not occur.

Using the explicit expressions for the helicity variables in the COM frame obtained in appendix C we can finally write the S-matrix in terms of the scattering angle θ. The only non-vanishing S-matrix element is

$$\begin{aligned} S^{|q|-\frac{1}{2}}_{f\to\bar{f}^\dagger} &= \mathcal{N} \, 2\,|q| \, \mathcal{M}^{|q|-\frac{1}{2}}_{-\frac{1}{2},\frac{1}{2}} \left[\sin\left(\frac{\theta}{2}\right) \right]^{2|q|-1} \quad \text{for } q > 0 \\ S^{|q|-\frac{1}{2}}_{\bar{f}^\dagger\to f} &= \mathcal{N} \, 2\,|q| \, \mathcal{M}^{|q|-\frac{1}{2}}_{\frac{1}{2},-\frac{1}{2}} \left[\sin\left(\frac{\theta}{2}\right) \right]^{2|q|-1} \quad \text{for } q < 0\,, \end{aligned} \tag{4.92}$$

where we have explicitly included the normalization coefficient $\mathcal{N} \equiv \sqrt{8\pi s}$ and the reduced matrix element $\mathcal{M}^{|q|-\frac{1}{2}}_{\mp\frac{1}{2},\pm\frac{1}{2}}$, which is *angle independent*. The factor $2|q|$ is from the prefactor $(2J+1)$ (for $J = |q| - 1/2$) introduced in the definition of the S-matrix Eq. (4.78). Note that for future convenience we have used the *in-out* notation for the physical helicities of incoming and outgoing fermions denoted as the subscripts $\mathcal{M}_{-h_{\rm in},h_{\rm out}}$, where $h_{\rm in}, h_{\rm out}$ are helicities in *out-out* formalism. In general, one needs a dynamical input to determine $\mathcal{M}$ in Eq. (4.92). However, as we will show in section 4.7 the higher partial waves do not contribute to the helicity-flip matrix element. When combined with the unitarity conditions (see section 4.8 for a detailed discussion) this implies that

$$\left|\mathcal{M}^{|q|-\frac{1}{2}}_{-\frac{1}{2},\frac{1}{2}}\right| \;=\; \left|\mathcal{M}^{|q|-\frac{1}{2}}_{\frac{1}{2},-\frac{1}{2}}\right| \;=\; 1\,. \tag{4.93}$$

Since the two helicity-flip processes never occur at the same time (they do or do not happen depending on the sign of q), we can set them to ∓ 1. As shown in detail in appendix F, the lowest partial wave S-matrix Eq. (4.92) with the reduced matrix elements Eq. (4.93) exactly reproduces the QM calculation of [68].

The result is rather interesting: in the limit of massless fermions, the S-matrix element is only non-vanishing for processes where the products of fermion helicities, h_f and $h_{f'}$, with q are positive, $h_f \cdot q = h_{f'} \cdot q > 0$ (in the out-out sense). It's even more striking once we remember that this discussion is in the all-outgoing convention, and so the physical interpretation in terms of in-out states is of a *positive* helicity fermion scattering into a *negative* helicity fermion for $q < 0$, or of a *negative* helicity fermion scattering into a *positive* helicity fermion for $q > 0$. In other words, our electric-magnetic S-matrix has a *selection rule* that tells us that the lowest partial wave always involves a helicity flip! In particular, forward or elastic scattering is forbidden by our selection rule since it does not flip the helicity of the fermion. This is the well-known Kazama-Yang result [68], and also the precursor of the

Rubakov-Callan effect [89, 19] in the scattering of two fermions and a monopole.

4.7 Fermion-Monopole Scattering: Higher Partial Waves

4.7.1 Massive fermions

We now consider the S-matrix elements for the higher partial waves in the fermion-monopole scattering process. Once again, it is convenient to start with a massive fermion. Following our derivation of the generalized Clebsch-Gordan coefficients, we have[19]

$$\mathcal{B}^J \sim \sum_{\sigma} \sum_{\sigma'} a_\sigma a'_{\sigma'} \frac{\left\langle \mathbf{f}\, p^{\flat\sigma}_{fM} \right\rangle \left\langle \mathbf{f}'\, p^{\flat\sigma'}_{f'M'} \right\rangle}{4p_c^2} \tilde{\mathcal{B}}^J(-q_\sigma, -q_{\sigma'}) \,, \tag{4.94}$$

where sum is taken over $\sigma = (+,-)$, $\sigma' = (+,-)$, while $q_+ = q - \frac{1}{2}$, $q_- = q + \frac{1}{2}$. We also included the coefficients a_σ (a'_σ) for the two possible tensor structures in the in (out) 3-point S-matrix elements. The $\tilde{\mathcal{B}}^J$ are given by

$$\tilde{\mathcal{B}}^J(\Delta, \Delta') \;=\; \frac{1}{(2p_c)^{2J}} \left(\langle p^{\flat-}_{fM}|^{J+\Delta} \langle p^{\flat+}_{fM}|^{J-\Delta} \right)^{\{\alpha_1,\ldots,\alpha_{2J}\}} \left(|p^{\flat-}_{f'M'}\rangle^{J+\Delta'} |p^{\flat+}_{f'M'}\rangle^{J-\Delta'} \right)_{\{\alpha_1,\ldots,\alpha_{2J}\}} . \tag{4.95}$$

Using Eq. (C.19) from appendix C.1, in the COM frame these become

$$\tilde{\mathcal{B}}^J(\Delta, \Delta') \;=\; (-1)^{J-\Delta'} \mathcal{D}^{J*}_{-\Delta,\Delta'}(\Omega_c) \,. \tag{4.96}$$

[19] Notice that this result is valid for all J, including the lowest partial wave case $J = |q| - 1/2$.

where $\Omega_c = \{\theta_c, \phi_c\}$ is the direction of the outgoing COM momenta (we chose the COM frame such that $\phi_c = 0$). Here $\mathcal{D}^J_{\Delta,-\Delta'}(\Omega)$ is the Wigner matrix [113, 110]

$$\mathcal{D}^J_{-\Delta,\Delta'}(\Omega) \;\equiv\; \mathcal{D}^J_{-\Delta,\Delta'}(\phi,\theta,-\phi) \;=\; e^{i\phi(\Delta+\Delta')}\, d^J_{-\Delta,\Delta'}(\theta)\,. \tag{4.97}$$

The standard definition of the Wigner d-matrix is $d^J_{m,m'}(\theta) = \langle J,m|\exp(-i\theta J_y)|J,m'\rangle$. The emergence of these specific $\mathcal{D}$-matrices is particularly satisfying, because they also go by another name: the spin-weighted spherical harmonics ${}_qY_{l,m}$ [115, 92], or monopole harmonics [115, 68]. Specifically[20]:

$$\mathcal{D}^{l*}_{q,m}(\Omega) \;=\; \sqrt{\frac{4\pi}{2l+1}}\; {}_qY_{l,m}(-\Omega)\;, \tag{4.98}$$

where $-\Omega = (\pi-\theta,-\phi)$. Monopole harmonics emerge in the solution of the Klein-Gordon or Dirac equations in the presence of a background magnetic field of a monopole [115, 68, 16]. It is reassuring to see them arise here in a completely relativistic setting, and based solely on LG and angular momentum arguments.

The J-partial wave matrix element for the COM scattering of a massive scalar monopole and a massive fermion is then

$$\begin{aligned} S^J \;&=\; \mathcal{N}\,(2J+1)\,\frac{\mathcal{M}^J}{4\,p_c^2} \\ &\Big\{a_1a_1'\,\big\langle \mathbf{f}\,p^{\flat-}_{fM}\big\rangle\,\big\langle \mathbf{f}'\,p^{\flat-}_{f'M'}\big\rangle\;\mathcal{D}^{J*}_{q+\frac12,-q-\frac12}(\Omega_c) \;+\; a_2a_1'\,\big\langle \mathbf{f}\,p^{\flat+}_{fM}\big\rangle\,\big\langle \mathbf{f}'\,p^{\flat-}_{f'M'}\big\rangle\;\mathcal{D}^{J*}_{q-\frac12,-q-\frac12}(\Omega_c) \\ &\quad a_1a_2'\,\big\langle \mathbf{f}\,p^{\flat-}_{fM}\big\rangle\big\langle \mathbf{f}'\,p^{\flat+}_{f'M'}\big\rangle\;\mathcal{D}^{J*}_{q+\frac12,-q+\frac12}(\Omega_c) \;+\; a_2a_2'\,\big\langle \mathbf{f}\,p^{\flat+}_{fM}\big\rangle\big\langle \mathbf{f}'\,p^{\flat+}_{f'M'}\big\rangle\;\mathcal{D}^{J*}_{q-\frac12,-q+\frac12}(\Omega_c)\Big\}\;, \end{aligned} \tag{4.99}$$

[20] Our ${}_qY_{lm}$ are defined according to the b-hemisphere definition of [115]

where the $(-1)^{J-\Delta'}$ prefactors have been absorbed into the coefficients a'_i, and $\mathcal{N} \equiv \sqrt{8\pi s}$.

4.7.2 Massless fermion

We now consider the massless limit for the fermions in the $J > |q| - \frac{1}{2}$ partial waves. The S-matrix Eq. (4.99) contains all of the possible helicity assignments, and so we can immediately extract the individual helicity amplitudes. For instance, the S-matrix for a helicity non-flip process $f \to f$ is obtained by unbolding the finial state massive fermion variable, and replacing the initial massive variable with P-conjugate $\hat{\eta}$-variable. Under this replacements, only the second term survives and Eq. (4.99) simplifies significantly to

$$S^J_{f\to f} \;=\; \mathcal{N}\,(2J+1)\,\mathcal{M}^J_{\frac{1}{2},-\frac{1}{2}}\;\mathcal{D}^{J*}_{q-\frac{1}{2},-q-\frac{1}{2}}(\Omega_c)\;, \tag{4.100}$$

where we dropped the $\frac{[f\,p^{\flat-}_{fM}]\langle f\,p^{\flat-}_{fM}\rangle}{4p_c^2}$ factor, which equals to 1 in the COM frame. Other cases can be worked out easily, and the general results are summarized in a compact expression as

$$S^J_{h_{\rm in}\to h_{\rm out}} \;=\; \mathcal{N}\,(2J+1)\,\mathcal{M}^J_{-h_{\rm in},h_{\rm out}}\;\mathcal{D}^{J*}_{q-h_{\rm in},-q+h_{\rm out}}(\Omega_c)\;. \tag{4.101}$$

As shown in appendix F, Eq. (4.101) exactly reproduces the angular dependence of the higher partial wave amplitudes in [68], obtained by a brute force solution of the Dirac equation in a monopole background.[21]

[21] We remind the reader that $h_{\rm in}$, $h_{\rm out}$ are defined in the *all-outgoing* convention, and so an incoming $f\,(\bar{f}^\dagger)$ has helicity $h_{\rm in} = \frac{1}{2}\,(-\frac{1}{2})$, while an outgoing $f\,(\bar{f}^\dagger)$ has helicity $h_{\rm out} = -\frac{1}{2}\,(\frac{1}{2})$. Note also that the indices on $\mathcal{M}^J$ are $-h_{\rm in}$ and $h_{\rm out}$, such that the labeling of $\mathcal{M}^J$ respects particle kind (f or $\bar{f}^\dagger$) rather than helicity in the *out-out* convention: $-\frac{1}{2} \to f$ and $+\frac{1}{2} \to \bar{f}^\dagger$. This will be useful to keep in mind when considering $\mathcal{M}^{J\dagger}$.

As in textbook QM scattering in a central potential, our partial wave expansion only determines the angular dependence of each partial wave, while the relative magnitude of the different partial waves is determined dynamically in the form of *phase shifts*. For the lowest partial wave, our selection rule forbids forward scattering, and so the full partial amplitude was completely fixed by unitarity. In contrast, for the higher partial waves, unitarity alone does not uniquely determine the amplitude, and some knowledge of the underlying dynamics is needed to specify the reduced matrix elements. To this end we extract the reduced matrix elements for the *helicity non-flip* amplitude from [68]:

$$\mathcal{M}^{J}_{\pm\frac{1}{2},\pm\frac{1}{2}} = e^{-i\pi\mu}, \tag{4.102}$$

where $\mu = \sqrt{\left(J+\frac{1}{2}\right)^2 - q^2}$. One can see that these are indeed merely phase shifts, and they are the only dynamical information needed to completely fix the S-matrix. The unitarity condition discussed in the next section then leads to

$$\left|\mathcal{M}^{J}_{\pm\frac{1}{2},\mp\frac{1}{2}}\right|^2 \;=\; 1 - \left|\mathcal{M}^{J}_{\pm\frac{1}{2},\pm\frac{1}{2}}\right|^2 \;=\; 0\,, \tag{4.103}$$

so the helicity-flip processes for $J > |q| - \frac{1}{2}$ vanish simply because a 100% of the probability goes to the helicity non-flip process Eq. (4.101).

To emphasize what we have achieved, note that *all* of the new information gained from the full solution of the QM scattering problem can be summarized in the phase shift Eq. (4.102). In this chapter we reproduced everything else based on LG and partial wave decomposition alone, in a manifestly relativistic setting. In particular, we reproduced the full angular dependence of all partial waves and the selection rule that requires a helicity-flip in the lowest partial wave.

4.8 Partial Wave Unitarity

To complete our analysis of charged fermion scattering off a massive scalar monopole, we need to discuss partial wave unitarity. Here we follow the standard derivation of partial wave unitarity given in [83], generalizing it to the electric-magnetic scattering case. Unitarity of the S-matrix implies

$$\frac{p_c}{16\pi^2\sqrt{s}}\int d\Omega_m \sum_{ab}\left(S_{(fM)_i\to ab}\, S^*_{(f^\dagger M)_f\to a^\dagger b^\dagger}\right) \;=\; \frac{16\pi^2\sqrt{s}}{p_c}\,\delta(\Omega_c)\,, \tag{4.104}$$

where the momenta of f_i (M_i) are directed along $\pm\hat{z}$ and the momenta of f_f (M_f) are directed along $\pm\hat{\Omega}_c$ with the angles (θ_c,ϕ_c). The intermediate states a,b can be either (f_m,M_m) or $(\bar{f}^\dagger_m,M_m)$ with their momenta along $\pm\hat{\Omega}_m$ with the angles (θ_m,ϕ_m).[22] We now wish to perform a partial wave expansion of the unitarity relation (4.104), in order to obtain a partial wave unitarity condition for our S-matrix. We begin by expanding the relevant S-matrix elements in partial waves, using Eq. (4.101), which we repeat here for completeness:

$$S_{h_{\rm in}\to h_{\rm out}} \;=\; \mathcal{N}\sum_J (2J+1)\;\mathcal{M}^J_{-h_{\rm in},h_{\rm out}}\;\mathcal{D}^{J*}_{q-h_{\rm in},-q+h_{\rm out}}(\Omega_m)\;, \tag{4.105}$$

where $\mathcal{N}\equiv\sqrt{8\pi s}$ is our usual normalization factor. Note that here, in contrast with the original Eq. (4.101), the argument of the $\mathcal{D}$-matrix is Ω_m rather than Ω_c. This is because we are considering the S-matrix for an in-state with COM momenta along the $\hat{z}$ axis and an

[22] Currently, we assume that the complete set of possible intermediate state consists of fermion and monopole pair $\{f,M\}$ (with all possible choices of fermion helicity). Of course, it is certainly possible to have a microscopic theory containing other possible states, e.g. dyon pair, or multi-particle states. However, note that what the S-matrix method does is to provide S-matrices consistent with the assumption of spectrum. Indeed, under this assumption, we find results in complete agreement with the full QM calculation with the *same* assumption made here.

out-state along the $\pm\hat{\Omega}_m$ direction. Similarly, we expand the inverse process as

$$S_{h_{\rm in}\to h_{\rm out}} \;=\; \mathcal{N}\sum_J (2J+1)\;\mathcal{M}^J_{-h_{\rm in},h_{\rm out}}\;\sum_{p=-J}^{J}\mathcal{D}^J_{p,q-h_{\rm in}}(\Omega_c)\;\mathcal{D}^{J*}_{p,-q+h_{\rm out}}(\Omega_m)\;. \tag{4.106}$$

This time we need two $\mathcal{D}$-matrices because we start from an in-state in the direction $\pm\hat{\Omega}_c$ and go to an out-state along $\pm\hat{\Omega}_m$. The explicit derivation of this particular angular dependence is presented in appendix C.1. Substituting the above expansions in Eq. (4.104), the unitarity relation becomes

$$\begin{aligned}
&\frac{1}{16\pi^2}\int d\Omega_m\;\sum_{J,J'}(2J+1)\,(2J'+1)\;\cdot\\
&\Bigg\{\;\mathcal{M}^J_{-\frac12,-\frac12}\,\mathcal{M}^{J'\dagger}_{-\frac12,-\frac12}\;\mathcal{D}^{J*}_{q-\frac12,-q-\frac12}(\Omega_m)\sum_{p=-J'}^{J'}\mathcal{D}^{J'*}_{p,q+\frac12}(\Omega_c)\;\mathcal{D}^{J'}_{p,-q-\frac12}(\Omega_m)\\
&\quad+\mathcal{M}^J_{-\frac12,\,\frac12}\,\mathcal{M}^{J'\dagger}_{\frac12,-\frac12}\;\mathcal{D}^{J*}_{q-\frac12,-q+\frac12}(\Omega_m)\sum_{p=-J'}^{J'}\mathcal{D}^{J'*}_{p,q+\frac12}(\Omega_c)\;\mathcal{D}^{J'}_{p,-q+\frac12}(\Omega_m)\Bigg\}\;=\;\delta(\Omega_c)\,.
\end{aligned} \tag{4.107}$$

We can perform the Ω_m integration using the orthogonality condition for $\mathcal{D}^J_{m,b}(\Omega_m)$,

$$\int d\Omega_m\;\mathcal{D}^{J*}_{a,b}(\Omega_m)\;\mathcal{D}^{J'}_{a',b'}(\Omega_m)\;=\;\frac{4\pi}{2J+1}\,\delta_{aa'}\,\delta_{bb'}\,\delta_{JJ'}\,. \tag{4.108}$$

Using this relation, our expression simplifies to

$$\frac{1}{4\pi}\sum_J(2J+1)\;\left(\mathcal{M}^J\mathcal{M}^{J\dagger}\right)_{-\frac12,-\frac12}\;\mathcal{D}^{J*}_{q-\frac12,q+\frac12}(\Omega_c)\;=\;\delta(\Omega_c)\,. \tag{4.109}$$

Eq. (4.109) is the unitarity relation applied to $f + M \to f + M$ scattering. Repeating the same steps for f, $\bar{f}^\dagger$ in the in and out state, we get the general relation Repeating this derivation for all other in/out- states, we get

$$\frac{1}{4\pi} \sum_J (2J+1) \left(\mathcal{M}^J \mathcal{M}^{J\dagger}\right)_{-h_{\rm in},h_{\rm out}} \mathcal{D}^{J*}_{q-h_{\rm in},q-h_{\rm out}}(\Omega_c) \;=\; \delta_{-h_{\rm in},h_{\rm out}}\, \delta(\Omega_c)\,. \quad (4.110)$$

Multiplying by $\mathcal{D}^{J}_{q-h_{\rm in},q-h_{\rm out}}(\Omega_c)$ and using Eq. (4.108), we have

$$\mathcal{M}^J \mathcal{M}^{J\dagger} \;=\; I\,, \quad (4.111)$$

where $\mathcal{M}^J$ is the 2×2 matrix representing f or $\bar{f}^\dagger$ in the in / out state, and I is the 2×2 identity matrix. In other words, the unitarity of the S-matrix leads to the unitarity of each individual *reduced matrix element* $\mathcal{M}^J$. This is also the standard result for non-magnetic amplitudes [83], which leads to the partial-wave unitarity bound [55]. Here we see that it holds for the electric-magnetic case as well, even though the eigenfunctions of the partial wave decomposition are modified by the extra angular momentum in the EM field. The unitarity condition Eq. (4.111) is key in reproducing the full helicity-flip amplitude for the $J = |q| - \frac{1}{2}$ partial wave in section 4.6, as well as the vanishing of the helicity-flip amplitudes for $J > |q| - \frac{1}{2}$ in section 4.7.2 (assuming that the helicity non-flip process is given by Eq. (4.102)).

4.9 Conclusions

In this chapter we have initiated the systematic study of electric-magnetic scattering amplitudes, using on-shell methods. We have identified the multi-particle representations of the Poincaré group that are necessary to incorporate asymptotic states with both electric and magnetic charges. At the heart of our study is the appearance of a new pairwise LG and its corresponding pairwise helicity, which describe the transformation of electric-magnetic multi-particle states relative to the direct product of the one-particle states. This pairwise helicity is non-zero for a charge-monopole pair and corresponds to the angular momentum stored in the asymptotic electromagnetic field, which is appropriately quantized if Dirac-Schwinger-Zwanziger charge quantization is satisfied. This novel pairwise helicity gains a simple and intuitive implementation in the scattering amplitude formalism, through the definition of pairwise spinor-helicity variables. We then used the pairwise spinor-helicity variables to formulate the general rules for building the electric-magnetic S-matrix. In particular, we were able to classify all 3-particle magnetic S-matrix elements, corresponding to decays of magnetically charged particles. Many of these electric-magnetic S-matrix elements are subject to simple selection rules among the spins/helicities and pairwise helicities of the various particles. In addition, we performed a pairwise LG covariant partial wave expansion for the generic $2 \to 2$ fermion-monopole scattering amplitude. For the lowest partial wave, our LG based selection rules allowed us to derive the famous helicity flip for the lowest partial wave. Furthermore, the well-known monopole spherical-harmonics appear naturally in our formalism, and the general results of [68] are fully reproduced up to dynamics-dependent phase shifts. We never have to introduce a Dirac string, and the resulting S-matrix elements are always manifestly Lorentz invariant. For monopoles that do not satisfy Dirac-Schwinger-Zwanziger charge quantization due to kinetic mixing with a hidden sector photon [103] a separate treatment is needed [105].

Recently the authors of ref. [58] discussed the need for a more careful definition of the S-

matrix; they define a "hard" S-matrix by evolving the asymptotic states with an asymptotic Hamiltonian which is not the free Hamiltonian, but allows for the emission and absorption of massless photons. This evolution builds up a cloud of photons representing the Coulomb fields of the charged in and out particles. In the presence of both electric and magnetic charges the Coulomb fields carry additional angular momentum which we have included explicitly using the pairwise LG. It would be interesting to see how this angular momentum could be handled in the "hard" S-matrix formalism. It will also be interesting to consider the double copy relation between dyons and Taub-NUT spaces [21, 80, 69] in light of our results.

Chapter 5

Dark Matter Freeze Out during an Early Cosmological Period of QCD Confinement

This chapter is heavily based on work previously published in collaboration with Dillon Berger, Seyda Ipek, and Tim Tait [12].

5.1 Introduction

The identity of the dark matter, necessary to explain a host of cosmological observations, is among the most pressing questions confronting particle physics today. The Standard Model (SM) contains no suitable fields to play the role of dark matter, and understanding how it must be amended to describe dark matter will inevitably provide important insights into the theory of fundamental particles and interactions. There are a plethora of theoretical ideas as to how to incorporate dark matter, and exploring how to test them is a major area of

activity in particle experiment.

Among the various candidates, the class of weakly interacting massive particles (WIMPs) remains extremely attractive, largely driven by the appealing opportunity to explain their relic density based on the strength of their interactions with the SM. Provided their interactions are roughly similar to the electroweak couplings, WIMPs are expected to initially be in chemical equilibrium with the SM plasma at early times, but to fall out of equilibrium when the temperature of the Universe falls below $T \sim m_\chi/20$, where m_χ is the mass of the WIMP. Provided the mass and cross section for annihilation into the SM are correlated appropriately [47], the observed cosmological abundance is relatively easily realized.

Vanilla theories of WIMPs are challenged by the null results from direct searches for dark matter scattering with heavy nuclei [6]. For many generic models of WIMP interactions with the SM, these searches exclude the required annihilation cross section for masses 1 GeV $\lesssim m_\chi \lesssim 10^4$ GeV. While it is possible to engineer interactions that allow for large annihilation while suppressing scattering (see [108, 24, 54, 50, 14, 64, 2] for a few examples), such limits, together with those derived from the null observations of WIMP annihilation products [5] and/or production at colliders [11, 1, 100], suggest that either Nature has been unkind in choosing which model of WIMPs to realize, or there is tension between realizing the observed relic density and the limits from experimental searches for WIMPs.

A key assumption under-pinning the mapping of the relic density to WIMP searches today is that the cosmological history of the Universe can be reliably extrapolated back to the time of freeze out. The standard picture extrapolates based on a theory containing the SM plus dark matter (and dark energy), with no other significant ingredients. The success of Big Bang Nucleosynthesis (BBN) in explaining the primordial abundances of the light elements could be taken as an argument that it is unlikely that cosmology has been very significantly altered at temperatures lower than $\sim$ 10 MeV, but this is far below the typical freeze-out temperature of a weak scale mass WIMP, which is more typically in the 5-100 GeV range.

Indeed, it has been shown that an early period of matter domination [57] or late entropy production [52] can alter the relic abundance for fixed WIMP model parameters, leading to substantially different mapping between the observed abundance and the expectations of direct searches.

In this article, we explore a different kind of nonstandard cosmology, in which the strong interaction described by Quantum Chromodynamics (QCD) undergoes an early phase of confinement, based on promoting the strong coupling α_s to a field, whose potential receives thermal corrections which cause it to take larger values at early times, relaxing to the canonical size some time before BBN [65, 29]. If the dark matter freeze out occurs during a period in which α_s is larger such that QCD is confined, the degrees of freedom of the Universe are radically different from the naive extrapolation, being composed largely of mesons and baryons rather than quarks and gluons. Similarly, the interactions of the dark matter with the hadrons are scaled up by the larger QCD scale, $\Lambda_{\rm QCD}$, leading to a very different annihilation cross section at the time of freeze-out than during the epoch in which experimental bounds are operative. We find that depending on the underlying form of the dark matter interactions with quarks, radical departures from the expected relic density are possible.

This article is organized as follows. In Section 5.2, we review the construction of a Universe in which α_s varies with temperature. In Section 5.3 we discuss the chiral perturbation theory which describes the mesons and their interactions with the dark matter during the period of early confinement, and in Section 5.4, we examine the relic density under different assumptions concerning α_s at the time of freeze-out, and contrast with experimental constraints derived today. We reserve Section 5.5 for our conclusions and outlook.

5.2 Early QCD Confinement

Following reference [65], we modify the gluon kinetic term in the SM Lagrangian to:

$$-\frac{1}{4g_{s0}^2}G^a_{\mu\nu}G_a^{\mu\nu} \quad \Rightarrow \quad -\frac{1}{4}\left(\frac{1}{g_{s0}^2}+\frac{S}{M_*}\right)G^a_{\mu\nu}G_a^{\mu\nu}\ , \tag{5.1}$$

where $G^a_{\mu\nu}$ is the gluon field strength, S is a gauge singlet real scalar field, and g_{s0} represents (after rescaling the kinetic term to canonical normalization) the SU(3) gauge coupling in the absence of a vacuum expectation value (VEV) for S. M_* is a parameter with dimensions of energy which parameterizes a non-renormalizable interaction between S and the gluons. It could represent the fluctuations of a radion or dilaton field, or by integrating out heavy vector-like SU(3)-charged particles which also couple to the scalar field S. In the latter case, the scale of the interaction is related to the mass of the new SU(3)-charged particles via $M_* \sim 4\pi M_Q/n_Q y_Q \alpha_s$, where n_Q is the number of SU(3)-charged fermions with mass M_Q and Yukawa coupling y_Q.

Engineering an early period of confinement, followed by subsequent deconfinement and return to a SM-like value of α_s before BBN imposes constraints on the potential for S, and its interactions with other fields (which determine the thermal corrections to its potential) [65]. Generally, mixed potential terms containing the SM Higgs doublet are present, and these may play an important role in the thermal history [29]. In this work, we remain agnostic concerning the specific dynamics which implement the shift in v_S leading to early confinement, and we assume that the terms mixing the S with the SM Higgs are small enough so as to be safely neglected.

A VEV for S generates a non-decoupling correction to the effective strong coupling constant through the dimension-5 interaction in Equation (5.1), which for negative v_s strengthens the

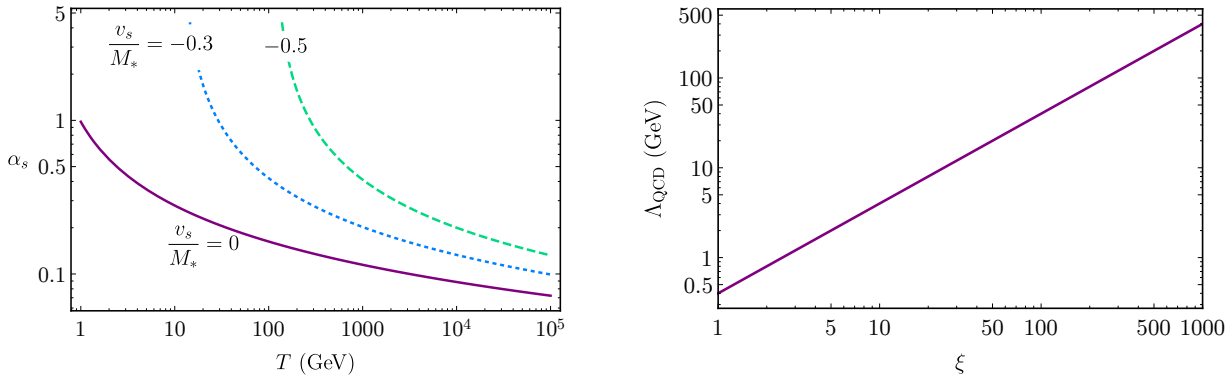

Figure 5.1: **Left panel:** Evolution of the strong coupling constant with temperature in the early Universe for three different values of v_s/M_*. Confinement takes place at temperatures for which $\alpha_s \gg 1$. **Right panel:** The scale of QCD confinement, $\Lambda_{\rm QCD}$, as a function of the parameter $\xi = \exp(24\pi^2/(2N_f - 33)v_S/M_*)$.

effective coupling strength. At one loop and at scale μ, the effective strong coupling is

$$\frac{1}{\alpha_s(\mu, v_s)} = \frac{33 - 2N_f}{12\pi} \ln\left(\frac{\mu^2}{\Lambda_0^2}\right) + 4\pi \frac{v_s}{M_*}, \tag{5.2}$$

where N_f is the number of active quark flavors at the scale $\mu \sim T$. Figure 5.1 shows the effective coupling as a function of temperature. QCD confinement occurs at a temperature $T_c \simeq \Lambda_{\rm QCD}$, where

$$\Lambda_{\rm QCD}(v_s) = \Lambda_{\rm QCD}^{\rm SM}\, e^{\frac{24\pi^2}{2N_f - 33}\frac{v_S}{M_*}}. \tag{5.3}$$

Here, $\Lambda_{\rm QCD}^{\rm SM} \simeq 400$ MeV is the SM value of the QCD confinement scale; we adjust g_{s0} such that it is realized for $v_s = 0$.

At scales below confinement, the relevant degrees of freedom are mesons, whose dynamics are described by chiral perturbation theory, the effective field theory of which is parameterized by coefficients which depend on $\Lambda_{\rm QCD}$. We find it convenient to parameterize the physics in

terms of the ratio of $\Lambda_{\rm QCD}$ to $\Lambda_{\rm QCD}^{\rm SM}$,

$$\xi \equiv \frac{\Lambda_{\rm QCD}}{\Lambda_{\rm QCD}^{\rm SM}} \simeq \exp\left(\frac{24\pi^2}{2N_f - 33}\frac{v_s}{M_*}\right). \tag{5.4}$$

The parameter ξ is typically sufficient to completely describe the physics of dark matter interactions during the period of early confinement.

5.3 Dark Matter Interactions and Chiral Perturbation Theory

The dynamics of the scenario we study are encoded in the Lagrangian:

$$\mathcal{L} \supset -\frac{1}{4}\left(\frac{1}{g_{s0}^2} + \frac{S}{M_*}\right) G^a_{\mu\nu} G_a^{\mu\nu} + \sum_q \left\{ i\bar{q}\not{D} q - y_q\, h\bar{q}_L q_R + \text{H.c.} \right\} + \mathcal{L}_\chi\,, \tag{5.5}$$

where $\mathcal{L}_\chi$ describes the dark matter and its interactions. We introduce a SM-singlet Dirac fermion field χ to represent the dark matter, and couple it to quarks,

$$\mathcal{L}_\chi = i\bar{\chi}\gamma^\mu\partial_\mu\chi - m_\chi\bar{\chi}\chi + \sum_{\bar{i},j}\left\{ \frac{\beta_{ij}}{M_S^2}\bar{\chi}\chi\ \bar{q}_i q_j + \frac{\lambda_{ij}}{M_V^2}\bar{\chi}\gamma^\mu\chi\ \bar{q}_i\gamma_\mu q_j \right\}, \tag{5.6}$$

where the couplings β_{ij}/M_S^2 and λ_{ij}/M_V^2 represent operators left behind by integrating out states with masses $\gg m_\chi$. Generically, one would also expect there to be interactions with the leptons or the Higgs doublet. We assume for simplicity that such interactions are subdominant if present.

In the case of the scalar interactions, S itself could act as the mediator, provided it has direct coupling to the dark matter. In that case, UV-completing will require additional states to

provide a renormalizable portal to $h\bar{q}q$, and the dimension six interaction written here will descend from a dimension seven operator after the SM Higgs gets its VEV. The vector interactions could represent a Z' from an additional U(1) gauge symmetry that couples to both quarks and dark matter. We will consider cases in which either scalar or vector interactions dominate over the other one. We follow the guidance of minimal flavor violation [36] in choosing the couplings such that

$$\beta_{ij} \equiv \pm\delta_{ij}\frac{y_i}{y_u} \ , \tag{5.7}$$

which is normalized to the coupling to up quarks, and with an over-all factor absorbed into M_S^2. The possibility of choosing either sign for β will play an important role, described in 5.21 below.

The vector couplings λ_{ij} are diagonal and have equal values for the up-type quarks, and equal (but different from the up-type) values for the down-type quarks,

$$\lambda_{ij} \equiv \begin{cases} \delta_{ij}, & j = u, c, t \\ (1+\alpha)\delta_{ij}, & j = d, s, b \ , \end{cases} \tag{5.8}$$

where α determines the difference between up- and down-type couplings. When $\alpha = 0$, the vector coupling assigns charges equivalent to baryon number, and the mesons decouple from the dark matter.

During early confinement, the Universe looks very different from the standard cosmological picture based on the SM extrapolation. (Massless) quark and gluon degrees of freedom are replaced by mesons and baryons, and chiral symmetry breaking induces a tadpole for the Higgs which is relevant for the evolution of its VEV. In order to determine how dark matter

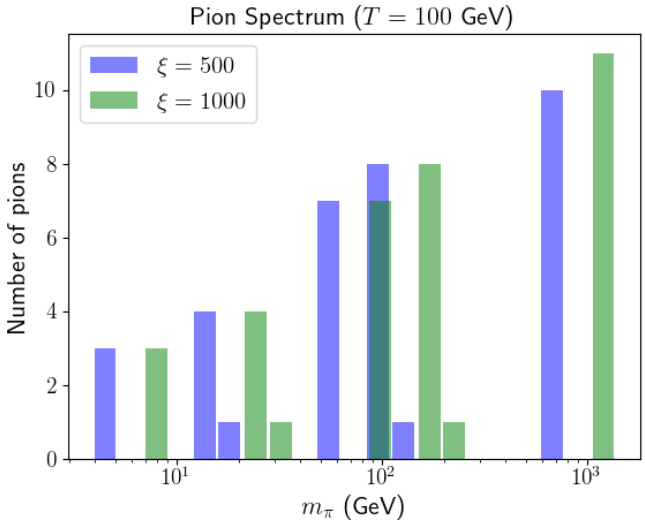

Figure 5.2: Spectrum of pion masses for two choices of ξ, with v_h corresponding to the Higgs VEV at $T = 100$ GeV.

interactions are affected by this early cosmological period of QCD confinement, we first give a description of this era in terms of chiral perturbation theory.

5.3.1 Chiral Perturbation Theory

In the limit $\Lambda_{\rm QCD} \gg m_t$, the QCD sector of the Lagrangian for quarks,

$$\mathcal{L} \supset \sum_q \left\{ i\bar{q}\not{D}q - y_q\, h\bar{q}_L q_R + \text{H.c.} \right\} \tag{5.9}$$

(where h is the SM Higgs radial mode) possesses an approximate global $\text{SU}(6)_L \times \text{SU}(6)_R$ chiral symmetry, which is softly broken by the Yukawa interactions. We work in the basis in which the y_q's are diagonal, for which all flavor-changing processes reside in the electroweak interactions. Non-perturbative QCD is expected to break $\text{SU}(6)_L \times \text{SU}(6)_R \to \text{SU}(6)_V$ to the diagonal subgroup, resulting in $6^2 - 1 = 35$ pions as pseudo-Nambu-Goldstone bosons.

At scales below $\Lambda_{\rm QCD}$, the pions are described by a nonlinear sigma model built out of

$U(x) \equiv \exp\left(i2T^a\pi^a(x)/f_\pi\right)$, where T^a are the SU(6) generators. The leading terms in the chiral Lagrangian (neglecting electroweak interactions) are

$$\mathcal{L}_{\rm ch} = \frac{f_\pi^2}{4}\ \mathrm{tr}(|D_\mu U|^2) + \kappa\ \ \mathrm{tr}(UM_q^\dagger + M_q U^\dagger)\ , \tag{5.10}$$

where f_π is the pion decay constant and κ is a constant with mass dimension 3, both of which represent the strong dynamics. The generators are normalized such that $\mathrm{tr}[T^aT^b] = \delta^{ab}/2$, leaving the π^a canonically normalized. The mass matrix M_q is a spurion representing the explicit $\mathrm{SU}(6)_L\times\ \mathrm{SU}(6)_R$ breaking from the Yukawa interactions,

$$M_q = \frac{1}{\sqrt{2}}h\ \mathrm{Diag}(y_u, y_d, y_s, y_c, y_b, y_t)\ . \tag{5.11}$$

Expanding the field U in Equation (5.10) to second order in π/f_π results in pion mass terms and a tadpole for the Higgs:

$$\mathcal{L}_{\rm ch} \supset \sqrt{2}\kappa\, y_t\, h - \frac{\kappa}{f_\pi^2}\ \mathrm{tr}[\{T^a, T^b\}M]\,\pi^a\pi^b\ , \tag{5.12}$$

both of which are controlled by κ. (In the tadpole term we keep only the top Yukawa as the contributions from light quarks are typically negligible.) We match f_π and κ to the SM pion mass, $m_{\pi 0} = 135$ MeV, and decay constant, $f_{\pi 0} = 94$ MeV at $\xi = 1$ and $v_h = v_h^0$, where $v_h^0 = 246$ GeV is the zero temperature SM Higgs VEV. Naive dimensional analysis provides the scaling for other values of ξ (for which the tadpole implies there will typically be a different v_h):

$$\kappa \simeq (220\ \mathrm{MeV})^3\,\xi^3\ , \qquad f_\pi \simeq 94\ \mathrm{MeV}\,\xi, \qquad m_\pi^2 \simeq m_{\pi 0}^2\,\xi\, v_h/v_h^0, \tag{5.13}$$

The resulting pion mass matrix is diagonalized numerically to determine the spectrum of mesons in the mass basis. Example spectra at $T = 100$ GeV for two different choices of ξ

are shown in Figure 5.2.

5.3.2 Finite Temperature Higgs Potential

As shown above, a cosmological era of early QCD confinement induces a tadpole for the Higgs radial mode h. If $\Lambda_{\rm QCD}$ is comparable in size to the weak scale, this tadpole can deform the Higgs potential by a relevant amount during the epoch of confinement. In addition, the plasma contains mesons (rather than quarks), which modifies the thermal corrections to the Higgs potential from the SM fermions.

We determine the Higgs VEV as a function of temperature by finding the global minimum of the finite-temperature Higgs potential. We assume that interaction terms between the Higgs and S are small enough to be neglected. We focus on a cosmological history where $\Lambda_{\rm QCD} > T_{\rm EW} \sim 150$ GeV, which requires $\xi \gtrsim 300$. We further assume that the S potential is such that there is a lower temperature T_d (which we treat as a free parameter) at which $\Lambda_{\rm QCD}$ returns to $\Lambda_{\rm QCD}^{\rm SM}$, implying that QCD deconfines and the subsequent evolution of the Universe is SM-like.

Under these assumptions, the finite temperature potential for the Higgs, $V(h,T)$ consists of the tree level SM potential,

$$V_0(h) = -\frac{1}{2}\mu^2 h^2 + \frac{\lambda}{4}h^4 \ , \tag{5.14}$$

whose parameters are adjusted to match the zero temperature VEV $v_h^0 = 246$ GeV and Higgs mass $m_h \simeq 126$ GeV. In three different temperature regimes, the form of the finite

temperature corrections is given as

$$V(h,T) = \begin{cases} V_0(h) + \dfrac{T^4}{2\pi^2} \displaystyle\sum_{i=h,W,Z,t} (-1)^F n_i J_{B/F}\left[m_i^2/T^2\right] & (T > \Lambda_{\rm QCD}) \\ V_0(h) - \sqrt{2}\kappa y_t h + \dfrac{T^4}{2\pi^2} \displaystyle\sum_{i=h,W,Z,\pi^a} n_i J_B\left[m_i^2/T^2\right] & (T_d < T < \Lambda_{\rm QCD})\,, \\ V_0(h) + \dfrac{T^4}{2\pi^2} \displaystyle\sum_{i=h,W,Z,t} (-1)^F n_i J_{B/F}\left[m_i^2/T^2\right] & (T < T_d)\ , \end{cases} \tag{5.15}$$

where $F = 0/1$ for bosons/fermions and n_i counts degrees of freedom: $n_h = n_\pi = 1$, $n_W = 6$, $n_Z = 3$, and $n_t = 12$. The functions $J_{B/F}$ are the bosonic/fermionic thermal functions,

$$J_{B/F}\left[m_i^2/T^2\right] = \int_0^\infty x^2 \log\left(1 - (-1)^F e^{-\sqrt{x^2 + m_i^2/T^2}}\right) \tag{5.16}$$

and $m_i^2(h)$ are the field dependent masses,

$$m_h^2 = -\mu^2 + 3\lambda h^2, \qquad m_W^2 = \frac{g_W^2}{4}h^2, \qquad m_Z^2 = \frac{g_W^2}{4\cos^2(\theta_w)}h^2, \qquad m_t^2 = \frac{y_t^2}{2}h^2. \tag{5.17}$$

We make use of the high temperature expansions of the thermal functions, which are given as

$$\begin{aligned} J_B\left(m^2(h)/T^2\right) &= -\frac{\pi^4}{45} + \frac{\pi^2}{12}\frac{m^2(h)}{T^2} - \frac{\pi}{6}\left(\frac{m^2(h)}{T^2}\right)^{3/2} + \mathcal{O}\left[\frac{m^4}{T^4}\log\left(\frac{m^2}{T^2}\right)\right]\ , \\ J_F\left(m^2(h)/T^2\right) &= \frac{7\pi^4}{360} - \frac{\pi^2}{24}\frac{m^2(h)}{T^2} + \mathcal{O}\left[\frac{m^4}{T^4}\log\left(\frac{m^2}{T^2}\right)\right]\ . \end{aligned} \tag{5.18}$$

The meson masses in the confined phase are calculated as described in the previous section. We find that for the values of ξ under consideration, the mesons containing top quarks are typically much heavier than the temperature during the period of early confinement such

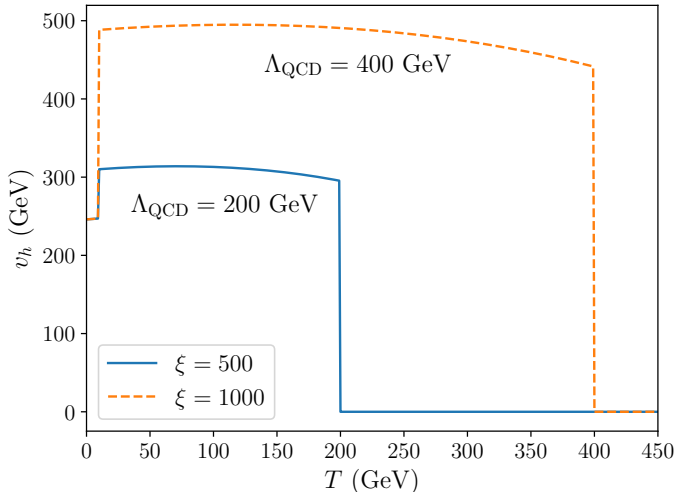

Figure 5.3: Higgs VEV as a function of temperature T for $\xi = 500, 1000$ and $T_d = 10$ GeV. The sudden changes occur at $T \simeq \Lambda_{\rm QCD}$ and T_d.

that they are Boltzmann suppressed. Hence the dominant thermal corrections are from the mesons containing bottom quarks. We keep all 35 mesons in our numerical calculations.

At high temperatures, the potential is dominated by the T^2h^2 term, driving $v_h \to 0$, and the electroweak symmetry is restored. At $T = \Lambda_{\rm QCD}$, chiral symmetry is broken via the quark condensate, and the tadpole triggers a non-zero Higgs VEV that is larger than v_h^0 for the ξ values we consider. At T_d, QCD deconfines and the Higgs VEV relaxes to its SM value. This behavior is shown in Figure 5.3 for $T_d = 10$ GeV and two values of ξ.

5.3.3 Dark Matter Interactions with pions

At leading order in chiral perturbation theory, the interactions with the dark matter map onto,

$$\frac{\kappa}{M_S^2}\,\bar{\chi}\chi\ \mathrm{tr}\left(U^\dagger\beta + U\beta^\dagger\right) + \frac{i}{M_V^2}\,\bar{\chi}\gamma^\mu\chi\ \mathrm{tr}\left((\partial_\mu U^\dagger)\,[\lambda, U] - [U^\dagger, \lambda^\dagger]\,(\partial_\mu U)\right)\ , \tag{5.19}$$

with κ and f_π determined as discussed in Section 5.3.1. Note that because the scalar interaction with dark matter is chosen to take the same form as the spurion containing the quark masses, a single hadronic coefficient κ determines both the pion masses and the dark matter couplings [9]. Expanding U to second order for Hermitian choices of β and λ produces:

$$\frac{2\kappa \ \mathrm{tr}\,[\beta]}{M_S^2}\ \bar{\chi}\chi + \frac{2\kappa}{f_\pi^2}\frac{1}{M_S^2}\ \mathrm{tr}[T^a T^b \beta]\ \bar{\chi}\chi\pi^a\pi^b + \frac{2i}{M_V^2} f^{abc}\ \mathrm{tr}[T^b\lambda]\ \bar{\chi}\gamma^\mu\chi\ \pi^a(\partial_\mu\pi^c)\,. \tag{5.20}$$

It is worth noting that the strength of the scalar interaction scales as $\kappa/f_\pi^2 \propto \xi$, whereas the vector-interaction strength is independent of it.

The first term in Equation (5.20) represents a contribution to the dark matter mass induced by the chiral condensate. At the time of freeze out, the effective mass is given by the sum of $m_\chi^{T=0}$, which to good approximation is m_χ in the Lagrangian (5.6), and this additional correction that is operative during confinement,

$$m_\chi^{T=T_F} = m_\chi^{T=0} + \Delta m_\chi\ , \quad \text{where}\ \ \Delta m_\chi \simeq (2\ \mathrm{eV})\,\xi^3 \left(\frac{10^6\ \mathrm{GeV}}{M_S}\right)^2\ . \tag{5.21}$$

For large values of ξ, the effective shift may be a few GeV, and may play a role in determining the relic abundance for dark masses of $O(10\ \mathrm{GeV})$. In Section 5.4 we present our results in terms of the $T = 0$ (unshifted) mass relevant for WIMP searches today. For dark matter masses of $O(\mathrm{GeV})$, the sign of the effective mass term may flip between the time of freeze out and today due to a sign difference between m_χ and β. For sufficiently complicated WIMP interactions, this could lead to non-trivial interference effects, but for the simple cases we consider here it is unimportant.

5.4 Dark Matter Parameter Space

In this section, we consider dark matter freezing out through either the scalar or vector interactions introduced above during an early cosmological period of QCD confinement. We contrast with the expectations from a standard cosmology and constraints from direct searches.

5.4.1 Relic Density

The Boltzmann equation describing the evolution of the density of dark matter in an expanding Universe can be written as [70]:

$$\frac{dn_\chi}{dt} + 3Hn_\chi = -\langle\sigma v\rangle(n_\chi^2 - n_{eq}^2)\,, \tag{5.22}$$

where n_χ is the co-moving number density of the dark matter, and n_{eq} is its equilibrium density at a given temperature. When the interaction rate drops below the expansion rate of the Universe, H, the dark matter number density stabilizes, leaving a relic of the species in the Universe today. The relic density can be solved for a non-relativistic species with a thermally averaged cross section approximated as $\langle\sigma v\rangle \sim a + 6b/x$ where $x \equiv m_\chi/T$. The resulting relic density is:

$$\Omega_\chi h^2 \approx \frac{1.04\times10^9}{M_{Pl}}\frac{x_F}{\sqrt{g_*}}\frac{1}{a+3b/x_F}\,, \tag{5.23}$$

where g_* counts the number of relativistic degrees of freedom at freeze-out and h parameterizes the Hubble scale. For the standard case of $\xi = 1$, we have $g_* = 92$. In an era of QCD confinement at $T \sim 10 - 100$ GeV, the degrees of freedom changes from the standard scenario since quarks and gluons confine into (heavy) mesons. For the cases we study, this corresponds to $g_* \simeq 26$ at the time of dark matter freeze-out. The freeze out temperature

$x_F = m_\chi/T_F$ can be solved for iteratively via

$$x_F = \ln\left(c(c+2)\sqrt{\frac{45}{8}}\frac{g_\chi}{2\pi^3}\frac{m_\chi M_{Pl}(a+6b/x_F)}{\sqrt{g_* x_F}}\right) , \tag{5.24}$$

where $g_\chi = 2$ for fermionic dark matter and $c = 1/2$ approximates the numerical solution well [70]. The parameters a, b in the annihilation cross section are model dependent. We compute them in Sections 5.4.3 and 5.4.4 for scalar and vector interactions, respectively.

The preceding discussion assumes that the freeze out takes place during a time of radiation domination, as is the case for a WIMP in the backdrop of a standard cosmology. It is generally expected that QCD confinement results in a shift in the vacuum energy of $c_0\Lambda_{\rm QCD}^4$, where c_0 is a dimensionless constant which naive dimensional analysis would suggest is order 1. The relic density in Equation (5.23) assumes that the subsequent deconfinement of QCD occurs before the onset of vacuum domination,

$$\Lambda_{\rm QCD} \gtrsim T_F \gtrsim \Lambda_{\rm QCD}\left(\frac{c_0}{g_*}\right)^{1/4} . \tag{5.25}$$

For $c_0 \sim 1$, this is a relatively narrow range which would involve some fine-tuning between the freeze out temperature and $\Lambda_{\rm QCD}$ for Equation (5.23) to hold. However, the tiny value of the vacuum energy inferred from cosmic acceleration in the current era could argue that there is some mechanism at work which dynamically cancels the influence of vacuum energy in different epochs, which would allow for a much wider period of radiation domination.

5.4.2 Limits from Direct Searches

Direct detection experiments such as XENON provide important bounds on parameter space based on the null results for dark matter scattering with nuclei. The rate for χ to scatter

with a nucleus N in the non-relativistic limit is,

$$\sigma_{\chi N} = \frac{1}{\pi}\frac{m_\chi^2 m_N^2}{(m_\chi + m_N)^2}[Z f_p + (A - Z) f_n]^2 \,, \tag{5.26}$$

where Z and A are the atomic number and mass number respectively and $f_{p/n}$ are the effective couplings to protons/neutrons, given by

$$\begin{aligned} &\text{Scalar Interaction}: f_{p/n} = \frac{1}{M_S^2}\left\{\sum_{q=u,d,s} f_{Tq}^{(p/n)} + \frac{2}{9} f_{Tg}^{(p/n)}\right\} \,, \\ &\text{Vector Interaction}: f_p = \frac{1}{M_V^2}(3+\alpha) \,, \quad f_n = \frac{1}{M_V^2}(3+2\alpha) \,, \end{aligned} \tag{5.27}$$

at leading order [98], with hadronic matrix elements f_{Tq}, and f_{Tg} defined as in references [60, 79].

5.4.3 Scalar-Mediator Results

It can be seen from Equation (5.20) that the strength of scalar interaction between dark matter and pions depend on the QCD confinement scale, $\Lambda_{\rm QCD} = \xi \Lambda_{\rm QCD}^{\rm SM}$. Consequently, for dark matter with purely scalar interactions, the relic density is a function of the mediator scale M_S, QCD confinement scale $\Lambda_{\rm QCD}$, and the mass of the dark matter at zero temperature, $m_\chi^{T=0}$. We consider $\xi = 1, 500, 1000$, where $\xi = 1$ represents the standard cosmological history and the other two choices correspond to $\Lambda_{\rm QCD} = 200, 400$ GeV, respectively.

The relic abundance is controlled by the thermally-averaged annihilation cross section at the time of freeze out ($T = T_F$) in the non-relativistic limit,

$$\langle \sigma_S v \rangle = \left(\frac{\kappa}{f_\pi^2 M_S^2}\right)^2 \sum_{\pi_a} \frac{\omega_a^2}{4\pi} \sqrt{1 - \frac{m_{\pi_a}^2}{m_\chi^2}} \langle v^2 \rangle + \mathcal{O}(\langle v^4 \rangle) \,. \tag{5.28}$$

Here ω_a are the eigenvalues of the 35×35 matrix $\mathrm{tr}(T^a T^b \beta)$, and the sum is over all the

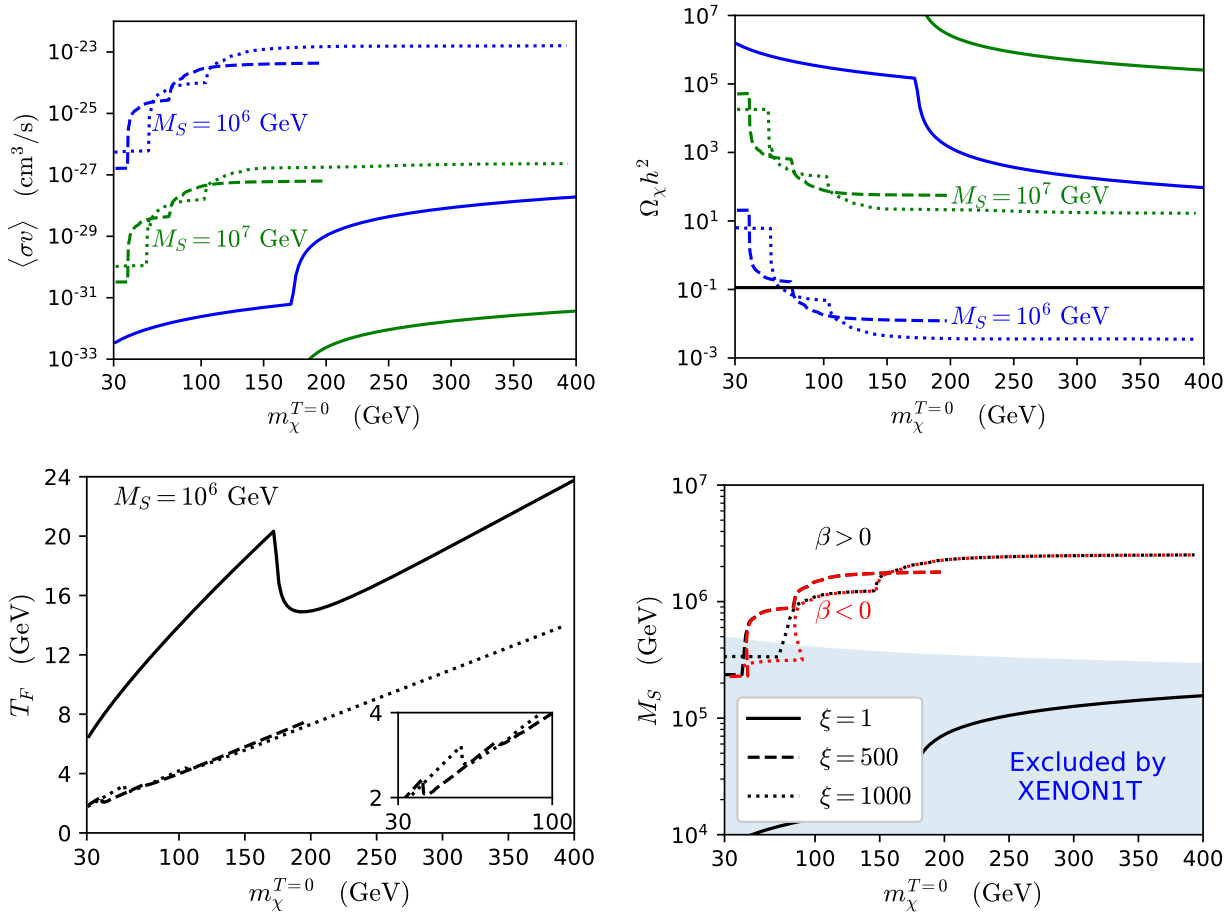

Figure 5.4: **(Top Left)** The thermally-averaged cross-sections at the time of freeze-out as a function of $m_\chi^{T=0}$ plotted for $M_S = 10^6$ GeV (blue), 10^7 GeV (green) and ξ =1 (solid), 500 (dashed), 1000 (dotted). **(Top Right)** Dark matter relic abundance today as a function of $m_\chi^{T=0}$ plotted for $M_S = 10^6$ GeV (blue), 10^7 GeV (green) and $\xi = 1, 500, 1000$. The horizontal solid line is the observed dark matter abundance. **(Bottom Left)** The freeze-out temperature T_F as a function of $m_\chi^{T=0}$ with $M_S = 10^6$ GeV, 10^7 GeV plotted for ξ =1 (solid), 500 (dashed), 1000 (dotted). **(Bottom Right)** We show the M_S values that produce the observed dark matter relic abundance as a function of $m_\chi^{T=0}$ for ξ =1 (solid), 500 (dashed), 1000 (dotted). For $\beta < 0$, the line is plotted in red. Shaded blue region is excluded by XENON1T. See text for details.

pions of mass[1] less than $m_\chi^{T=T_F}$. Note that scalar interactions lead to p-wave suppressed annihilation, for which $a = 0$. The relic abundance today is given by $\rho_\chi = m_\chi^{T=0} n_\chi$, whereas the energy density immediately after freeze out is $m_\chi^{T=T_F} n_\chi$. The shift in m_χ between the time of freeze out and the present epoch introduces an additional correction to the relic

[1]Our choice of couplings β_{ij} aligned with the Yukawa interactions leads to diagonal interactions between the dark matter and the pion mass eigenstates.

density today:

$$\Omega_\chi^{T=0} h^2 = \frac{m_\chi^{T=0}}{m_\chi^{T=0} + \Delta m_\chi} \Omega_\chi^{T=T_F} h^2. \tag{5.29}$$

In Figure 5.4, we show the annihilation cross section, relic density today, and freeze out temperature, for $\xi = 1, 500, 1000$ and two representative values of M_S, as a function of the dark matter mass today. In the final panel, we show the value of M_S for each dark matter mass (today) required to reproduce the observed relic density, for the same values of ξ considered. Also plotted on that panel are the current XENON1T constraints [6]. Comparing $\xi = 1$, the standard cosmological scenario, to $\xi = 500, 1000$ cases makes it clear that freeze-out during an early cosmological period of QCD confinement, which can realize the observed relic density for weaker couplings, can make the difference between a freeze-out relic WIMP being allowed versus strongly excluded by direct searches.

There are a number of features in Figure 5.4 that warrant further discussion:

- The $\xi \gg 1$ lines end when $m_\chi^{T=T_F} \sim \Lambda_{\rm QCD} \equiv \xi \Lambda_{\rm QCD}^{\rm SM}$, at which point the dark matter mass is heavier than the QCD scale, and the resulting annihilation would be into quarks and not into pions.

- For standard cosmology, with $\xi = 1$, the kink in the annihilation cross section at $m_\chi \sim 173$ GeV corresponds to the annihilation channel into top quarks opening up. Similarly, the kinks in the $\xi = 500, 1000$ lines correspond to new channels into heavier pions.

- As mentioned earlier, the annihilation cross section is enhanced by the QCD scale. Therefore this scenario accommodates larger values of the mediator scale, $M_S \sim 10^6$ GeV, compared to a standard WIMP scenario.

- The effect of the quark-condensate contribution to the dark matter mass can be seen

in the bottom-right panel. Depending on the sign of β in 5.21, there are two values of $m_\chi^{T=T_F}$ which correspond to a single $m_\chi^{T=0}$ for modest dark matter masses.

- The bottom left panel implies that a scenario in which the QCD deconfinement brings the dark matter back into equilibrium with quarks after it has frozen out from interacting with mesons is never realized, for deconfinement happening below a few GeV.

5.4.4 Vector-Mediator Results

For vector interactions, our choice of minimally flavor-violating interactions λ_{ij} with the quarks results in leading interactions with a pair of pions, as in Equation (5.20). In the non-relativistic limit, the thermally-averaged annihilation cross section is,

$$\langle \sigma_V v \rangle = \sum_{a,b=1}^{35} \frac{\Omega_{ab}}{24\pi} m_\chi^2 (1 - \gamma_{ab} + \rho_{ab})^{3/2} \left[1 + \left(1 + \frac{9}{4} \frac{\gamma_{ab} - 2\rho_{ab}}{1 - \gamma_{ab} + \rho_{ab}} \right) \frac{\langle v^2 \rangle}{2} + \mathcal{O}(\langle v^4 \rangle) \right] \quad (5.30)$$

summed over pairs of mesons for which $m_{\pi_a} + m_{\pi_b} \leq 2m_\chi$. Note that vector interactions do not induce a shift in the mass of the dark matter from the chiral condensate. The coupling matrix Ω_{ab} is given by

$$\Omega_{ab} \equiv \sum_{c,d=1}^{35} \frac{1}{M_V^4} f^{abc} \, \mathrm{tr}[T^c \lambda] \, f^{abd} \, \mathrm{tr}[T^d \lambda] \propto \frac{\alpha^2}{M_V^4} \, , \quad (5.31)$$

where we focus on $\alpha = 1$ for simplicity. The kinematic factors are defined as $\gamma_{ab} \equiv (m_{\pi_a}^2 + m_{\pi_b}^2)/(2m_\chi^2)$ and $\rho_{ab} \equiv (m_{\pi_a}^2 - m_{\pi_b}^2)^2/(16 m_\chi^4)$.

In Figure 5.5 we show the resulting annihilation cross section, relic density, and freeze-out temperature, as a function of the dark matter mass at zero temperature $m_\chi^{T=0}$, for two choices of $M_V = 100$ GeV, 1 TeV and $\xi = 1, 500, 1000$, where $\xi = 1$ corresponds to the standard picture of freeze-out through annihilation into quarks. In the final panel, we show the value of M_V for each dark matter mass required to reproduce the observed relic density for a given

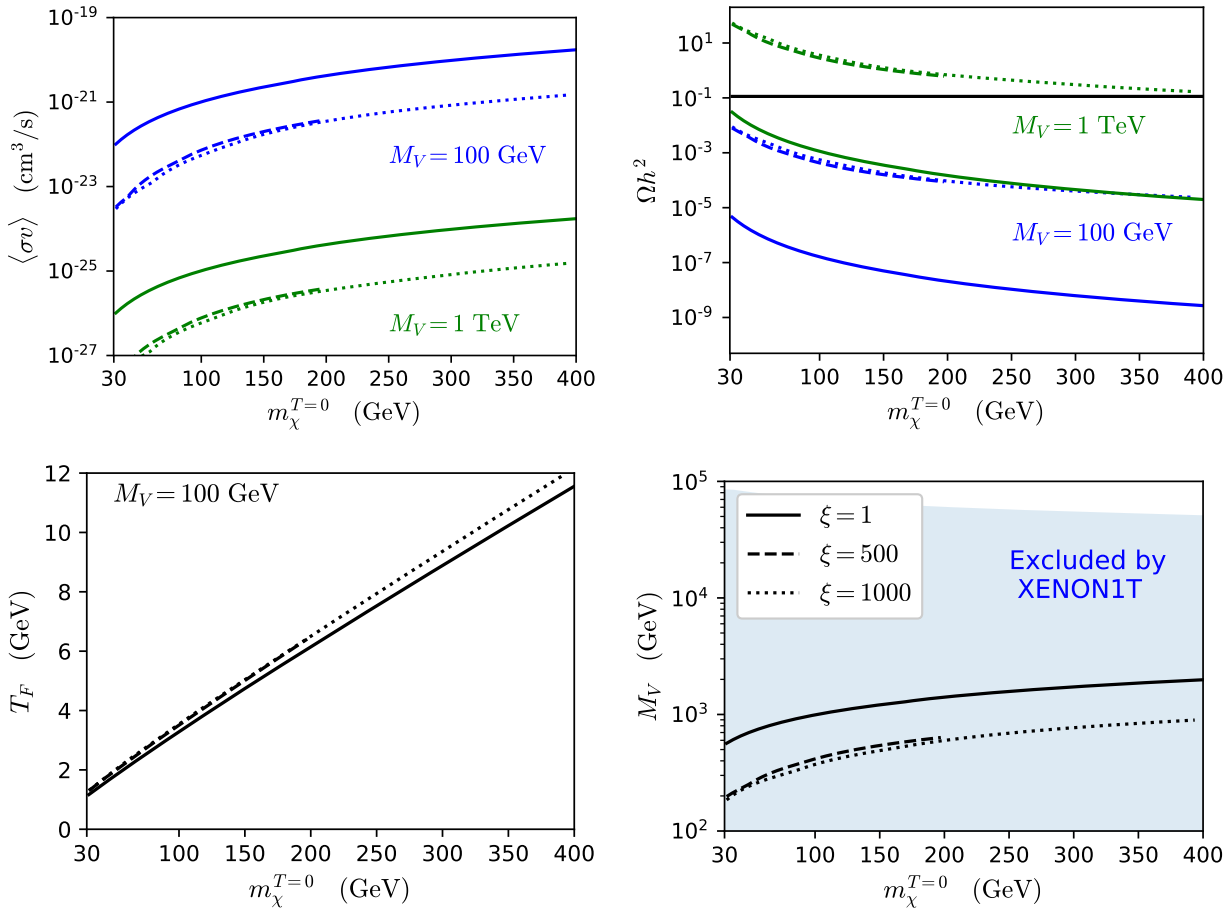

Figure 5.5: **(Top Left)** The thermally-averaged cross-sections at the time of freeze-out as a function of $m_\chi^{T=0}$ plotted for $M_V = 100$ GeV (blue), 1 TeV (green) and ξ =1 (solid), 500 (dashed), 1000 (dotted). **(Top Right)** The generated relic abundance today as a function of $m_\chi^{T=0}$ plotted for $M_V = 100$ GeV (blue), 1 TeV (green) and ξ =1 (solid), 500 (dashed), 1000 (dotted). The horizontal solid line is the observed dark matter abundance. **(Bottom Left)** The freeze-out temperature as a function of $m_\chi^{T=0}$ with $M_V = 100$ GeV plotted for ξ =1 (solid), 500 (dashed), 1000 (dotted). **(Bottom Right)** Coupling as a function of $m_\chi^{T=0}$ to produce the observed relic density plotted for ξ =1 (solid), 500 (dashed), 1000 (dotted). Shaded blue region is excluded by XENON1T. See text for details.

choice of ξ.

Unlike the scalar interactions, vector interactions do not get the $\xi-$enhancement from QCD confinement. On the contrary the annihilation cross-section is smaller than the standard WIMP scenario because the annihilation products, namely the new pions, are heavier than SM quarks at the same temperature in standard cosmology. Hence, the vector scenario does

worse than the standard WIMP case within this cosmological history.

5.5 Conclusions

The standard picture of freeze out is a compelling picture for the mechanism by which dark matter is produced in the early Universe, and the primary motivation for WIMP dark matter. Common wisdom states that the WIMP paradigm is in trouble, but this is the result of comparing freeze out in a standard cosmology to searches for WIMPs. In this article, we have explored the possibility that the cosmology looks radically different at the time of freeze out, in particular exploring the idea that QCD could have undergone an early period of confinement before relaxing to the behavior observed at low temperatures today. We find that for a scalar mediator, the dark matter mass is shifted by the chiral condensate, and its coupling to pions is enhanced during early confinement, allowing for parameter space which allows for freeze out production while remaining safe from constraints from XENON1T today, rescuing some of the WIMP parameter space. On the other hand, for a vector mediator we find that the differences between freeze out during early confinement and the standard cosmology are more modest, and the entire parameter space remains ruled out by XENON1T. Our work highlights the fact that a modified cosmology may largely distort the apparent messages from astrophysical observations of dark matter to inform particle physics model building.

Chapter 6

Conclusions

Throughout this thesis, we considered QFTs with two different goals: to study the dynamics of gauge theories and/or to study possible extensions of the SM which explain phenomena beyond the SM.

In the pursuit of the dynamics of gauge theories, we examined SUSY QFTs on $\mathbb{R}^4$, $\mathbb{R}^3$, and $\mathbb{R}^3 \times \mathbb{S}^1$ where the theory on the cylinder interpolates between the 3D and 4D theories. In Chapter 2, we derived the fundamental zero modes of the KK monopole. The existence of these zero modes explains how the 4D dynamics imparted by the KK monopole decouples from the 3D dynamics of the theory to arrive at a truly 3Dtheory, and in some examples, these zero modes become active in the 4D limit and are necessary to arrive at the correct instanton-induced superpotential. In Chapter 3, we calculated quantum corrections to the classical moduli space in 3D SUSY QCD with $F < N$ flavors. These quantum corrections "smooth out" the boundaries of the classical moduli space, allowing one to connect the coordinate charts in all regions of the moduli space. When implemented as a Lagrange multiplier in the superpotential, these corrections explain how the Coulomb branches of the theory reproduce the appropriate 4D result in the large radius limit on a cyliner and how

theories with F flavors flow to theories with $F-1$ flavors under large mass deformations.

The study of electric-magnetic scattering in Chapter 4 makes progress towards both goals. The on-shell methods developed in said chapter allow us to calcualte the dynamics in gauge theories with magnetic charges where little was calculable. In particular, we derive new selection rules for these scattering processes and fully relativistic answers for fermion-monopole scattering which agree with previous non-relativistic results. Furthermore, this formalism could help explain phenomena which is a result of magnetic charges in beyond the SM model building.

Finally, in Chapter 5, we discuss a model beyond the SM which could explain the observed dark matter abundance. This model consider thermal freeze out in a universe where QCD experiences an early phase transition. The phase transition ensures that the hadrons are the active degrees of freedom during thermal freeze out which alters the relationship between the dark matter couplings, mass, and relic density. While most models of dark matter with masses and couplings of order the electroweak scale are in tension with bounds from direct detection experiments, this altered relationship between the dark matter's observables allows the model to explain the observed dark matter relic abundance without contradicting direct detection observations.

Bibliography

[1] M. Aaboud et al. Search for dark matter and other new phenomena in events with an energetic jet and large missing transverse momentum using the ATLAS detector. *JHEP*, 01:126, 2018.

[2] M. Abdullah, A. DiFranzo, A. Rajaraman, T. M. P. Tait, P. Tanedo, and A. M. Wijangco. Hidden on-shell mediators for the Galactic Center γ-ray excess. *Phys. Rev.*, D90:035004, 2014.

[3] O. Aharony, A. Hanany, K. A. Intriligator, N. Seiberg, and M. J. Strassler. Aspects of N=2 supersymmetric gauge theories in three-dimensions. *Nucl. Phys. B*, 499:67–99, 1997.

[4] O. Aharony, S. S. Razamat, N. Seiberg, and B. Willett. 3d dualities from 4d dualities. *JHEP*, 07:149, 2013.

[5] M. L. Ahnen et al. Limits to Dark Matter Annihilation Cross-Section from a Combined Analysis of MAGIC and Fermi-LAT Observations of Dwarf Satellite Galaxies. *JCAP*, 1602:039, 2016.

[6] E. Aprile et al. Dark Matter Search Results from a One Ton-Year Exposure of XENON1T. *Phys. Rev. Lett.*, 121(11):111302, 2018.

[7] N. Arkani-Hamed, T.-C. Huang, and Y.-t. Huang. Scattering Amplitudes For All Masses and Spins. 9 2017.

[8] M. F. Atiyah, N. J. Hitchin, V. G. Drinfeld, and Y. I. Manin. Construction of Instantons. *Phys. Lett. A*, 65:185–187, 1978.

[9] Y. Bai and T. M. P. Tait. Inelastic Dark Matter at the LHC. *Phys. Lett.*, B710:335–338, 2012.

[10] A. A. Belavin, A. M. Polyakov, A. S. Schwartz, and Y. S. Tyupkin. Pseudoparticle Solutions of the Yang-Mills Equations. *Phys. Lett. B*, 59:85–87, 1975.

[11] M. Beltran, D. Hooper, E. W. Kolb, and Z. C. Krusberg. Deducing the nature of dark matter from direct and indirect detection experiments in the absence of collider signatures of new physics. *Phys. Rev.*, D80:043509, 2009.

[12] D. Berger, S. Ipek, T. M. P. Tait, and M. Waterbury. Dark Matter Freeze Out during an Early Cosmological Period of QCD Confinement. *JHEP*, 07:192, 2020.

[13] Z. Bern, L. J. Dixon, D. C. Dunbar, and D. A. Kosower. Fusing gauge theory tree amplitudes into loop amplitudes. *Nucl. Phys. B*, 435:59–101, 1995.

[14] C. Boehm, M. J. Dolan, C. McCabe, M. Spannowsky, and C. J. Wallace. Extended gamma-ray emission from Coy Dark Matter. *JCAP*, 1405:009, 2014.

[15] E. B. Bogomolny. Stability of Classical Solutions. *Sov. J. Nucl. Phys.*, 24:449, 1976.

[16] D. G. Boulware, L. S. Brown, R. N. Cahn, S. D. Ellis, and C.-k. Lee. Scattering on Magnetic Charge. *Phys. Rev.*, D14:2708, 1976.

[17] F. Bruckmann, D. Nogradi, and P. van Baal. Constituent monopoles through the eyes of fermion zero modes. *Nucl. Phys. B*, 666:197–229, 2003.

[18] F. Brummer, J. Jaeckel, and V. V. Khoze. Magnetic Mixing: Electric Minicharges from Magnetic Monopoles. *JHEP*, 06:037, 2009.

[19] C. G. Callan, Jr. Monopole Catalysis of Baryon Decay. *Nucl. Phys.*, B212:391–400, 1983.

[20] C. Callias. Index Theorems on Open Spaces. *Commun. Math. Phys.*, 62:213–234, 1978.

[21] S. Caron-Huot and Z. Zahraee. Integrability of Black Hole Orbits in Maximal Supergravity. *JHEP*, 07:179, 2019.

[22] A. Cherman, T. Schäfer, and M. Ünsal. Chiral Lagrangian from Duality and Monopole Operators in Compactified QCD. *Phys. Rev. Lett.*, 117(8):081601, 2016.

[23] C. Cheung. *TASI Lectures on Scattering Amplitudes*, pages 571–623. 2018.

[24] M. Cirelli, N. Fornengo, and A. Strumia. Minimal dark matter. *Nucl. Phys.*, B753:178–194, 2006.

[25] S. Coleman. *Aspects of Symmetry: Selected Erice Lectures*. Cambridge University Press, Cambridge, U.K., 1985.

[26] K. Colwell and J. Terning. S-Duality and Helicity Amplitudes. *JHEP*, 03:068, 2016.

[27] E. Conde, E. Joung, and K. Mkrtchyan. Spinor-Helicity Three-Point Amplitudes from Local Cubic Interactions. *JHEP*, 08:040, 2016.

[28] S. F. Cordes. The Instanton Induced Superpotential in Supersymmetric QCD. *Nucl. Phys. B*, 273:629–648, 1986.

[29] D. Croon, J. N. Howard, S. Ipek, and T. M. P. Tait. QCD Baryogenesis. 2019.

[30] C. Csáki, S. Hong, Y. Shirman, O. Telem, and J. Terning. Multi-particle Representations of the Poincaré Group. 10 2020.

[31] C. Csaki, S. Hong, Y. Shirman, O. Telem, J. Terning, and M. Waterbury. Scattering Amplitudes for Monopoles: Pairwise Little Group and Pairwise Helicity. 9 2020.

[32] C. Csáki, M. Martone, Y. Shirman, P. Tanedo, and J. Terning. Dynamics of 3D SUSY Gauge Theories with Antisymmetric Matter. *JHEP*, 08:141, 2014.

[33] C. Csáki, M. Martone, Y. Shirman, and J. Terning. Pre-ADS Superpotential from Confined Monopoles. *JHEP*, 05:188, 2018.

[34] C. Csaki, Y. Shirman, and J. Terning. Anomaly Constraints on Monopoles and Dyons. *Phys. Rev. D*, 81:125028, 2010.

[35] C. Csaki, Y. Shirman, J. Terning, and M. Waterbury. Kaluza-Klein Monopoles and their Zero Modes. *Phys. Rev. Lett.*, 120(7):071603, 2018.

[36] G. D'Ambrosio, G. F. Giudice, G. Isidori, and A. Strumia. Minimal flavor violation: An Effective field theory approach. *Nucl. Phys.*, B645:155–187, 2002.

[37] N. M. Davies, T. J. Hollowood, V. V. Khoze, and M. P. Mattis. Gluino condensate and magnetic monopoles in supersymmetric gluodynamics. *Nucl. Phys. B*, 559:123–142, 1999.

[38] J. de Boer, K. Hori, H. Ooguri, and Y. Oz. Mirror symmetry in three-dimensional gauge theories, quivers and D-branes. *Nucl. Phys. B*, 493:101–147, 1997.

[39] J. de Boer, K. Hori, and Y. Oz. Dynamics of N=2 supersymmetric gauge theories in three-dimensions. *Nucl. Phys. B*, 500:163–191, 1997.

[40] P. A. Dirac. The Theory of magnetic poles. *Phys. Rev.*, 74:817–830, 1948.

[41] P. A. M. Dirac. Quantised singularities in the electromagnetic field,. *Proc. Roy. Soc. Lond. A*, 133(821):60–72, 1931.

[42] N. Dorey, T. J. Hollowood, V. V. Khoze, and M. P. Mattis. The Calculus of many instantons. *Phys. Rept.*, 371:231–459, 2002.

[43] N. Dorey, V. V. Khoze, M. P. Mattis, D. Tong, and S. Vandoren. Instantons, three-dimensional gauge theory, and the Atiyah-Hitchin manifold. *Nucl. Phys. B*, 502:59–93, 1997.

[44] N. Dorey, D. Tong, and S. Vandoren. Instanton effects in three-dimensional supersymmetric gauge theories with matter. *JHEP*, 04:005, 1998.

[45] G. Durieux, T. Kitahara, C. S. Machado, Y. Shadmi, and Y. Weiss. Constructing massive on-shell contact terms. 8 2020.

[46] H. Elvang and Y.-t. Huang. Scattering Amplitudes. 8 2013.

[47] J. L. Feng and J. Kumar. The WIMPless Miracle: Dark-Matter Particles without Weak-Scale Masses or Weak Interactions. *Phys. Rev. Lett.*, 101:231301, 2008.

[48] D. Finnell and P. Pouliot. Instanton calculations versus exact results in four-dimensional SUSY gauge theories. *Nucl. Phys. B*, 453:225–239, 1995.

[49] D. Forde. Direct extraction of one-loop integral coefficients. *Phys. Rev. D*, 75:125019, 2007.

[50] M. Freytsis and Z. Ligeti. On dark matter models with uniquely spin-dependent detection possibilities. *Phys. Rev.*, D83:115009, 2011.

[51] L. P. Gamberg and K. A. Milton. Dual quantum electrodynamics: Dyon-dyon and charge monopole scattering in a high-energy approximation. *Phys. Rev. D*, 61:075013, 2000.

[52] G. B. Gelmini and P. Gondolo. Neutralino with the right cold dark matter abundance in (almost) any supersymmetric model. *Phys. Rev.*, D74:023510, 2006.

[53] C. Gomez Sanchez and B. Holdom. Monopoles, strings and dark matter. *Phys. Rev. D*, 83:123524, 2011.

[54] J. Goodman, M. Ibe, A. Rajaraman, W. Shepherd, T. M. P. Tait, and H.-B. Yu. Constraints on Dark Matter from Colliders. *Phys. Rev.*, D82:116010, 2010.

[55] K. Griest and M. Kamionkowski. Unitarity Limits on the Mass and Radius of Dark Matter Particles. *Phys. Rev. Lett.*, 64:615, 1990.

[56] A. Guevara, A. Ochirov, and J. Vines. Scattering of Spinning Black Holes from Exponentiated Soft Factors. *JHEP*, 09:056, 2019.

[57] S. Hamdan and J. Unwin. Dark Matter Freeze-out During Matter Domination. *Mod. Phys. Lett.*, A33(29):1850181, 2018.

[58] H. Hannesdottir and M. D. Schwartz. S -Matrix for massless particles. *Phys. Rev. D*, 101(10):105001, 2020.

[59] J. M. Henn and J. C. Plefka. *Scattering Amplitudes in Gauge Theories*, volume 883. Springer, Berlin, 2014.

[60] R. J. Hill and M. P. Solon. Standard Model anatomy of WIMP dark matter direct detection II: QCD analysis and hadronic matrix elements. *Phys. Rev.*, D91:043505, 2015.

[61] A. Hook and J. Huang. Bounding millimagnetically charged particles with magnetars. *Phys. Rev. D*, 96(5):055010, 2017.

[62] Y.-T. Huang, U. Kol, and D. O'Connell. Double copy of electric-magnetic duality. *Phys. Rev. D*, 102(4):046005, 2020.

[63] K. A. Intriligator, R. G. Leigh, and N. Seiberg. Exact superpotentials in four-dimensions. *Phys. Rev. D*, 50:1092–1104, 1994.

[64] S. Ipek, D. McKeen, and A. E. Nelson. A Renormalizable Model for the Galactic Center Gamma Ray Excess from Dark Matter Annihilation. *Phys. Rev.*, D90(5):055021, 2014.

[65] S. Ipek and T. M. P. Tait. Early Cosmological Period of QCD Confinement. *Phys. Rev. Lett.*, 122(11):112001, 2019.

[66] R. Jackiw and C. Rebbi. Solitons with Fermion Number 1/2. *Phys. Rev. D*, 13:3398–3409, 1976.

[67] M. Jiang, J. Shu, M.-L. Xiao, and Y.-H. Zheng. New Selection Rules from Angular Momentum Conservation. 1 2020.

[68] Y. Kazama, C. N. Yang, and A. S. Goldhaber. Scattering of a Dirac Particle with Charge Ze by a Fixed Magnetic Monopole. *Phys. Rev.*, D15:2287–2299, 1977.

[69] U. Kol and M. Porrati. Gravitational Wu-Yang Monopoles. *Phys. Rev. D*, 101(12):126009, 2020.

[70] E. W. Kolb and M. S. Turner. The Early Universe. *Front. Phys.*, 69:1–547, 1990.

[71] D. A. Kosower. Next-to-maximal helicity violating amplitudes in gauge theory. *Phys. Rev. D*, 71:045007, 2005.

[72] T. C. Kraan and P. van Baal. Periodic instantons with nontrivial holonomy. *Nucl. Phys. B*, 533:627–659, 1998.

[73] L. Laperashvili and H. B. Nielsen. Dirac relation and renormalization group equations for electric and magnetic fine structure constants. *Mod. Phys. Lett. A*, 14:2797, 1999.

[74] K.-M. Lee. Instantons and magnetic monopoles on R**3 x S**1 with arbitrary simple gauge groups. *Phys. Lett. B*, 426:323–328, 1998.

[75] K.-M. Lee and C.-h. Lu. SU(2) calorons and magnetic monopoles. *Phys. Rev. D*, 58:025011, 1998.

[76] K.-M. Lee and P. Yi. Monopoles and instantons on partially compactified D-branes. *Phys. Rev. D*, 56:3711–3717, 1997.

[77] H. Lipkin, W. Weisberger, and M. Peshkin. Magnetic charge quantization and angular momentum. *Annals Phys.*, 53:203–214, 1969.

[78] S. Mandelstam. Vortices and Quark Confinement in Nonabelian Gauge Theories. *Phys. Rept.*, 23:245–249, 1976.

[79] K. A. Mohan, D. Sengupta, T. M. P. Tait, B. Yan, and C. P. Yuan. Direct Detection and LHC constraints on a t-Channel Simplified Model of Majorana Dark Matter at One Loop. *JHEP*, 05:115, 2019.

[80] N. Moynihan and J. Murugan. On-Shell Electric-Magnetic Duality and the Dual Graviton. 2 2020.

[81] T. M. W. Nye and M. A. Singer. An L**2 index theorem for Dirac operators on S**1 x R**3. 9 2000.

[82] G. Ossola, C. G. Papadopoulos, and R. Pittau. Reducing full one-loop amplitudes to scalar integrals at the integrand level. *Nucl. Phys. B*, 763:147–169, 2007.

[83] H. Pilkuhn. *Relativistic Particle Physics*. 1 1979.

[84] A. M. Polyakov. Particle Spectrum in the Quantum Field Theory. *JETP Lett.*, 20:194–195, 1974.

[85] A. M. Polyakov. Quark Confinement and Topology of Gauge Groups. *Nucl. Phys. B*, 120:429–458, 1977.

[86] E. Poppitz, T. Schäfer, and M. Unsal. Continuity, Deconfinement, and (Super) Yang-Mills Theory. *JHEP*, 10:115, 2012.

[87] E. Poppitz and M. Unsal. Index theorem for topological excitations on R**3 x S**1 and Chern-Simons theory. *JHEP*, 03:027, 2009.

[88] E. Poppitz and M. Unsal. Seiberg-Witten and 'Polyakov-like' magnetic bion confinements are continuously connected. *JHEP*, 07:082, 2011.

[89] V. A. Rubakov. Superheavy Magnetic Monopoles and Proton Decay. *JETP Lett.*, 33:644–646, 1981. [Pisma Zh. Eksp. Teor. Fiz.33,658(1981)].

[90] P. Schuster and N. Toro. Continuous-spin particle field theory with helicity correspondence. *Phys. Rev. D*, 91:025023, 2015.

[91] J. S. Schwinger. A Magnetic model of matter. *Science*, 165:757–761, 1969.

[92] J. S. Schwinger, K. A. Milton, W.-y. Tsai, J. DeRaad, Lester L., and D. C. Clark. Nonrelativistic Dyon-Dyon Scattering. *Annals Phys.*, 101:451, 1976.

[93] N. Seiberg. Naturalness versus supersymmetric nonrenormalization theorems. *Phys. Lett. B*, 318:469–475, 1993.

[94] N. Seiberg and E. Witten. Electric - magnetic duality, monopole condensation, and confinement in N=2 supersymmetric Yang-Mills theory. *Nucl. Phys. B*, 426:19–52, 1994. [Erratum: Nucl.Phys.B 430, 485–486 (1994)].

[95] N. Seiberg and E. Witten. Gauge dynamics and compactification to three-dimensions. In *Conference on the Mathematical Beauty of Physics (In Memory of C. Itzykson)*, 6 1996.

[96] M. Shifman. *Advanced topics in quantum field theory.* Cambridge Univ. Press, Cambridge, UK, 2012.

[97] M. Shifman and M. Unsal. On Yang-Mills Theories with Chiral Matter at Strong Coupling. *Phys. Rev. D*, 79:105010, 2009.

[98] M. A. Shifman, A. I. Vainshtein, and V. I. Zakharov. Remarks on Higgs Boson Interactions with Nucleons. *Phys. Lett.*, 78B:443–446, 1978.

[99] Y. Shirman and M. Waterbury. Deformations of the moduli space and superpotential flows in 3D SUSY QCD. *Phys. Rev. D*, 99(12):125002, 2019.

[100] A. M. Sirunyan et al. Search for dark matter produced with an energetic jet or a hadronically decaying W or Z boson at $\sqrt{s} = 13$ TeV. *JHEP*, 07:014, 2017.

[101] G. 't Hooft. Magnetic Monopoles in Unified Gauge Theories. *Nucl. Phys. B*, 79:276–284, 1974.

[102] G. 't Hooft. Computation of the Quantum Effects Due to a Four-Dimensional Pseudoparticle. *Phys. Rev. D*, 14:3432–3450, 1976. [Erratum: Phys.Rev.D 18, 2199 (1978)].

[103] J. Terning and C. B. Verhaaren. Dark Monopoles and $SL(2, \mathbb{Z})$ Duality. *JHEP*, 12:123, 2018.

[104] J. Terning and C. B. Verhaaren. Resolving the Weinberg Paradox with Topology. *JHEP*, 03:177, 2019.

[105] J. Terning and C. B. Verhaaren. Spurious Poles in the Scattering of Electric and Magnetic Charges. *JHEP*, 12:153, 2020.

[106] J. J. Thomson. On momentum in the electric field. *Phil. Mag.*, 8:331, 1904.

[107] D. Tong. TASI lectures on solitons: Instantons, monopoles, vortices and kinks. In *Theoretical Advanced Study Institute in Elementary Particle Physics: Many Dimensions of String Theory*, 6 2005.

[108] D. Tucker-Smith and N. Weiner. Inelastic dark matter. *Phys. Rev.*, D64:043502, 2001.

[109] S. Vandoren and P. van Nieuwenhuizen. Lectures on instantons. 2 2008.

[110] D. Varshalovich, A. Moskalev, and V. Khersonsky. *Quantum Theory of Angular Momentum: Irreducible Tensors, Spherical Harmonics, Vector Coupling Coefficients, 3nj Symbols*. World Scientific, Singapore, 1988.

[111] S. Weinberg. Photons and gravitons in perturbation theory: Derivation of Maxwell's and Einstein's equations. *Phys. Rev.*, 138:B988–B1002, 1965.

[112] S. Weinberg. *The Quantum theory of fields. Vol. 1: Foundations*. Cambridge University Press, 2005.

[113] E. P. Wigner. On Unitary Representations of the Inhomogeneous Lorentz Group. *Annals Math.*, 40:149–204, 1939.

[114] E. Witten. Perturbative gauge theory as a string theory in twistor space. *Commun. Math. Phys.*, 252:189–258, 2004.

[115] T. T. Wu and C. N. Yang. Dirac Monopole Without Strings: Monopole Harmonics. *Nucl. Phys. B*, 107:365, 1976.

[116] T. T. Wu and C. N. Yang. Dirac's Monopole Without Strings: Classical Lagrangian Theory. *Phys. Rev. D*, 14:437–445, 1976.

[117] D. Zwanziger. Quantum field theory of particles with both electric and magnetic charges. *Phys. Rev.*, 176:1489–1495, 1968.

[118] D. Zwanziger. Local Lagrangian quantum field theory of electric and magnetic charges. *Phys. Rev. D*, 3:880, 1971.

[119] D. Zwanziger. Angular distributions and a selection rule in charge-pole reactions. *Phys. Rev. D*, 6:458–470, Jul 1972.

Appendix A

Squark Correlation Function Calculation

This appendix first appeared in work previously published in collaboration with Yuri Shirman [99].

In this appendix, we discuss the evaluation of the path integral for an SU(2) theory with one flavor which leads to (3.4). We begin by deriving the instanton-monopole integration measure, collective coordinates, one loop determinants and all. Then we derive the fermionic zero mode functions and evaluate the integral. As a preparation for this discussion, let us recall properties of the single monopole configuration corresponding to the first non-trivial solution of the classical equations of motion [84, 101]

$$\begin{aligned} A_i^a(r) &= \epsilon^{aij}\frac{n^j}{r}F(vr)\,, \quad \sigma^a(r) = vn^a H(vr)\,, \\ F(\rho) &= 1 - \frac{\rho}{\sinh\rho}\,, \quad H(\rho) = \frac{\cosh\rho}{\sinh\rho} - \frac{1}{\rho}\,. \end{aligned} \tag{A.1}$$

Such solutions satisfy the lower bound of the Bogomolnyi bound and are exact since the adjoint scalar has no classical potential. There remain quantum fluctuations of the fields in

this classical background. Some of these fluctuations do not have a corresponding change in the action. These are the zero modes of the instanton-monopole. Index theorems guarantee a certain number of zero modes.

Specifically, the single monopole has four bosonic zero modes: three for the position of the monopole and one for a left over U(1) transformation. If we add a fermion ψ to the theory, it also acquires zero modes satisfying

$$(i\mathcal{D}_\mu\bar{\sigma}^\mu)\psi = (i\partial_i\sigma^i + A_i^a\sigma^i T^a + \sigma^a T^a)\psi = 0\,, \tag{A.2}$$

where the number of zero mode solutions and T^a depend on the representation of ψ. We normalize our generators such that $\mathrm{Tr}(T^aT^b) = \delta^{ab}/2$ in the fundamental representation. Fermions in the adjoint representation have two zero modes, and fermions in the fundamental representation have a single zero mode.

A.1 Monopole-Instanton Measure

As discussed in section 3.2, the monopole contribution to the squark correlation function is (3.1). In this formula, all fields have been expanded around their classical solution $\phi = \phi_{cl.} + \phi_{qu.}$. The quantum fluctuations come in two types: non-zero modes and zero modes. To leading order, the non-zero mode fluctuations are gaussian and their evaluation reduces to determinants of $\Delta_- = \not{\mathcal{D}}_{cl}\bar{\not{\mathcal{D}}}_{cl}$ and $\Delta_+ = \bar{\not{\mathcal{D}}}_{cl}\not{\mathcal{D}}_{cl}$. Δ_- has zero modes in self-dual configurations which are excluded from the determinants (denoted with a det$'$). In 3D, the contributions of non-zero modes do not cancel even in supersymmetric theories [43, 44]. As a result, the path integral of the $\mathcal{N} = 2$ theory with F fundamental flavors is proportional to a factor of $(R_{adj})^{3/4}\,(R_{fund})^{-F/2}$, where the ratio of determinants $R_{\mathcal{R}}$ for an arbitrary

representation $\mathcal{R}$ is given by

$$R_{\mathcal{R}} = \frac{\det \Delta_+}{\det' \Delta_-} = \lim_{\mu \to 0} \left[\mu^{I_{\mathcal{R}}(0)} \exp\left(- \int_{\mu^2}^{\infty} \frac{dM^2}{M^2} I_{\mathcal{R}}(M^2) \right) \right] . \tag{A.3}$$

$I_{\mathcal{R}}(M^2)$ is the generalized zero mode index for representation $\mathcal{R}$. The ratio of non-zero mode determinants is $R_{adj} = (2v)^4$ for the adjoint and $R_{fund} = v^2$ for the fundamental representation [44].

After converting the zero mode integrals to collective coordinates and using zero mode solutions normalized to one, the path integral measure becomes [43]

$$\int [D\phi_0] = \int \frac{d^3z}{(2\pi)^{3/2}} (S_{cl})^{3/2} \int \frac{d\theta}{(2\pi)^{1/2}} \left(\frac{S_{cl}}{v^2} \right)^{1/2} \int d^2\xi \int d\chi \int d\bar{\chi} \, , \tag{A.4}$$

where z and θ make up the bosonic collective coordinates, and the ξ, χ and $\bar{\chi}$ are Grassmannian collective coordinates for the gauginos and quarks respectively. If we expand the effective squark action in supersymmetric gauge couplings, the correlation function simplifies to

$$\begin{aligned} \langle \bar{q}^i(x) q_i(x) \rangle = \frac{(R_{adj})^{3/4} (R_{fund})^{-1/2}}{2\pi} \frac{(S_{cl})^2}{v} e^{-S_{cl}} \int d^3z \int d^2\xi \int d\chi d\bar{\chi} \\ \times \bar{q}(x) q(x) \int d^3y_1 \, (q^* \lambda \psi) \int d^3y_2 \, \left(\bar{q}^* \lambda \bar{\psi} \right) . \end{aligned} \tag{A.5}$$

Now we turn to deriving the fermionic zero modes.

A.2 Gaugino Zero Modes

Reverting to σ^a being the fourth component of the four-vector gauge field A_μ, the gaugino has zero mode solutions resulting from supersymmetry transformations on the monopole

field configuration

$$\lambda^a{}_\alpha^{[\beta]}(r) = \frac{-1}{\sqrt{2}}(\sigma^{\mu\nu})_\alpha{}^\beta F^a{}_{\mu\nu} \equiv \sqrt{2}(\sigma^k)_\alpha{}^\beta B^a_k(r)\,, \tag{A.6}$$

where $B^a_k(r)$ is the k^{th} component of the a^{th} color magnetic field, $B^a_k = -\frac{1}{2}\epsilon_{ijk}F^{a\,ij}$, in monopole background and β labels the two zero modes. Explicit evaluation finds

$$B^a_k(r) = (\delta^a_k - n^k n^a)\frac{vH(vr)}{r}(1 - F(vr)) + n^k n^a \frac{F(vr)}{r^2}(2 - F(vr))\,. \tag{A.7}$$

After normalizing the gaugino zero modes and introducing a dimensionless function $\tilde{B}^a_k(vr) = \frac{1}{v^2}B^a_k$ we find

$$\lambda^a{}_\alpha^{[\beta]}(r) = \sqrt{\frac{g^2v^3}{4\pi}}(\sigma^k)_\alpha{}^\beta \tilde{B}^a_k(vr)\,. \tag{A.8}$$

A.3 Quark Zero Modes

Zero mode solutions for fundamental fermions were found in [66] and are given by

$$\psi_{i\alpha}(r) = (\sigma^2)_{i\alpha}C\exp\left[-\int_0^r dr\left(\frac{v}{2}H(vr) + \frac{F(vr)}{r}\right)\right], \tag{A.9}$$

where C is the normalization constant. In supersymmetric gauge theories, there is a closed form solution,

$$\psi_{i\alpha}(r) = (\sigma^2)_{i\alpha}\sqrt{\frac{v^3}{8\pi}}\frac{\tanh\frac{vr}{2}}{\sqrt{vr\sinh vr}} := (\sigma^2)_{i\alpha}\sqrt{\frac{v^3}{8\pi}}X(vr)\,, \tag{A.10}$$

where $X(r)$ is implicitly defined. Similar solutions for the anti-fundamental modes can be found by raising indices with the anti-symmetric tensor, ϵ^{ij}. Reintroducing the Grassmannian coordinate, χ, to the fermion field, the zero mode is $(\psi_0)_{i\alpha} = \psi_{i\alpha}\chi$.

A.4 Evalulating the integral

Inserting (A.8) and (A.10) into (A.5) then performing the Grassmann integration and replacing the products of squark operators with their Green's functions,[1] one finds

$$\langle \bar{q}^i(x) q_i(x) \rangle = \frac{v^2}{g^4} e^{-S_{cl}} \frac{g^2}{16\pi^3} \int d^3z \prod_{i=1,2} \int d^3y_i \frac{e^{-\frac{v}{2}|x-y_i|}}{v|x-y_i|} \Omega(v|z-y_i|)\,, \tag{A.11}$$

where $\Omega(\rho) = \delta^k_a X(\rho) \tilde{B}^a_k(\rho)$. Shifting the center of integration such that $y_i \to y_i + z$ and $z \to z + x$, the x dependence drops out. The angular y_i integrals can be evaluated and the integral simplifies to

$$\langle \bar{q}^i(x) q_i(x) \rangle = \frac{v^2}{g^4} e^{-S_{cl}} g^2 I\,, \tag{A.12}$$

where $I = 4 \int d\rho_z \prod_{i=1,2} \int d\rho_i \rho_i (e^{-|\rho_z - \rho_i|/2} - e^{-|\rho_z + \rho_i|/2}) \Omega(\rho_i)$. Note that the ρ_i are the dimensionless magnitudes of the 3D vectors $\rho_i = v|\vec{y_i}|$. It takes some work, but one can show that the integrand of I is positive definite and converges quickly. Thus our answer is

$$\langle \bar{q}^i(x) q_i(x) \rangle \sim g^2 \left(\frac{v^2}{g^4} \right) e^{-S_{cl}}\,, \tag{A.13}$$

which is non-holomorphic due to the factor of v^2/g^4. As explained in [44, 86], this non-holomorphic factor reflects finite renormalization of g^2 and can be absorbed into the definition of the kinetic terms in the low energy theory. After taking this into account, the correlation function becomes a holomorphic relation between chiral operators $YM = g^2$.

[1] The integral should be dominated by regions where the squarks are essentially free, massive fields. In these regions, the Green's function is $q_i^*(x) q^j(y) = G_i^j(|x-y|) \sim \delta_i^j e^{-v|x-y|/2} (4\pi|x-y|)^{-1}$.

Appendix B

Notation and Conventions for Chapter 4

This appendix first appeared in work previously published in collaboration with Csaba Csáki, Sungwoo Hong, Yuri Shirman, Ofri Telem, and John Terning [31].

B.1 Notation

We work in mostly-minus signature $(+,-,-,-)$. Our Pauli matrices are defined as

$$(\sigma^\mu)_{\alpha\dot{\alpha}} \;=\; (I\,,\,\vec{\sigma}) \quad , \quad (\bar{\sigma}^\mu)^{\dot{\alpha}\alpha} \;=\; (I\,,\,-\vec{\sigma})\,, \tag{B.1}$$

where

$$\sigma^1 \;=\; \begin{pmatrix} 0 & 1 \\ 1 & 0 \end{pmatrix} \;,\; \sigma^2 \;=\; \begin{pmatrix} 0 & -i \\ i & 0 \end{pmatrix} \;,\; \sigma^3 \;=\; \begin{pmatrix} 1 & 0 \\ 0 & -1 \end{pmatrix} . \tag{B.2}$$

Undotted indices are raised and lowered by the two index epsilon symbol

$$\epsilon^{\alpha\beta} \;=\; \epsilon_{\alpha\beta} \;=\; \begin{pmatrix} 0 & 1 \\ -1 & 0 \end{pmatrix} , \tag{B.3}$$

following a northwest-southeast convention:

$$\lambda^\alpha \;=\; \epsilon^{\alpha\beta}\lambda_\beta \;,\; \lambda_\alpha \;=\; \lambda^\beta \epsilon_{\beta\alpha} \,. \tag{B.4}$$

Similarly, dotted indices are raised and lowered with

$$\epsilon^{\dot\alpha\dot\beta} \;=\; \epsilon_{\dot\alpha\dot\beta} \;=\; \begin{pmatrix} 0 & -1 \\ 1 & 0 \end{pmatrix} , \tag{B.5}$$

following a northwest-southeast convention:

$$\tilde\lambda^{\dot\alpha} \;=\; \tilde\lambda_{\dot\beta}\, \epsilon^{\dot\beta\dot\alpha} \;,\; \tilde\lambda_{\dot\alpha} \;=\; \epsilon_{\dot\alpha\dot\beta}\, \tilde\lambda^{\dot\beta} \,. \tag{B.6}$$

We define symmetrized products as:

$$
\begin{aligned}
&(\ |a_1\rangle^{n_1} \ \cdot \ldots \cdot \ |a_k\rangle^{n_k} \ )_{\{\alpha_1,\ldots\alpha_{2J}\}} \ \equiv \\
&\mathcal{N} \sum_{\sigma_k} |a_1\rangle_{\alpha_{\sigma_k(1)}} \cdot \ldots \cdot |a_1\rangle_{\alpha_{\sigma_k(n_1)}} \cdot \ldots \cdot |a_k\rangle_{\alpha_{\sigma_k(2J-n_k+1)}} \cdot \ldots \cdot |a_k\rangle_{\alpha_{\sigma_k(2J)}} \, ,
\end{aligned}
\tag{B.7}
$$

where $\sum n_i = 2J$, and the sum is over permutations on k elements. We choose the normalization factor to be

$$
\mathcal{N} \ = \ \left[(2J)! \prod_{i=1}^{k} (n_i)! \right]^{-\frac{1}{2}} \, . \tag{B.8}
$$

This choice of normalization gives us Wigner $\mathcal{D}$-matrices when contracting symmetric products of spinors in the COM frame.

B.1.1 Conventions

The fermions in our paper are all left-handed Weyl, while their hermitian conjugates are right-handed:

$$
f \ \equiv \ \text{LH Weyl} \quad , \quad f^\dagger \ \equiv \ \text{RH Weyl} \, . \tag{B.9}
$$

We work in the all-outgoing convention for the S-matrix, for consistency with the rest of the scattering S-matrix literature. In practice it means that $h = \frac{1}{2}\,(-\frac{1}{2})$ for the initial

(i.e. originally incoming but crossed to outgoing) LH (RH) Weyl fermions, and $h = -\frac{1}{2}\,(\frac{1}{2})$ for the final (outgoing) LH (RH) Weyl fermions.

Reduced matrix elements are labeled as

$$\mathcal{M}^{J}_{-h_{\rm in},h_{\rm out}} \tag{B.10}$$

in our all-outgoing convention, $h_{\rm in} = \frac{1}{2}\,(-\frac{1}{2})$ for incoming $f\,(\bar{f}^{\,\dagger})$, and $h_{\rm out} = -\frac{1}{2}\,(\frac{1}{2})$ for outgoing $f\,(\bar{f}^{\,\dagger})$. This means that the labels on $\mathcal{M}^{J}$ respect particle identity: $\mathcal{M}^{J}_{-\frac{1}{2},\frac{1}{2}}$ is for $f \to \bar{f}^{\,\dagger}$ while $\mathcal{M}^{J}_{\frac{1}{2},-\frac{1}{2}}$ is for $\bar{f}^{\,\dagger} \to f$, etc.

Appendix C

Spinor-helicity variables in the COM frame and in the heavy monopole limit

This appendix first appeared in work previously published in collaboration with Csaba Csáki, Sungwoo Hong, Yuri Shirman, Ofri Telem, and John Terning [31].

In the COM frame of a dyon pair i, j we have

$$\begin{aligned} p_i^\mu &= (E_i^c, \ +\hat{p}_c) \\ p_j^\mu &= \left(E_j^c, \ -\hat{p}_c\right) , \end{aligned} \tag{C.1}$$

where $\hat{p}_c$ is in the direction given by $\{\theta_c, \phi_c\}$ and

$$p_c \;=\; \sqrt{\frac{(p_i \cdot p_j)^2 - m_i^2 m_j^2}{s}} \quad , \quad E^c_{i,j} = \sqrt{m^2_{i,j} + p^2_{\rm c}}\,. \tag{C.2}$$

In this case, the Lorentz transformation L_p taking the reference momenta Eq. (4.13) to p_i, p_j is just a rotation

$$L_p \;=\; R_z\left(\phi_c\right)\, R_y\left(\theta_c\right)\,. \tag{C.3}$$

Acting with the spinor version of this transformation on the reference pairwise spinors $|k_{ij}^{\flat\pm}\rangle_\alpha$, $\left[k_{ij}^{\flat\pm}\right|_{\dot\alpha}$, etc. we get

$$|p_{ij}^{\flat\pm}\rangle_\alpha \;=\; \sqrt{2p_c}\,|\pm\hat{p}_c\rangle_\alpha \quad , \quad \left[p_{ij}^{\flat\pm}\right|_{\dot\alpha} \;=\; \sqrt{2p_c}\,[\pm\,\hat{p}_c|_{\dot\alpha}\,, \tag{C.4}$$

where we use "-" instead of $-$ inside the brackets for ease of reading. In the equation above we use the notation

$$\begin{aligned} |\hat{n}\rangle_\alpha \;&\equiv\; \begin{pmatrix} c_n \\ \\ s_n \end{pmatrix} \quad , \quad [\hat{n}|_{\dot\alpha} \;\equiv\; (c_n\;,\; s_n^*) \\ |\text{-}\hat{n}\rangle_\alpha \;&\equiv\; \begin{pmatrix} -s_n^* \\ \\ c_n \end{pmatrix} \quad , \quad [\text{-}\hat{n}|_{\dot\alpha} \;\equiv\; (-s_n\;,\; c_n)\,. \end{aligned} \tag{C.5}$$

where $s_n = e^{i\phi_n}\sin\left(\frac{\theta_n}{2}\right)$, $c_n = \cos\left(\frac{\theta_n}{2}\right)$. In particular, under a parity transformation $\hat{n} \leftrightarrow$

$-\hat{n}$, we have

$$|\hat{n}\rangle_\alpha \;\leftrightarrow\; -e^{i\phi_n}\,|\text{-}\hat{n}\rangle_\alpha \quad , \quad [\hat{n}|_{\dot\alpha} \;\leftrightarrow\; -e^{-i\phi_n}\,[\text{-}\hat{n}|_{\dot\alpha}\ . \tag{C.6}$$

The expressions for $\langle \pm\hat{n}|^\alpha$ and $|\pm\hat{n}]^{\dot\alpha}$ are obtained by raising the spinor indices with $\epsilon^{\alpha\beta}$ and $\epsilon^{\dot\alpha\dot\beta}$, following the northwest-southeast convention for α and the southwest-northeast convention for $\dot\alpha$. Explicitly,

$$\begin{aligned}
\langle\hat{n}|^\alpha &= (s_n\ ,\ -c_n) \qquad , \qquad |\hat{n}]^{\dot\alpha} = \begin{pmatrix} s_n^* \\ -c_n \end{pmatrix} \\
\langle\text{-}\hat{n}|^\alpha &= (c_n\ ,\ s_n^*) \qquad , \qquad |\text{-}\hat{n}]^{\dot\alpha} = \begin{pmatrix} c_n \\ s_n \end{pmatrix} .
\end{aligned} \tag{C.7}$$

Also, since in the center of mass frame $\hat{p}_i = -\hat{p}_j = \hat{p}_c$, we automatically get the following relations in the $m_i \to 0$ limit

$$\begin{aligned}
|p_{ij}^{\flat+}\rangle_\alpha &= |\,i\,\rangle_\alpha \qquad , \qquad \left[p_{ij}^{\flat+}\right|_{\dot\alpha} = [\,i\,|_{\dot\alpha} \\
|p_{ij}^{\flat-}\rangle_\alpha &= \sqrt{2p_c}\,|\hat{\eta}_i\rangle_\alpha \qquad , \qquad \left[p_{ij}^{\flat-}\right|_{\dot\alpha} = \sqrt{2p_c}\,[\hat{\eta}_i|_{\dot\alpha}\ ,
\end{aligned} \tag{C.8}$$

where $|i\rangle_\alpha$, $[i|_{\dot\alpha}$ are the standard massless spinor-helicity variables, and $|\hat{\eta}_i\rangle_\alpha$, $[\hat{\eta}_i|_{\dot\alpha}$ are the (dimensionless) Parity-conjugate massless spinors that appear in the massless limit of the massive spinors $|\mathbf{i}\rangle_\alpha^I$, $[\mathbf{i}|_{\dot\alpha}^I$ (see [7] for their definition). Consequently, the following contrac-

tions vanish:

$$\begin{aligned}
\left[p_{ij}^{\flat+}\, i\right] &= \left\langle i\, p_{ij}^{\flat+}\right\rangle = \left[\hat{\eta}_i\, p_{ij}^{\flat-}\right] = \left\langle p_{ij}^{\flat-}\, \hat{\eta}_i\right\rangle = 0 \\
\left[p_{ij}^{\flat-}\, i\right] &= \left\langle i\, p_{ij}^{\flat-}\right\rangle = \left[\hat{\eta}_i\, p_{ij}^{\flat+}\right] = \left\langle p_{ij}^{\flat+}\, \hat{\eta}_i\right\rangle = 2p_c\,,
\end{aligned} \tag{C.9}$$

since $[\text{-}\hat{n}\,|\,\hat{n}] = \langle\hat{n}\,|\,\text{-}\hat{n}\rangle = 1$. Note that the above equations are Lorentz *and* LG invariant, and so hold in any other reference frame as well.

C.1 $2 \to 2$ scattering in the COM frame and Wigner $\mathcal{D}$-matrices

We now explicitly present the relevant formulas for $2 \to 2$ scattering in the COM frame. We take the colliding momenta to be

$$\begin{aligned}
p_i^\mu &= (E_i^c,\, \hat{n}\, p_c\,) \quad , \quad p_j^\mu = \left(E_j^c,\, -\hat{n}\, p_c\right) \\
\tilde{p}_i^\mu &= \left(E_i^c,\, \hat{k}\, p_c\right) \quad , \quad \tilde{p}_j^\mu = \left(E_j^c,\, -\hat{k}\, p_c\right)\,,
\end{aligned} \tag{C.10}$$

where $\hat{n}$ is in the (θ_n, ϕ_n) direction and $\hat{k}$ is in the (θ_k, ϕ_k) direction. Later we will specialize to the case $\theta_n = 0$ in which the initial momenta point along the $\hat{z}$ direction. From Eq. (C.5) we have

$$\begin{aligned}
\left\langle \text{-}\hat{n}\,|\,\text{-}\hat{k}\right\rangle^* &= \left\langle \hat{n}\,|\,\hat{k}\right\rangle = s_n\, c_k - c_n\, s_k \\
-\left\langle \hat{n}\,|\,\text{-}\hat{k}\right\rangle^* &= \left\langle \text{-}\hat{n}\,|\,\hat{k}\right\rangle = c_n\, c_k + s_n^*\, s_k\,.
\end{aligned} \tag{C.11}$$

where $s_i = e^{i\phi_i}\sin(\theta_i/2)$, $c_i = \cos(\theta_i/2)$ for $i = n, k$. We put a | to separate contractions involving a "-" for ease of reading. The expression for square brackets are obtained by $[ab] = \langle ba\rangle^*$.

When writing down $2 \to 2$ electric-magnetic S-matrix elements, we encounter the ubiquitous spinor contraction

$$\tilde{\mathcal{B}}^J(\Delta,\Delta') \quad = \quad \left(\langle \text{-}\hat{n}|^{J+\Delta}\langle\,\hat{n}|^{J-\Delta}\right)^{\{\alpha_1,\ldots,\alpha_{2J}\}}\left(|\,\text{-}\hat{k}\rangle^{J+\Delta'}|\,\hat{k}\rangle^{J-\Delta'}\right)_{\{\alpha_1,\ldots,\alpha_{2J}\}}. \tag{C.12}$$

By simple combinatorics, this expression simplifies to the sum

$$\tilde{\mathcal{B}}^J(\Delta,\Delta') \quad = \quad \sum_i w_i \left\langle \text{-}\hat{n}\,|\,\text{-}\hat{k}\right\rangle^i \left\langle \hat{n}\,|\,\hat{k}\right\rangle^{i-\Delta-\Delta'} \left\langle \text{-}\hat{n}\,|\,\hat{k}\right\rangle^{J+\Delta-i} \left\langle \hat{n}\,|\,\text{-}\hat{k}\right\rangle^{J+\Delta'-i} \tag{C.13}$$

where the sum is over $\max(0,\Delta+\Delta') \le i \le J + \min(\Delta,\Delta')$. The coefficients ω_i are combinatoric factors denoting the number of equivalent contractions [67],

$$w^i = \frac{\sqrt{J+\Delta)!\,(J-\Delta)!\;(J+\Delta')!\;(J-\Delta')!}}{i!\,(i-\Delta-\Delta')!\;(J+\Delta-i)!\,i!\;(J+\Delta'-i)!}\,. \tag{C.14}$$

Note that to get w^i we have used our particular normalization for symmetrized products, Eq. (B.8). Substituting the values Eq. (C.11) in Eq. (C.12), one can check explicitly that the following relation holds:

$$\tilde{\mathcal{B}}^J(\Delta,\Delta') \quad = \quad (-1)^{J-\Delta'}\sum_{p=-J}^{J}\mathcal{D}^J_{p,-\Delta}(\phi_n,\theta_n,-\phi_n)\;\mathcal{D}^{J*}_{p,\Delta'}(\phi_k,\theta_k,-\phi_k)\;. \tag{C.15}$$

$\mathcal{D}^{J}_{m,m'}(\alpha,\beta,\gamma)$ is the Wigner $\mathcal{D}$-matrix, defined as

$$\mathcal{D}^{J}_{m,m'}(\alpha,\beta,\gamma) \;\equiv\; \langle J,m|\mathcal{R}(\alpha,\beta,\gamma)|J,m'\rangle = e^{-i\,(m\,\alpha\,+\,m'\,\gamma)}\; d^{J}_{m,m'}(\beta)\;, \tag{C.16}$$

where $\mathcal{R}(\alpha,\beta,\gamma) = e^{-i\alpha J_z}e^{-i\beta J_y}e^{-i\gamma J_z}$ is a 3-dimensional rotation operator, and therefore

$$d^{J}_{m,m'}(\beta) \equiv \left\langle J,m\,|\,e^{-iJ_y\beta}\,|\,J,m'\right\rangle. \tag{C.17}$$

Since our $\mathcal{D}$-matrices always involve $\gamma=-\alpha=-\phi$, $\beta=\theta$, we use the shorthand notation

$$\mathcal{D}^{J}_{m,m'}(\Omega) \;\equiv\; \mathcal{D}^{J}_{m,m'}(\phi,\theta,-\phi)\;, \tag{C.18}$$

where $\Omega=\{\theta,\phi\}$. In the particular case where the initial momenta are along the $\pm\hat{z}$ direction, we have $\theta_n=0$, and Eq. (C.15) reduces to

$$\tilde{\mathcal{B}}^{J}(\Delta,\Delta') \quad=\quad (-1)^{J-\Delta'}\,\mathcal{D}^{J*}_{-\Delta,\Delta'}(\Omega_k)\;. \tag{C.19}$$

We make use of this expression in section 4.6, where we consider $2\to 2$ electric-magnetic S-matrix elements in the COM frame.

C.2 The heavy particle limit

In the $m_j \to \infty$ limit, Eq. (4.32) leads to very simple expressions for the spatial parts of the pairwise momenta,

$$\vec{p}_{ij}^{\,\flat\pm} \quad = \quad \pm\,\vec{p}_i\,. \tag{C.20}$$

Note that in this limit $p_i \sim p_c$ up to $\mathcal{O}\left(m_j^{-1}\right)$ corrections. That implies

$$|p_{ij}^{\flat\pm}\rangle_\alpha \;=\; \sqrt{2p_c}\,|\pm\hat{p}_i\rangle_\alpha \quad , \quad \left[p_{ij}^{\flat\pm}\right|_{\dot\alpha} \;=\; \sqrt{2p_c}\,\left[\pm\,\hat{p}_i\right|_{\dot\alpha}\,, \tag{C.21}$$

and we are free to use all the expressions derived throughout appendix C for the COM frame also in any other frame with the substitution $\hat{p}_c \to \hat{p}_i$. This is correct up to $\mathcal{O}\left(m_j^{-1}\right)$ corrections.

Appendix D

Definition of the electric-magnetic S-matrix

In this section we define the S-matrix rigorously following Weinberg [112], making changes when necessary to adapt to the electric-magnetic case. We work in the Heisenberg picture, where all of the time dependence is concentrated in the operators rather than in the quantum states. As in the standard definition of the S-matrix, we separate the full Hamiltonian of the system into a free and interacting part, as in Eq. (4.24). Note that in the case of electric-magnetic scattering, the free part H_0 and the full Hamiltonian H have *different* conserved angular momentum operators,

$$\left[H, \vec{J}\right] \;=\; \left[H_0, \vec{J}_0\right] \;=\; 0, \quad \vec{J} \;\neq\; \vec{J}_0\,. \tag{D.1}$$

This means that the Lorentz group is represented differently on the eigenstates of H and H_0. We'll return to this point below.

As a first step towards the definition of the S-matrix, we define the eigenstates $|\alpha;\,\text{free}\rangle$ of the non-interacting part H_0 such that,

$$H_0\,|\alpha;\,\text{free}\rangle \;=\; E_\alpha\,|\alpha;\,\text{free}\rangle\,. \tag{D.2}$$

The label α denotes the different eigenstates of H_0. Since H_0 is free, its eigenfunctions are just direct products (or sums of direct products) of one-particle states,

$$|\alpha;\,\text{free}\rangle \;=\; \prod_{i\in\alpha} |p_i;\,s_i;\,n_i\rangle\,, \tag{D.3}$$

where p_i and s_i are the momentum and spin/helicity of each particle, and n_i denotes its charges and gauge representations.

As in [112], we define our in (out) states as eigenstates of H. Since the interaction V vanishes asymptotically, the eigenstates of H and H_0 coincide, and we can write

$$H\,|\alpha;\,\pm\,\rangle \;=\; E_\alpha\,|\alpha;\,\pm\,\rangle\,, \tag{D.4}$$

where '+' denotes in states and '$-$' denotes out states. In Weinberg's definition, the labels in (out) define two different eigenbases of H, which differ by their asymptotic forms at $t \to \pm\infty$. From this limiting relation and using $J = J_0$ (valid in his case but *not* in ours), he deduces how the Lorentz group is represented on in/out- states, and more importantly, that the *in*- and *out*- representations are identical.

In the case of an electric-magnetic S-matrix, $J \neq J_0$ by the non-vanishing asymptotic value of

the angular momentum in the EM field. Inspired by Zwanziger [119], we follow an opposite route to Weinberg, namely, we *define* our in out states by their *different* representations under the Lorentz group, and derive the implications for the S-matrix. The transformation rule that we impose on our *in*- and *out*- states is given in Eq. (4.26), and we repeat it here for completeness,

$$\begin{aligned} U(\Lambda)\,|p_1,\ldots,p_n\,;\pm\rangle &= \prod_i \mathcal{D}(W_i)\;|\Lambda p_1,\ldots,\Lambda p_n\,;\pm\rangle\, e^{\pm i\,\Sigma} \\ U_{\text{free}}(\Lambda)\,|p_1''\ldots p_l''\,;\text{free}\rangle &= \prod_i \mathcal{D}(W_i)|\Lambda p_1''\ldots\Lambda p_l''\,;\text{free}\rangle\,, \end{aligned} \tag{D.5}$$

where $\Sigma \equiv \sum_{i>j} q_{ij}\,\phi(p_i,p_j,\Lambda)$. We explicitly present the momenta p_i of the particles involved but suppress their spin/helicity labels, which are implicit in the LG transformations $\mathcal{D}(W_i)$. The magnetic part of the transformation for in/out-states is evident in the q_{ij} dependence of Σ, where $q_{ij} = e_i g_j - e_j g_i$ is the pairwise helicity of each particle pair. In section 4.2.3 we prove that these transformation rules constitute a unitary representation of the Lorentz group, by explicitly constructing them through the method of induced representations. The transformation rule Eq. (D.5) is a departure from Weinberg's standard definition of the S-matrix, in the sense that the Lorentz group is represented *differently* on *in*- and *out*- sates.

Having defined our in/out states in terms of their representations under Lorentz transformation, we can now take their $t \to \pm\infty$ limits to get relations similar to Weinberg's Eq. 3.1.12. In these limits, we would like to make the statement that our *in*- and *out*- states approach free states, since the interaction term V vanishes for $t \to \pm\infty$. However, our naive expectation is hindered by the extra phases in the transformation of our in- and out-states.

To compensate for that, we define our *compensated* free states:

$$|p_1'' \dots p_l''\,;\,(\text{free}\,\pm)\,\rangle \;\equiv\; C_\pm(p_1'' \dots p_l'')\,|p_1'' \dots p_l''\,;\,\text{free}\,\rangle\,, \tag{D.6}$$

where $C_\pm$ is a "compensator" function of the momenta which satisfies

$$\begin{aligned} C_\pm(p_1'' \dots p_l'') &= e^{\pm i\Sigma}\, C_\pm(\Lambda p_1'' \dots \Lambda p_l'') \\ |C_\pm(p_1'' \dots p_l'')|^2 &= 1\,. \end{aligned} \tag{D.7}$$

The compensator functions are unique up to a constant phase, and we can construct them explicitly from our pairwise spinor-helicity variables, as we demonstrate for the $2 \to 2$ case in section 4.8.

Because of the compensator functions, the compensated free states have the same transformation rule as their in/out- counterparts, so they can serve as the right limits at $t \to \pm\infty$. We now make this statement in a more formal manner. Since we are working in the Heisenberg picture, we define time dependent superpositions of in, out, and free states as

$$\begin{aligned} |g, t;\,\pm\,\rangle &= \exp\left(-i\,H\,t\right) \int d\alpha\, g(\alpha)\,|\alpha;\,\pm\,\rangle \\ |g, t;\,(\text{free}\,\pm)\rangle &= \exp\left(-i\,H_0\,t\right) \int d\alpha\, g(\alpha)\,|\alpha;\,(\text{free}\,\pm)\,\rangle\,. \end{aligned} \tag{D.8}$$

Taking the $t \to \pm\infty$ limit of our in/out- superpositions, and noting that $H \to H_0$ in this

limit, we get the limiting forms

$$\lim_{t\to\mp\infty} |g,t\,;\pm\rangle \quad = \quad \lim_{t\to\mp\infty} |g,t\,;\,(\text{free}\,\pm)\,\rangle\,. \tag{D.9}$$

A different way of stating the same relation is the formal expression

$$|\alpha;\pm\rangle \quad = \quad \Omega(\mp\infty)\,|\alpha;\,(\text{free}\,\pm)\,\rangle\,, \tag{D.10}$$

where $\Omega(t) \equiv \exp(iHt)\exp(-iH_0t)$. This relation should be understood in terms of superpositions as in Eq. (D.8). The S-matrix is defined as usual as:

$$S_{\beta\alpha} \;=\; \langle\beta;-\,|\,\alpha;+\rangle\;, \tag{D.11}$$

or equivalently as

$$S_{\beta\alpha} \;=\; \langle\beta;\,(\text{free}\,-)\;|S|\,\alpha;\,(\text{free}\,+)\,\rangle\;, \tag{D.12}$$

where $S \equiv \Omega^\dagger(\infty)\,\Omega(-\infty)$.

Appendix E

Zwanziger's Vectors

The first derivation of the LG transformation for electric-magnetic S-matrix elements was given by Zwanziger for $q_{ij} = 1$ in a seminal paper [119]. Beyond deriving the LG transformation similarly[1] to our section 4.2.3, Zwanziger also defined LG covariant vectors, which he used to construct manifestly LG covariant S-matrix elements. Unfortunately, Zwanziger's vectors were explicitly Lorentz non-invariant, as they have an explicit dependence on an arbitrary direction $\hat{n}$. This was not a major detractor from his formalism, though, since all of the $\hat{n}$ dependence canceled out when taking the absolute value squared of the S-matrix. Our use of pairwise spinors rather than vectors eliminates this $\hat{n}$ dependence, up to our choice of the canonical Lorentz transformation L_p which takes $k_{i,j} \to p_{i,j}$. However, this is no different from the usual choice of a canonical Lorentz transformation in the standard Wigner method. The other main detractor from using Zwanziger's pairwise vectors was the fact that they have pairwise helicity ± 1 rather than $\pm\frac{1}{2}$, which excludes writing down S-matrix elements with half integer q. Our formalism closes this gap, and allows us to write down pairwise LG covariant S-matrix elements in their most general form.

[1]The main difference between our derivation and Zwanziger's original derivation is our choice of the reference momenta $k_{i,j}$ to be the COM momenta rather than the momenta in the monopole rest frame. This makes our formalism more symmetric and suitable for the introduction of pairwise spinors.

In this appendix we define Zwanziger's vectors in terms of our pairwise spinor-helicity variables, and reproduce his results from section V of [119]. To define LG covariant vectors, we first pick a reference vector n^μ and define:

$$\begin{aligned} a_+^\mu &= i\sqrt{\frac{\langle p_{ij}^{\flat+}|n|p_{ij}^{\flat-}]}{\langle p_{ij}^{\flat-}|n|p_{ij}^{\flat+}]}}\,\langle p_{ij}^{\flat-}|\sigma^\mu|p_{ij}^{\flat+}] \\ a_-^\mu &= a_+^{\mu *}\,. \end{aligned} \tag{E.1}$$

We've constructed these vectors so that $(a_+ + a_-)\cdot n = 0$. Additionally, we have $a_\pm \cdot p_i = a_\pm \cdot p_j = 0$. To see this, note that

$$a_+ \cdot p_i \;\sim\; \langle p_{ij}^{\flat-}|\, i\,|p_{ij}^{\flat+}]\;, \tag{E.2}$$

and since p_i is a linear combination of $p_{ij}^{\flat+}$ and $p_{ij}^{\flat-}$ the whole expression is zero by the Dirac equation. By similar arguments $a_\pm \cdot p_i = a_\pm \cdot p_j = 0$.

Finally, we reproduce Zwanziger's Eq. (5.9):

$$\begin{aligned} a_+^\mu a_+^{\nu *} &= \langle p_{ij}^{\flat-}|\sigma^\mu|p_{ij}^{\flat+}]\,\langle p_{ij}^{\flat+}|\sigma^\nu|p_{ij}^{\flat-}] \\ a_-^\mu a_-^{\nu *} &= \langle p_{ij}^{\flat+}|\sigma^\mu|p_{ij}^{\flat-}]\,\langle p_{ij}^{\flat-}|\sigma^\nu|p_{ij}^{\flat+}]\;. \end{aligned} \tag{E.3}$$

Using the identity

$$\langle v|\sigma^\mu|u]\,\langle u|\sigma^\nu|v] \;\;=\;\; \frac{1}{v\cdot u}\,[v^\mu u^\nu \,+\, u^\mu v^\nu \,-\, (v\cdot u)\;g^{\mu\nu} + i\,\epsilon^{\mu\nu\rho\sigma}\,v_\mu u_\rho]\;, \tag{E.4}$$

valid for any null vector u, v, we have

$$a^\mu_\pm\,a^{\nu *}_\pm \;\;=\;\; \frac{1}{(p^{\flat +}_{ij}\cdot p^{\flat -}_{ij})}\,\Big[p^{\mu;\flat +}_{ij}p^{\nu;\flat -}_{ij} \,+\, p^{\mu;\flat -}_{ij}p^{\nu;\flat +}_{ij} \,-\, \big(p^{\flat +}_{ij}\cdot p^{\flat -}_{ij}\big)\;g^{\mu\nu} \,\mp\, i\,\epsilon^{\mu\nu\rho\sigma}\,p^{\flat +}_{\mu;ij}p^{\flat -}_{\rho;ij}\Big]\;, \tag{E.5}$$

or explicitly

$$\begin{aligned} a^\mu_\pm\,a^{\nu *}_\pm \;\;=\;\; & -\,g^{\mu\nu} + \frac{(p_i\cdot p_j)\;\big(p^\mu_i p^\nu_j \,+\, p^\mu_j p^\nu_i\big) - m_j^2\,p^\mu_i p^\nu_i \,-\, m_i^2\,p^\mu_j p^\nu_j}{(p_i\cdot p_j)^2 - m_i^2\,m_j^2} \,- \\ & \mp\frac{i\,\epsilon^{\mu\nu\rho\sigma}\,p_{\mu;i}p_{\nu;j}}{\sqrt{(p_i\cdot p_j)^2 - m_i^2\,m_j^2}}\,. \end{aligned} \tag{E.6}$$

This is exactly Zwanziger's Eq. (5.9). Contracting this with $g^{\mu\nu}$, we see that

$$-\frac{1}{2}(a_\pm\cdot a^*_\pm) \;=\; 1\,, \tag{E.7}$$

and so $\hat\epsilon^\mu \equiv \frac{i}{2}(a^\mu_+ + a^{\mu *}_+)$ and $\hat\zeta^\mu \equiv \frac{1}{2}(a^\mu_+ - a^{\mu *}_+)$ are two orthonormal vectors, orthogonal to $p^\mu_{i,j}$. By definition $\hat\epsilon\cdot n = 0$.

To show the LG covariance of $a^\mu_\pm$, we follow Zwanziger's argument. We note that

$$a^\mu_\pm(\Lambda p_i, \Lambda p_j, n) \;=\; \Lambda^\mu{}_\nu \, a^\nu_\pm(p_i, p_j, \Lambda^{-1} n)\,. \tag{E.8}$$

As we Lorentz transform, n, $\hat{\epsilon}$ remains in the plane orthogonal to $p_{i,j}$ and so is rotated by the angle ϕ_{ij} such that

$$\cos\phi_{ij} \;=\; \hat{\epsilon}(\Lambda^{-1} n) \cdot \hat{\epsilon}(n)\,. \tag{E.9}$$

Since $\hat{\zeta} \cdot \hat{\epsilon} = 0$ and is also in the $\hat{\zeta}$ same plane orthogonal to $p_{i,j}$, it is rotated by the same angle. But since $a^\mu_\pm = i\hat{\epsilon}^\mu \pm \hat{\zeta}^\mu$, this rotation amounts to a phase factor $\exp(\pm i\phi_{ij})$ for $a^\mu_\pm$. Summing up, we have

$$a^\mu_\pm(\Lambda p_i, \Lambda p_j, n) \;=\; \Lambda^\mu{}_\nu \, a^\nu_\pm(p_i, p_j, n) \exp(\pm i\phi_{ij})\,. \tag{E.10}$$

The last thing to show is that the angle ϕ_{ij} is the same LG angle as in Eq. (4.22). But Zwanziger shows that we can always fix the $U(1)$ ambiguity in the definition of $L(p_i, p_j)$ such that:

$$L(p_i, p_j)^\mu_2 \;=\; \hat{\epsilon}^\mu\,, \tag{E.11}$$

and consequently the LG rotation angle is exactly the rotation angle of $\hat{\epsilon}$.

Appendix F

Comparison of amplitude formalism to QM calculations

Here we show that Eq. (4.101) exactly reproduces the angular dependence of the higher partial amplitudes in [68]. Starting from their partial amplitude

$$S^J_{f\to f} \;=\; S^J_{\bar f\to \bar f} \;=$$
$$\mathcal{N}\; e^{-i\pi\mu}\,\frac{\mu}{\cos(\theta_c/2)}\,\left[\sqrt{\frac{4\pi}{2j}}\;{}_qY_{j-\frac{1}{2},-q}(-\Omega_c)\;-\;\sqrt{\frac{4\pi}{2j+2}}\;{}_qY_{j+\frac{1}{2},-q}(-\Omega_c)\right], \tag{F.1}$$

where $-\Omega_c = (\pi-\theta_c,-\phi_c)$ and $\mu \equiv \sqrt{(J+\frac{1}{2})^2-q^2}$. and using the relation Eq. (4.98) between the ${}_qY_{lm}$ and Wigner $\mathcal{D}$-matrices, we can cast it in the form

$$S^J_{f\to f} \;=\; S^J_{\bar f\to \bar f} \;=\; \mathcal{N}\, e^{-i\pi\mu}\;\frac{\mu}{\cos(\theta_c/2)}\,\left[\mathcal{D}^{J-\frac{1}{2}\,*}_{q,-q}(\Omega_c)+\mathcal{D}^{J+\frac{1}{2}\,*}_{q,-q}(\Omega_c)\right]. \tag{F.2}$$

Finally we can use $\mathcal{D}$-matrix identities in sec 4.8.2 of [110] to transform this expression to

$$S^J_{f\to f} \;=\; S^J_{\bar f\to \bar f} \;=$$

$$\mathcal{N}\;(2J+1)\,e^{-i\pi\mu}\;\mathcal{D}^{J*}_{q-\frac{1}{2},-q-\frac{1}{2}}(\Omega_c) \;=\; \mathcal{N}\;(2J+1)\,e^{-i\pi\mu}\;\mathcal{D}^{J*}_{q+\frac{1}{2},-q+\frac{1}{2}}(\Omega_c)\,. \tag{F.3}$$

Comparing this to the result obtained in our amplitude formalism,Eq. (4.101), implies that

$$\mathcal{M}^J_{\pm\frac{1}{2},\pm\frac{1}{2}} \;=\; e^{-i\pi\mu}\,. \tag{F.4}$$

where $\mu=\sqrt{\left(J+\frac{1}{2}\right)^2-q^2}$. Combining this expression with the unitarity condition leads to

$$\left|\mathcal{M}^J_{\pm\frac{1}{2},\mp\frac{1}{2}}\right|^2 \;=\; 1-\left|\mathcal{M}^J_{\pm\frac{1}{2},\pm\frac{1}{2}}\right|^2 \;=\; 0\,, \tag{F.5}$$

for helicity-flip $J>|g|-\frac{1}{2}$ processes in an agreement with the explicit calculation in [68].